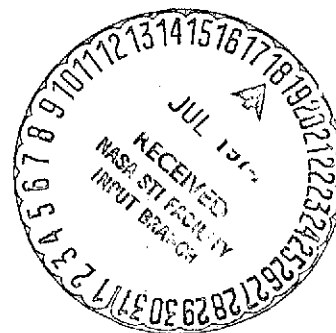ROTATION IN VIBRATION, OPTIMIZATION, AND

AEROELASTIC STABILITY PROBLEMS

Stanford University   NGL-05-020-243

A DISSERTATION

SUBMITTED TO THE DEPARTMENT OF AERONAUTICS AND ASTRONAUTICS

AND THE COMMITTEE ON GRADUATE STUDIES

OF STANFORD UNIVERSITY

IN PARTIAL FULFILLMENT OF THE REQUIREMENTS

FOR THE DEGREE OF

DOCTOR OF PHILOSOPHY

By

Krishna Rao Venkata Kaza

May 1974

ABSTRACT

A study on the effects of rotation in the areas of vibrations, dynamic stability, optimization, and aeroelasticity is presented. The governing equations of motion for the study of vibration and dynamic stability of a rapidly rotating deformable body are developed starting from the nonlinear theory of elasticity. Through some selected examples, some common features such as the limitations of the classical theory of elasticity, the choice of axis system, the property of self-adjointness, the phenomenon of frequency splitting, shortcomings of stability methods as applied to gyroscopic systems, and the effect of internal and external damping on stability in gyroscopic systems are identified and discussed. Then the experience gained from this general study is profitably applied to three specific problems. In the first problem exact vibration frequencies in two perpendicular planes of a rotating uniform beam inclined at an arbitrary angle to the axis of rotation are calculated. Also, a stability analysis of this beam is performed with the angle of inclination and rotational speed as parameters. Existence of several interesting bands of instabilities is shown. Optimum depth and thus the optimum mass distribution of a rotating beam with a given fundamental flapping frequency and rotational speed is calculated in the second problem using a numerical

- iii -

iterative method, based on a transition matrix approach, to solve the
resulting two-point nonlinear boundary-value problem. It is shown that
even in the presence of rotation the optimal structure is characterized
by the condition that specific Lagrangian density is constant. In the
last problem the effect of steady coning angle and internal damping at
the blade flapping hinge on whirl flutter stability in prop-rotors is
investigated. The developed mathematical equations and their analyses
are applied to two wind tunnel models studied in previous investigations.
The results indicate that these new parameters have a marked influence on
stability, and that they may even change the critical flutter mode. The
destabilizing effect of damping at the blade flapping hinge is discovered
to be analogous to the effects of internal damping in gyroscopic systems.
It is shown that this internal damping might help to explain why some
previous investigations show good correlation between theory and exper-
iment and some do not.

ACKNOWLEDGMENTS

TABLE OF CONTENTS

TABLE OF CONTENTS (Cont'd)

LIST OF TABLES

LIST OF SYMBOLS

Symbol	Description
A	area of cross section, Eq. (3.64); arbitrary constant, Eq. (5.28)
A_n	constant coefficients, Eq. (3.43) ($n = 1, 2, \ldots$)
a	lift coefficient
a_i	constant coefficients, Eq. (4.7)
B_n	constant coefficients, Eq. (3.44) ($n = 1, 2, \ldots$)
C_ℓ, C_d	lift and drag coefficients, Eq. (A.28)
C_{do}	defined in Eq. (A.36)
C_θ, C_ψ	viscous damping coefficients in pitch and yaw directions, Eq. (A.24)
C_β'	viscous damping coefficient at blade flapping hinge
C_β	effective flap damping of the rotor, Eq. (A.26)
c	blade chord; fixed constant, 1.875
c_e, c_i	external and internal damping coefficients
D_c	dissipation function
$\{dF_n\}$	elemental force vector

LIST OF SYMBOLS (Cont'd)

Symbol	Description
dm_n	mass of the blade element, dr
dm_s	mass of the nacelle element, ds
$E(i,j)$	value of the state vector $y(i)$ with jth set of boundary conditions
EI	bending stiffness of a symmetric shaft, Eq. (3.36)
EI_{yy}, EI_{zz}	flapwise and chordwise bending stiffness, Eqs. (3.57) and (3.58)
$\vec{F}_x$	surface tractions per unit area (before deformation)
H	Hamiltonian function
$\vec{H}_o$	angular momentum of the body about o
h	distance between the pivot point and the propeller center
$\tilde{I}$	idem tensor
$I_o, I_1, I_2, I_\beta, I_\theta,$ etc.	moments of inertias, Eq. (A.19)
$\vec{i}, \vec{j}, \vec{k}$	unit vector triad of the mean axis system
$K_\beta', K_\beta, K_\theta, K_\psi$	spring constants, Eqs. (A.21) and (A.23)
K_{do}, K_{d1}, K_{d2}	drag derivatives, Eq. (A.28)
L	length of the beam

Symbol	Description
m	mass of the body, Eq. (2.15); mass per unit length of the beam, Eq. (3.36)
m_b	mass per unit length of the blade
m_n	mass per unit length of nacelle
N	number of blades
n	number of modes
$\vec{n}_x$	unit vector normal to the surface before deformation
O	propeller center, Fig. 6.1
O_s	origin of inertial axis system, Fig. 6.1
O_β	hinge position on the axis of the blade, Fig. 6.1
o	origin of body fixed mean axis system; center of mass of the body; suffix representing steady-state or reference values
P_1, P_2	constants, Eq. (3.77)
Q_1, Q_2	constants, Eq. (3.78)
$\vec{q}$	displacement vector; vector, Eq. (A.38)
R	blade radius measured from the axis of rotation
$\vec{R}_x$	body force per unit volume

Symbol	Description
r	running coordinate along the blade axis
r_e	distance between the hinge center and the axis of rotation
r'	$r - r_e$
$\vec{r}$	position vector of mass point after deformation with respect to body fixed mean axis system
$\vec{r}'$	position vector of mass point with respect to inertial axis system
$\vec{r}'_o$	position vector of mass point in the undeformed state
$\vec{r}_u$	position vector of mass point before deformation expressed with respect to body fixed mean axis system
S	surface area
T	kinetic energy, Eq. (A.10); mass moment, Eq. (3.61)
$T_\ell(x)$	depth of the beam along the span
T_o	depth of the beam at the root
t	nondimensional depth. Eq. (5.4); time coordinate
U_p, U_T, U_r, U	perpendicular, tangential, radial and resultant velocities experienced by the blade element

Symbol	Description
$\dot{u}$	defined in Eq. (5.3)
u, v, w	elastic displacements associated with xyz system
u', v', w'	elastic displacements associated with $x'y'z'$ system
V	volume of the body
$\vec{V}$	velocity of the center of mass with respect to xyz system
$X_s, Y_s, Z_s, 0_s$	inertial axis system, Fig. 6.1
$X_{gn}, Y_{gn}, Z_{gn}, 0_s$	axis system fixed to nacelle, Fig. 6.1
$X_r, Y_r, Z_r, 0$	axis system fixed to the nth blade, rotating but not flapping
$X_b, Y_b, Z_b, 0$	axis system fixed to the blade, both rotating and flapping
x, y, z	body fixed mean axis system
x', y', z'	inertial axis system
x_b, y_b, z_b	coordinates of a point on the blade in X_b, Y_b, Z_b system
x_c, y_c, z_c	coordinates of 0 in X_{gn}, Y_{gn}, Z_{gn} system
x_e, y_e, z_e	coordinates of hinge center in X_r, Y_r, Z_r system

Symbol	Description
x_{gn}, y_{gn}, z_{gn}	coordinates of a point of the nacelle in X_{gn}, Y_{gn}, Z_{gn} system
x_s, y_s, z_s	coordinates of a point on the blade in X_s, Y_s, Z_s system
α	effective angle of attack of the blade element
α_o	defined in Eq. (A.36)
β_n	flapping angle of nth blade
$\beta_o, \bar{\beta}_n, \beta_\theta, \beta_\psi$	defined in Eq. (A.11)
$\gamma, \gamma_\theta, \gamma_\psi, \gamma_\beta, \gamma_{\beta 1}$	frequency ratios, Eqs. (6.1), (A.23), and (A.26)
$\delta(\ )$	variation or perturbation, Eq. (5.20)
ϵ	nondimensional hinge offset, Eq. (A.36); constant governing step size, Eq. (5.24)
$\zeta_\beta, \zeta_\theta, \zeta_\psi$	damping coefficients, Eq. (A.26)
θ, ψ	pitch and yaw deflection
λ	eigenvalue, Eq. (3.73); material constant, Eq. (3.10); and inflow ratio, Eq. (A.36)
λ_c	$\lambda \cos \beta_o$

Symbol	Description
$\tilde{\lambda}$	adjoint variable vector, Eq. (5.12)
μ	material constant, Eq. (2.12); real part of eigenvalue λ ; and eigenvalue, Eq. (6.1)
μ_o	real part of eigenvalue, Eq. (6.1); constant defined in Eq. (A.36)
ν_1	rotational frequency parameter, $\Omega_o/(\omega_{NR})_1$
ν_R	frequency parameter, $\omega_R/(\omega_{NR})_1$
$(\nu_R)_{11}$	frequency parameter, $(\omega_R)_{11}/(\omega_{NR})_1$
$(\nu_R)_{1n}, (\nu_R)_{2n}$	rotating frequency parameters of nth mode; $(\nu_R)_n$ splits into $(\nu_R)_{1n}$ and $(\nu_R)_{2n}$
ξ, η, ζ	coordinates of a mass point in the deformed state with respect to xyz system
ρ	mass density
$\tilde{\sigma}$	Eulerian stress tensor
τ	nondimensional time
$\bar{\tau}_0, \bar{\tau}_1, \bar{\tau}_2,$ etc.	defined in Eq. (A.36)
ν	helical angle of the typical blade element
ϕ	characteristic function, Eq. (3.41)

LIST OF SYMBOLS (Cont'd)

Symbol	Description
ϕ_n, ψ_n	characteristic functions of nth mode in y and z directions, Eqs. (4.13) and (4.14)
ϕ_n	azimuth angle of nth blade
χ	nondimensional coordinate along blade axis
$\vec{\Omega}$	angular velocity of the body relative to xyz axis system
Ω_o	propeller rotational speed; steady-state rotation of the shaft, Eq. (3.35)
$\omega, \omega_1, \omega_2, \omega_3, \omega_4$	whirl frequencies
$\vec{\omega}$	rotation vector of the displacement field, Eq. (2.13)
$(\omega_{NR})_1$	nonrotating fundamental frequency, Eq. (5.4)
$(\omega_{NR})_n$	nonrotating frequency of nth mode, Eq. (3.32)
$(\omega_R)_n$	rotating frequency of nth mode, Eq. (4.2)
$(\omega_R)_{1n}, (\omega_R)_{2n}$	rotating frequencies of nth mode, Eq. (3.44)
$\omega_\theta, \omega_\psi, \omega_\beta$	nonrotating frequencies, Eq. (A.23)
$\omega_{\beta 1}, \omega_{\beta 1d}$	rotating frequencies of rotor without and with damping

Note:
$d\vec{F}_x$, $d\vec{M}_x$, dV_x , dS_s , etc. are elemental quantities.

$\frac{d}{dt}$ ( ) $= \frac{\partial}{\partial t}$ ( ) $+ \vec{\Omega}$ x ( ). Subscript o denotes reference or steady-state values. Dots over symbols indicate differentiation with respect to time, and primes indicate differentiation with respect to τ .

The above nomenclature is followed in the majority of the thesis. However, because the study involves several areas there may be an overlapping of terminology. Where this is the case, this fact will be pointed out.

I.   INTRODUCTION

1.1   BACKGROUND AND OBJECTIVES

Engineering science provides many examples in vibrations, dynamic stability, optimization, and aeroelasticity involving the effects of rapid rotation. Some examples are the rotating shaft, the rotating disk, the rotating propeller blade, the spinning space vehicle, and the spinning planet. These bodies may be of one-dimensional or two-dimensional or three-dimensional configurations; may be rigid or deformable; may or may not suffer external kinematic constraints; and may be subjected to both conservative and nonconservative external forces. The term rapid rotation means that the additional forces experienced by the body due to rotation are of the same order as those acting on the body in the absence of rotation. Most of these problems are understood in a piecewise manner, and satisfactory analytical treatments have been given in the literature. However, several unresolved discrepancies remain in the literature, particularly in the areas of vibrations, dynamic stability, and aeroelasticity of deformable bodies. Thus, the subject of effects of rotation covers a broad spectrum of both applied and academic objectives, methods and applications even when the topic is restricted to structural dynamics. Hence, one can recognize multiple stages to a study. The stages

considered in this dissertation are: 1) the development of the equations of motion of an unrestrained, deformable, and rapidly rotating body, and a systematic reduction of these equations to specific cases; 2) a general study of vibration and stability of a rapidly rotating deformable body; 3) consideration of some common phenomena such as frequency splitting, orthogonality between the modes, the effect of choice of axis systems, and the effect of internal and external damping on stability; and 4) application of the experience gained in stages 1-3 to three problems of practical engineering interest.

The first problem considered is a slender beam, capable of bending in two planes perpendicular to its neutral axis and simultaneously rotating about an axis inclined at an arbitrary angle to its neutral axis. The angle between the neutral axis of the beam and the plane perpendicular to the axis of rotation is called coning angle, and the beam is referred to as a coned beam. The exact vibration frequencies of this beam are calculated at various coning angles and rotational speeds. The principal motivating factor for this investigation is the fact that both coriolis and centrifugal forces appear due to coning angle. Another is the need for an exact vibration, dynamic response, and stability analysis of the rotor blade with coning angle, in view of the use of precone in several V/STOL designs.

The second problem concerns application of control theory methods to the mass optimization of structures having dynamic constraints in the presence of rotation. The model considered for this study is a rotating cantilever beam with given fundamental flapping frequency.

The motivating factor for this investigation is a more general one of avoiding unnecessary weight, which increases overall weight and in turn increases the direct operating costs of V/STOL prop-rotor configurations.

The third investigation is aimed at better understanding of whirl flutter in prop-rotors. Whirl flutter is an aeroelastic instability that can occur on a flexibly mounted aircraft prop-rotor/power-plant combination, and involves coupling of inertial, elastic, centrifugal, coriolis, aerodynamic, and damping forces. Whirl flutter is a design consideration in every V/STOL aircraft configuration which makes use of rotors or propellers for lift or thrust. The primary factor that motivates this study is the lack of agreement between theory and experiment in some specific cases.

1.2 SCOPE OF THE THESIS

The common factor in all the problems studied in this thesis is rapid rotation. Two types of mathematical models — the elastic continuum model and the concentrated mass and stiffness model — are used to represent the structure of rapidly rotating deformable bodies. A "viscous" representation is adopted for both internal and external damping.

This thesis comprises seven chapters and one appendix. In Chapter II, using an elastic continuum model and the nonlinear theory of elasticity, the equations of motion of a rapidly rotating deformable body are developed. Then these equations are linearized about a steady state condition in Chapter III, and the equations for free vibration

are obtained. Though the explicit need for nonlinear elasticity theory is well known in the static theory of elasticity in order to derive the equations for deflection of a beam subjected to axial loads, it has apparently not been used explicitly in deriving the free vibration motion equations for rotating beams simply because it is easier to avoid complexity by treating centrifugal forces by an "effective applied load" concept. As a result, the explicit need for nonlinear elasticity theory in the presence of rotation is not even mentioned in the literature. The effective applied load concept is well suited for rotating beams, but for a general elastic body it is not easily implemented. Hence, the explicit need for the nonlinear theory of elasticity in the presence of rotation is emphasized. With regard to stability, simple examples are used to illustrate shortcomings of the kinetic method of stability as applied to gyroscopic conservative systems, and the consequent need for the introduction of imperfections to extract all the possible instabilities of the systems. The advantage of using a body fixed rotating coordinate system to detect the instabilities due to imperfections is emphasized. Also, the effects of internal and external damping in gyroscopic systems are discussed. Finally, vibration and stability of a beam at various rotational speeds are studied with coning angle as a parameter, and some interesting instability bands are found.

Chapter IV is devoted to the calculation of exact vibration frequencies and mode shapes of a rotating beam with coning angle. These results are used to validate the application of Galerkin's method to this class of problems.

Least weight design with dynamic constraints is the problem of Chapter V. A rotating beam with given fundamental frequency and rotational speed is optimized for least weight using optimal control theory methods to derive the necessary conditions for an extremal. A numerical solution technique, called the transition matrix approach, is adapted to solve the resulting two-point boundary-value problem. The numerical results appear to be somewhat unusual. Optimality of the structure is characterized by the constancy of a specific Lagrangian density which includes the potential energy density of the equilibrium centrifugal forces. This observation is consistent with the corresponding one for nonrotating structures.

A whirl flutter study in prop-rotors in the propeller mode of operation, aimed at better correlation between theory and experiment in some specific cases, forms the contents of Chapter VI. In this problem the power-plant-nacelle-propeller combination is represented by a concentrated mass and stiffness mathematical model. It is shown in Chapter III that the coning angle of the beam changes the blade flapping frequency, and that internal damping has a destabilizing effect on stability in gyroscopic systems. Given the importance of flapping frequency and internal damping on whirl flutter, two additional parameters — coning angle of the blades and internal damping at the blade flapping hinge — are introduced in the formulation. The equations of motion are derived by a Lagrangian approach. Quasi-steady blade element theory is used to generate aerodynamic forces of the windmilling prop-rotor. A linearized version of these equations is applied to two wind-tunnel

models from previous investigations, and the whirl flutter stability boundaries are obtained. The results indicate that these parameters have a marked effect on stability. It is also shown that internal damping might even explain why some investigations show good correlation between theory and experiment and some do not.

In a concluding chapter are discussed some limitations of the continuum mathematical model for analytical treatment of the problems in the presence of rotation. Some common features of problems involving effects of rotation are summarized. Possible extensions for this investigation are suggested.

II. EQUATIONS OF MOTION OF A RAPIDLY

ROTATING DEFORMABLE BODY

2.1 INTRODUCTION

The quantitative theoretical treatment of any class of engineering problems requires a physical idealization, appropriate laws of physics, a resulting mathematical model, mathematical equations, and their analysis. In this chapter the governing equations of motion for the study of vibration and stability of a three-dimensional, unconstrained, deformable, and rapidly rotating body are derived by considering the body as an elastic continuum. The derivation is straightforward, and appears implicitly in the literature (Ref. 2.1 for example). It is reviewed in this chapter with multiple objectives: 1) to use these general equations in the following chapter to extract general inferences concerning the influence of rapid rotation on the equations of motion, and on the frequencies and mode shapes of a rotating deformable body; 2) to obtain the equations of motion of some examples considered in the following chapters as a special case of these general equations; 3) to make explicit the necessity of employing nonlinear elasticity theory to study vibration in the presence of rotation; and 4) to maintain consistency in notation.

2.2 EQUILIBRIUM EQUATIONS

Let us consider a body of total mass m as shown in Fig. 2.1. This body may undergo displacements with respect to an orthogonal body-fixed system xyz with the origin at o , the center of mass of the body in the undeformed state. We shall denote by $\vec{r}_u = \vec{i}x + \vec{j}y + \vec{k}z$ the position vector relative to axes xyz of an element of mass dm in the undeformed state, by $\vec{q} = \vec{i}u(x,y,z,t) + \vec{j}v(x,y,z,t) + \vec{k}w(x,y,z,t)$ the elastic displacement vector of the element, and by $\vec{r} = \vec{r}_u + \vec{q} = \vec{i}\xi + \vec{j}\eta + \vec{k}\zeta$ the position vector relative to axes xyz of the element of mass in the deformed state. All these vectors are referred to the same set of rectangular Cartesian coordinates xyz . The variables x,y,z,t and ξ,η,ζ,t are called Lagrangian and Eulerian variables, respectively. The components of $\vec{q}$ need not be infinitesimally small. The absolute position of dm in the deformed state is given by $\vec{r}_o + \vec{r}_u + q$, where $\vec{r}_o$ is the position vector of the center of mass of the body in the undeformed state relative to the inertial axis system $x'y'z'$.

If the body is acted on by surface tractions per unit of area designated by the vector $\vec{F}_x$ and by body forces per unit of volume designated by the vector $\vec{R}_x$, then the equations for linear momentum $\vec{G}$ and angular momentum $\vec{H}_o$ are given by

$$\vec{G} = \iiint_{V_x} \frac{d\vec{r}'}{dt} \rho_x \, dV_x \qquad (2.1)$$

$$\vec{H}_o = \iiint_{V_x} \vec{r} \times \frac{d\vec{r}'}{dt} \rho_x \, dV_x \qquad (2.2)$$

- 8 -
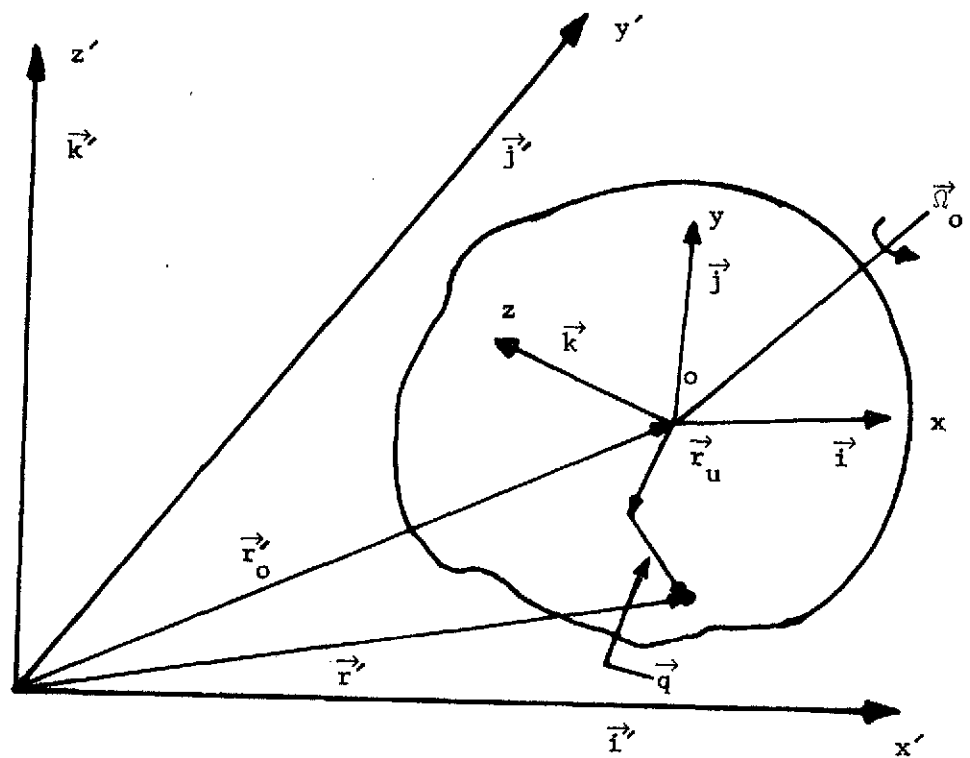
FIG. 2.1--Rapidly rotating, three-dimensional, unconstrained, and deformable body — $\vec{r}_u$, position vector of mass point before deformation; $\vec{q}$, elastic displacement; $\vec{r}_o$, position vector to the center of mass o; $\vec{r}'$, position vector to the mass point after deformation; $\vec{\Omega}_o$, steady angular velocity of the body.

where suffix 'x' indicates that the corresponding quantities are referred to the initial state, and $\frac{d(\ )}{dt} = \frac{\partial(\ )}{\partial t} + \vec{\Omega} \times (\ )$. Here, $\vec{\Omega}$ is the angular velocity of the body expressed with respect to the xyz system. If we introduce the relation

$$\vec{r'} = \vec{r'_o} + \vec{r}$$ (2.3)

into Eqs. (2.1) and (2.2) we obtain

$$\vec{G} = m\vec{V} + \iiint_{V_x} \left(\frac{\partial \vec{q}}{\partial t} + \vec{\Omega} \times \vec{q} \right) \rho_x \, dV_x$$ (2.4)

$$\vec{H}_o = \widetilde{I}_o \cdot \vec{\Omega} + \widetilde{I'}_o \cdot \vec{\Omega}$$

$$+ \iiint_{V_x} \left(\vec{r}_u \times \frac{\partial \vec{q}}{\partial t} \right) \rho_x \, dV_x + \iiint_{V_x} (\vec{q} \times \vec{V}) \rho_x \, dV_x$$ (2.5).

Here $\vec{V}$ is the linear velocity of the point o expressed in the xyz system, and $\widetilde{I}_o$ and $\widetilde{I'}_o$ are inertial tensors given by

$$\widetilde{I}_o = \iiint_{V_x} (r_u^2 \widetilde{I} - \vec{r}_u \vec{r}_u) \rho_x \, dV_x$$

$$\widetilde{I'}_o = \iiint_{V_x} (2\vec{r}_u \cdot \vec{q} \, \widetilde{I} - \vec{r}_u \vec{q} - \vec{q} \, \vec{r}_u + q^2 \widetilde{I} - \vec{q} \, \vec{q}) \rho_x \, dV_x$$ (2.6)

- 10 -

and $\tilde{I}$ is the idem or unit tensor. While obtaining Eqs. (2.4) and (2.5), we made use of the fact that o is the center of mass of the body.

Applying the law of linear momentum (see Ref. 2.2), we get

$$\frac{d\vec{G}}{dt} = \iiint\limits_{V_x} \vec{R}_x \, dV_x + \iint\limits_{S_x} \vec{F}_x \, dS_x \qquad (2.7)$$

Similarly, the law of angular momentum leads to

$$\frac{d\vec{H}_o}{dt} = \iiint\limits_{V_x} (\vec{r} \times \vec{R}_x) \, dV_x + \iint\limits_{S_x} (\vec{r} \times \vec{F}_x) \, dS_x \qquad (2.8)$$

Equations (2.7) and (2.8) govern the motion of the body, but they provide no information concerning the internal or elastic response. The equations that govern the elastic response are referred to as elemental equations, and they must be obtained by considering the stress and strain within the body.

According to Novozhilov [2.1], deformable bodies are divided into two types: massive bodies and flexible bodies. In the former type, the extension is of the same order of magnitude in all three of its dimensions; and in the latter type, the extension in one or two directions is small compared to that in remaining dimensions. The choice of the elemental equations depends on the type of the body. The classical equations of elasticity are applicable to all massive bodies and to a particular class of flexible bodies (such as rods, plates, and shells). In particular, they may be used in the study of bending and

torsion of thin rods when they are not subjected to the simultaneous action of axial forces, and the angles of rotations of the sections are small compared to unity and at the same time small compared to strains. Hence, for rapidly rotating bodies, particularly when flexible, the classical theory is no good, since these bodies are subjected to equilibrium stresses, and the angles of rotations of the sections are not small compared to strains. Then, the next question concerns the type of nonlinear theory to be used. This was discussed by Milne [2.3]. The present writer agrees with this discussion, since the equations for most engineering type problems can be derived with certain assumptions. The assumptions that are appropriate for this nonlinear theory are as follows:

(1) No body couples, no couple stresses.

(2) Elongations and shears small compared to unity.

(3) Infinitesimal strains.

(4) Linear stress-strain law (Hooke's law).

It is to be noted that there is no restriction on the magnitude of displacements and rotations. The appropriate elemental equations of equilibrium, compatibility, boundary conditions, and stress-strain law can be deduced from Ref. 2.1 as

$$\left. \begin{array}{c} \rho_x \; \dfrac{d^2 \vec{r}'}{dt^2} - \vec{\nabla}_x \cdot [\tilde{\sigma} \cdot (\tilde{I} + \vec{\nabla}_x \vec{q}')] - \vec{R}_x = 0 \\ \\ \sigma_{ij} = \sigma_{ji} \end{array} \right\} \qquad (2.9)$$

$$E_{ij} = e_{ij} + \tfrac{1}{2} (e_{ki} - \omega_{ki})(e_{kj} - \omega_{kj}) \qquad (2.10)$$

and

$$\tilde{\sigma} \cdot (\tilde{I} + \vec{\nabla}_x \vec{q}) \cdot \vec{n}_x = \vec{F}_x \qquad (2.11)$$

$$\tilde{\sigma} = 2\mu\tilde{E} + \tilde{I}\lambda\vec{\nabla}_x \cdot \vec{q} \qquad (2.12)$$

where

$$e_{ij} = \frac{1}{2}\left(\frac{\partial u_i}{\partial x_j} + \frac{\partial u_j}{\partial x_i}\right)$$

$$\qquad (2.13)$$

$$\omega_{ij} = \frac{1}{2}\left(\frac{\partial u_j}{\partial x_i} - \frac{\partial u_i}{\partial x_j}\right)$$

The suffix 'x' , which indicates that the quantities are referred to the initial state, will be omitted here onwards for simplicity, since the areas and volumes do not change due to deformation in view of the assumption that shears and elongations are small compared to unity.

2.3 SPECIFICATION OF BODY AXES

In the absence of kinematic constraints the elastic boundary value problem is the Neumann problem. The solution of such a problem is arbitrary to the extent of a rigid-body displacement and rotation. This arbitrariness can be resolved with the choice of the body axes. A thorough discussion on choosing the appropriate body axes was presented by Milne [2.4]. In all, there are three possible choices: namely, attached, mean, and principal axes. Attached axes are specified by the condition

that the rigid-body displacements and rotations are zero. Mean axes are chosen in such a way that at every instant the linear and angular momenta of the motion with respect to the body axes are identically zero. The basic requirement in the case of principal axes is that the tensor $\tilde{I}'_o$ should be diagonal. It was also illustrated by Milne [2.3] that the conditions for both mean axes and principal axes will be identical for shapes which are typical of aeroplanes, in which transverse displacement relative to a plane or line contributes the main deformation. We shall use the mean axes in all our discussions. These axes are given by the conditions

$$\left. \begin{aligned} \iiint\limits_V \rho \vec{q}\, dV &= 0 \\[2em] \iiint\limits_V \rho\, [(\vec{r}_u + \vec{q}) \times \vec{q}]\, dV &= 0 \end{aligned} \right\} \tag{2.14}$$

It is to be noted that the first of Eqs. (2.14) implies that the origin of the mean axis system xyz is always at the center of mass of the body. Substituting Eqs. (2.14) into Eqs. (2.7) and (2.8), we obtain the overall body equations as

$$\frac{d}{dt}\,(m\vec{V}) = \iiint\limits_V \vec{R}\, dV + \iint\limits_S \vec{F}\, dS \tag{2.15}$$

$$\frac{d}{dt}\,(\tilde{I}_o \cdot \vec{\Omega} + \tilde{I}'_o \cdot \vec{\Omega}) = \iiint\limits_V (\vec{r} \times \vec{R})\, dV + \iint\limits_S (\vec{r} \times \vec{F})\, dS \tag{2.16}$$

There is no change in the elemental Eqs. (2.9), (2.10), (2.11), and (2.12) of the body.

We note that the motion of the body is described by a "hybrid" set of equations, since Eqs. (2.15) and (2.16) are six ordinary differential equations, and Eq. (2.9) leads to three partial differential equations. Further, all these equations are nonlinear. These equations form the bases for mathematical analyses of the vibration, dynamic stability, and aeroelastic behavior of an unconstrained, three-dimensional, rapidly rotating and deformable body. The equations of motion of some of the examples considered in the latter chapters are obtained as special cases of these general equations.

III. VIBRATION OF A RAPIDLY ROTATING

DEFORMABLE BODY

3.1 INTRODUCTION

In the previous chapter we developed the equations of motion of a
rapidly rotating, three-dimensional, unconstrained, and deformable body
for the study of vibration, dynamic stability, and aeroelastic behavior.
In this chapter we shall deduce the linearized equations of motion of
vibration of the same body in a vacuum and shall present a brief dis-
cussion concerning the magnitude and character of the influence of ro-
tation on the equations of motion of vibration, and on the frequencies
and mode shapes. Then, these discussions will be followed up by several
examples, though all of them are not new, in order to extract some com-
mon features of the effects of rotation. These features include choice
of axis system, the property of self-adjointness, the phenomenon of
frequency splitting, shortcomings of stability methods as applied to
gyroscopic systems, and the role of internal damping on stability.
Finally, vibration and stability analysis of a rotating beam with
coning angle as a parameter will be presented. This analysis is
believed to be new.

The experience gained in this chapter, particularly on the effect
of coning on the frequencies of the rotating beam and on the influence

of internal damping on stability in gyroscopic systems, is applied to the whirl flutter problem in Chapter VI.

3.2 EQUATIONS OF VIBRATION IN A VACUUM

The most general model for the vibration problem is an unconstrained, three-dimensional, rapidly rotating, deformable body, whose motion is assumed to be stable. A small perturbation motion about some stable steady-state condition can be called vibration. As mentioned earlier, the elastic problem is of a Neumann type, and hence the solution is arbitrary to the extent of a rigid-body translation and rotation. This arbitrariness was resolved by properly fixing the reference axis system, which is the mean axis system in our case. These axes will translate $(\vec{V}_o = \text{constant})$ and rotate $(\vec{\Omega}_o = \text{constant})$ with the body. Motions, which satisfy the equations of motion when no external forces act on the system with respect to the mean axes, might be called general motions. Of all these motions, only those involving steady non-rotating translation $(\vec{V}_o = \text{constant} , \vec{\Omega}_o = 0)$ of the mean axes are normally called free vibration motions. All other motions involving steady translation and rotation $(\vec{V}_o = \text{constant} , \vec{\Omega}_o = \text{constant})$ of the mean axes will be here onwards termed as vibrational motion with rotation, and the associated frequencies and modes will be called frequencies with rotation and modes with rotation.

In the absence of external forces, the equations of motion for vibration of a steadily rotating, uniformly translating, unconstrained, and deformable body can be deduced from Eqs. (2.15), (2.16), (2.9),

- 17 -

(2.10), (2.11), and (2.12). They are with respect to the mean axes as follows:

$$\frac{d}{dt} (m\vec{V}) = 0 \tag{3.1}$$

$$\frac{d}{dt} \left[\iiint_V \left(\vec{r} \times \frac{d\vec{r}}{dt} \right) \rho \, dV \right] = 0 \tag{3.2}$$

$$\rho \, \frac{d^2 \vec{r}'}{dt^2} - \vec{\nabla} \cdot [\tilde{\sigma} \cdot (\tilde{I} + \vec{\nabla} \vec{q})] = 0 \tag{3.3}$$

$$\tilde{\sigma} \cdot (\tilde{I} + \vec{\nabla} \vec{q}) \cdot \vec{n} = 0 \tag{3.4}$$

Equations (2.10) and (2.12) are unaltered.

The above set of equations are nonlinear. We shall linearize them about the steady state condition. Let us use the suffix '1' for the characteristics of the perturbed condition $(\vec{\Omega} = \vec{\Omega}_1, \vec{V} = \vec{V}_1)$, suffix 'o' for the characteristics of the steady-state condition and the same quantities for the perturbations. Then, the disturbed motion will be of the form

$$\vec{q}_1 = \vec{q}_o + \vec{q}$$

$$\tilde{\sigma}_1 = \tilde{\sigma}_o + \tilde{\sigma}$$

$$\vec{\Omega}_1 = \vec{\Omega}_o + \vec{\Omega} \qquad \text{(Cont'd)}$$

- 18 -

and

$$\vec{V}_1 = \vec{V}_o + \frac{d\vec{r}_1}{dt}$$

$$\vec{r}_1 = \vec{r}_u + \vec{q}_o + \vec{q}$$

$$(\rho_x)_1 = (\rho_x)$$

$$\text{etc.} \tag{3.5}$$

Application of Eqs. (3.1), (3.2), (3.3), and (3.4) at both steady-state condition and the disturbed condition leads to

$$\frac{d}{dt}\left\{ \iiint\limits_{V_x} \left\{ \left[(\vec{r}_u + \vec{q}_o) \times [(\vec{\Omega}_o + \vec{\Omega}) \times (\vec{r}_u + \vec{q}_o)] \right] \right.\right.$$

$$+ (\vec{r}_u + \vec{q}_o) \times (\vec{\Omega}_o \times \vec{q}_o) + \vec{q} \times [\vec{\Omega}_o \times (\vec{r}_u + \vec{q}_o)]$$

$$\left.\left. + \vec{q} \times (\vec{\Omega}_o \times \vec{q}) \right\} \rho_x \, dV_x \right\} = 0 \tag{3.6}$$

$$\text{div} \left[\tilde{\sigma} \cdot (\tilde{I} + \vec{\nabla}_x \vec{q}_o + \vec{\nabla}_x \vec{q}) \right] + \vec{\nabla}_x \cdot (\tilde{\sigma}_o \cdot \vec{\nabla}_x \vec{q}) - \rho_x \frac{d^2\vec{q}}{dt^2} = 0 \tag{3.7}$$

$$\left[\tilde{\sigma} \cdot (\tilde{I} + \vec{\nabla} \tilde{q}_o + \vec{\nabla} \vec{q}) \right] \cdot \vec{n} + \tilde{\sigma}_o \cdot \vec{\nabla} \vec{q} \cdot \vec{n} = 0 \tag{3.8}$$

and

$$\vec{\nabla} \cdot [\tilde{\sigma}_o \cdot (\tilde{I} + \vec{\nabla}\vec{q}_o)] = \rho \frac{d^2}{dt^2}(\vec{r}_u + \vec{q}_o) \qquad (3.9)$$

It should be noted that the equation governing the overall linear translational motion is automatically satisfied, whereas that of the angular motion couples the rigid body motions and the elastic deformations. If $\vec{\mathfrak{N}}_o = 0$, it can be seen from Eq. (3.6) that the coupling between rigid body motions and elastic motions will be eliminated.

We shall make two more assumptions: 1) the disturbances are small, which enables us to discard the terms $\tilde{\sigma} \cdot$ grad $\vec{q}$ from Eqs. (3.7) and (3.8) and simplifies Eq. (2.12) with the use of Eq. (2.10) as

$$\tilde{\sigma} = 2\mu\tilde{e} + \tilde{I}\lambda\vec{\nabla} \cdot \vec{q} \qquad (3.10)$$

and 2) the difference between the geometry of the initial undeformed state (natural state) and the undisturbed steady state $(\vec{\mathfrak{N}}_o = $ constant , $\vec{V}_o = $ constant) is comparatively small; this allows us to omit the terms grad $\vec{q}_o$ from Eqs. (3.7) — (3.9).

After the above simplifications, the linear equations or the variational equations of the system can be written as

$$\rho \frac{d^2\vec{q}}{dt^2} - \vec{\nabla} \cdot \tilde{\sigma} + \vec{\nabla} \cdot (\tilde{\sigma}_o \cdot \vec{\nabla}\vec{q}) = 0 \qquad (3.11)$$

and the boundary conditions as

$$\tilde{\sigma} \cdot \vec{n} + \tilde{\sigma}_o \cdot \vec{\nabla} \vec{q} \cdot \vec{n} = 0 \tag{3.12}$$

Equation (3.6) remains unchanged, and the equilibrium stress tensor $\tilde{\sigma}_o$ can be obtained from Eq. (3.9) as

$$\vec{\nabla} \cdot \tilde{\sigma}_o = \rho \, \{\vec{\Omega}_o \times [\vec{\Omega}_o \times (\vec{r}_u + \vec{q}_o)]\}$$

$$= \rho \, (\vec{\Omega}_o \vec{\Omega}_o - \tilde{I}\Omega_o^2) \cdot (\vec{r}_u + \vec{q}_o) \tag{3.13}$$

Substituting Eq. (3.10) into Eqs. (3.11) and (3.12), we obtain

$$\rho \left[\frac{\partial^2 \vec{q}}{\partial t^2} + \vec{\Omega}_o \times (\vec{\Omega}_o \times \vec{q}) + 2\vec{\Omega}_o \times \frac{\partial \vec{q}}{\partial t} \right]$$

$$- \mu \nabla^2 \vec{q} - (\lambda + \mu) \, \vec{\nabla} \vec{\nabla} \cdot \vec{q} - \vec{\nabla} \cdot (\tilde{\sigma}_o \cdot \vec{\nabla} \vec{q}) = 0 \tag{3.14}$$

$$\lambda \vec{n} \, (\vec{\nabla} \cdot \vec{q}) + \vec{n} \cdot \vec{\nabla}_s \vec{q} 2\mu + \tilde{\sigma}_o \cdot \vec{\nabla} \vec{q} \cdot \vec{n} = 0 \tag{3.15}$$

where suffix 's' represents the symmetric part of the operator $\vec{\nabla}$.

Using the principle of virtual displacements, Eqs. (3.11) and (3.12) can be combined and expressed in integral form as

$$\iiint\limits_V \left[\vec{\nabla} \cdot \tilde{\sigma} + \vec{\nabla} \cdot (\tilde{\sigma}_o \cdot \vec{\nabla} \vec{q}) - \rho \, \frac{d^2 \vec{q}}{dt^2} \right] \cdot \delta \vec{q}_m \rho \, dV$$

$$- \iint\limits_S (\tilde{\sigma} \cdot \vec{n} - \tilde{\sigma}_o \cdot \vec{\nabla} \vec{q} \cdot \vec{n}) \cdot \delta \vec{q}_m \, dS = 0 \tag{3.16}$$

where $\delta\vec{q}_m$ is the virtual displacement. Equation (3.16) can be written in a compact integral form if we take into account that

$$\iiint\limits_{V} \vec{\nabla} \cdot \vec{A}\ dV = \oiint \vec{A} \cdot \vec{n}\ dS \qquad (3.17)$$

$$\vec{\nabla} \cdot (\widetilde{\sigma} \cdot \delta\vec{q}_m) = (\vec{\nabla} \cdot \widetilde{\sigma}) \cdot \delta\vec{q}_m + \widetilde{\sigma} : (\vec{\nabla}\delta\vec{q}_m)^*$$

$$= (\vec{\nabla} \cdot \widetilde{\sigma}) \cdot \delta\vec{q}_m + \widetilde{\sigma} : \vec{\nabla}_s \delta\vec{q}_m \qquad (3.18)$$

where A is any vector and '*' represents transpose. While simplifying Eq. (3.18), the symmetric property of the stress tensor $\widetilde{\sigma}$ is used. Consequently, we obtain

$$\iiint\limits_{V} \rho \left[\frac{\partial^2 \vec{q}}{\partial t^2} + \vec{\Omega}_o \times (\vec{\Omega}_o \times \vec{q}) + 2\vec{\Omega}_o \times \frac{\partial \vec{q}}{\partial t} \right] \cdot \delta\vec{q}_m\ dV$$

$$+ \iiint\limits_{V} \widetilde{\sigma} : (\vec{\nabla}_s \delta\vec{q}_m)\ dV$$

$$+ \iiint\limits_{V} \widetilde{\sigma}_o : [\vec{\nabla} \vec{q} \cdot (\vec{\nabla}\delta\vec{q}_m)^*]\ dV = 0 \qquad (3.19)$$

To ensure equilibrium, the rotational Eqs. (3.6) must be satisfied. The physical explanation for this is more involved. A discussion on this was presented by Milne [3.1]. The necessary conditions for steady rotation of the vibrating body are: 1) mean and principal axis must coincide, and 2) the diagonal element of $\widetilde{I}'_o$ which corresponds

to the axis of rotation must be zero. These two conditions ensure that the rotation about the appropriate principal axis of the reference configuration is stable. For the elastic body, the principal axes are given by the condition that the inertia tensor $\tilde{I}'_o$ should be diagonal. When the overall motion is stable, the elemental equations of equilibrium (3.14) and the associated boundary conditions given by Eq. (3.15) govern the vibrational motion of the rapidly rotating, unconstrained, and deformable body.

Let us examine Eq. (3.19) term by term to understand the effect of each individual term on the frequency of the body. If $\vec{\Omega}_o = 0$, Eq. (3.19) reads

$$\iiint_V \rho\, \frac{\partial^2 \vec{q}}{\partial t^2} \cdot \delta\vec{q}\; dV + \iiint_V \tilde{\sigma} : \vec{\nabla}_s \vec{q}\; dV = 0 \qquad (3.20)$$

or in the differential form as

$$\rho\, \frac{\partial^2 \vec{q}}{\partial t^2} - \mu \nabla^2 \vec{q} - (\lambda + \mu)\, \vec{\nabla}\, \vec{\nabla} \cdot \vec{q} = 0 \qquad (3.21)$$

and the associated boundary conditions are

$$\lambda \vec{n}\, (\vec{\nabla} \cdot \vec{q}) + 2\mu \vec{n} \cdot \vec{\nabla}_s \vec{q} = 0 \qquad (3.22)$$

The boundary-value problem represented by Eqs. (3.21) and (3.22) is self-adjoint according to Courant and Hilbert [3.2], since it arises from a functional with a homogeneous quadratic integrand. Knowing

the problem is self-adjoint, we can state that the eigenvalues λ^2 ($\lambda^2 = -\omega^2$, ω being the natural frequency) are real, and the eigenvectors are orthogonal. It is to be noted that the symbol λ is used both for the eigenvalue and for one of the material constants. A thorough discussion on these eigenfunctions and their use in obtaining the approximate solutions of dynamic response problems was presented by Bisplinghoff and Ashley [3.3], Bolotin [3.4], and Courant and Hilbert [3.2] among others. Also, it should be noted that when $\vec{\Omega}_o = 0$, the overall Eq. (3.6) of rotational equilibrium is decoupled from the elemental equations.

Now, let us return to the discussion on vibration of the rapidly rotating body. The constant rotation $\vec{\Omega}_o$ adds three additional terms to the elemental equations, which can be seen either from Eq. (3.14) or from Eq. (3.19). The centrifugal inertial term $[\vec{\Omega}_o \times (\vec{\Omega}_o \times \vec{q})]$ shows that the natural frequencies ($n = 1, 2, \ldots$) will be altered. The change in the frequencies of a rotating shaft is due to this term. Also, this term may give rise to some constant terms, such as the one that appears in the equation of motion of a beam rotating about an axis inclined at an arbitrary angle to the axis of the beam. The coriolis term $2\vec{\Omega}_o \times (\partial\vec{q}/\partial t)$ leads to the result that, as shown later, the linear eigenvalue problem governed by Eqs. (3.14) and (3.15) is not self-adjoint. Consequently, the modes will no longer be orthogonal. An example of this case occurs in the whirling vibration of a shaft with heavy disks attached to it. Another effect of the above two terms either individually or collectively is the phenomenon of

frequency splitting, which will be discussed later. Another interesting aspect of these two terms is that they may cause static instability, as in the case of a symmetric shaft, or they may cause self-excited vibration as in the case of an unsymmetric shaft. Further, the coriolis term does have a marked influence on the effect of damping on stability, as will be seen in the shaft problems. The stability of some simple systems involving these terms will be discussed in later sections.

The third additional term, $\vec{\nabla} \cdot (\tilde{\sigma}_o \cdot \vec{\nabla} \vec{q})$, changes the frequencies of vibration. The increase in the frequencies of the helicopter rotor blade with increase in rotational speed is an example of this effect.

When the frequency spectrum of the nonrotating structure contains multiple roots, these roots may be split during rotation into a distinct series. For example, a nonrotating elastic shaft has an infinite number of natural frequencies in any plane passing through its axis. Upon introducing rotation, each natural frequency is split into two; these frequencies are called whirl frequencies. In another example, Backus and Gilbert [3.5,3.6] predicted the frequency splitting for the earth's first two spheroidal modes and verified their prediction, within experimental accuracy, by seismographic measurements of response to the violent Chilean earthquake of May, 1960. This fact was brought to the attention of aeroelasticians by Ashley [3.7]. This phenomenon of frequency splitting depends, as shown through examples later, on the nature of the system and the coordinate system used.

Earlier, we stated that the differential equations and the associated boundary conditions of the vibration problem of a rapidly rotating body, in general, are not self-adjoint. Now, we shall demonstrate this fact. First, we shall assume

$$\vec{q} = \vec{\psi}(x,y,z) \, e^{\lambda t} \quad , \quad \lambda = \mu + i\omega \qquad (3.23)$$

where $\vec{\psi}$ is a vector function. Substituting Eq. (3.23) into Eqs. (3.14) and (3.15), we can write the resulting equations in compact form as

$$\tilde{L}(\vec{\psi}) = \lambda^2 \tilde{N}(\vec{\psi}) \qquad (3.24)$$

$$B_n(\vec{\psi}) = 0 \qquad (n = 1, 2, \ldots, 6) \qquad (3.25)$$

where

$$\tilde{L}(\vec{\psi}) = \mu \nabla^2 \vec{\psi} - (\lambda + \mu) \vec{\nabla} \vec{\nabla} \cdot \vec{\psi} + (\vec{\nabla} \cdot \tilde{\sigma}_0) \cdot \vec{\nabla} \vec{\psi} \qquad (3.26)$$

$$\tilde{N}(\vec{\psi}) = \rho \lambda^2 \left[\vec{\psi} + \frac{\vec{\Omega}_0 \times (\vec{\Omega}_0 \times \vec{\psi})}{\lambda^2} + \frac{2\vec{\Omega}_0 \times \vec{\psi}}{\lambda} \right] \qquad (3.27)$$

$$B_n(\vec{\psi}) = \lambda \vec{\nabla} \cdot \vec{\psi} \cdot \vec{n} + 2\mu \vec{\nabla} \vec{\psi} \cdot \vec{n} + \tilde{\sigma}_0 \cdot \vec{\nabla} \vec{\psi} \cdot \vec{n} \qquad (3.28)$$

The boundary-value problem represented by Eqs. (3.24) and (3.25) is said to be self-adjoint if, for any two arbitrary comparison vectors

$\vec{K_1}$ and $\vec{K_2}$, the following identities are satisfied:

$$\iiint\limits_V \vec{K_2} \cdot \tilde{L}(\vec{K_1}) \, dV = \iiint \vec{K_1} \cdot \tilde{L}(\vec{K_2}) \, dV \qquad (3.29)$$

$$\iiint\limits_V \vec{K_2} \cdot \tilde{N}(\vec{K_1}) \, dV = \iiint \vec{K_1} \cdot \tilde{N}(\vec{K_2}) \, dV \qquad (3.30)$$

Since the tensor differential operator $\tilde{L}$ and the boundary conditions given by Eq. (3.25) constitute the Euler-Lagrangian equations and the natural boundary conditions for the variational problem of finding stationary values of a functional with a homogeneous quadratic integrand, it is self-adjoint according to Courant and Hilbert [3.2]. However, the linear tensor operator $\tilde{N}$ contains a nonsymmetric coriolis term. As a result of this, Eq. (3.30) is not satisfied. Thus, the boundary-value problem is not self-adjoint. It is concluded that the vibration modes are not orthogonal and cannot exist independently of each other. They merely represent the possible harmonic modes of vibration of a rotating body. Consequently, it is incorrect to speak of them as normal modes of vibration. As stated earlier, they must be referred to as vibration modes with rotation.

A direct analysis of the eigenvalues of a nonself-adjoint boundary-value problem is extremely difficult. The possibility of using approximate and numerical methods is considered. The most effective approximate method is to express the components of the displacement vector as a series in a system of coordinate functions (called also as characteristic functions or eigenfunctions) which satisfy all the boundary

conditions. Application of Galerkin's method, as described by Bis-
plinghoff and Ashley [3.3] and several others, reduces the problem to
one of solving a system of ordinary differential equations in the co-
efficients of the series.

Now, there is a physical argument behind the use of normal coor-
dinates in representing any distortions of the rotating body as the
sum of distortions in its principal modes of nonrotating body. Another
issue is the application of Galerkin's method in which convergence
is not conclusively proved, particularly to nonself-adjoint boundary-
value problems. These two issues are more involved, and hence we will
not go into the details. However, some discussion on these issues can
be found in Bishop [3.8] and Bolotin [3.4], respectively. Our rationale
to justify this approach is based on a comparison of exact results (if
not available, experimental results) with those obtained by Galerkin's
method. A problem, vibration of a rotating beam with a coning angle,
is solved both by Galerkin's method and by an exact method (in the
numerical sense), and the results are compared in the next chapter.

The solution of Eq. (3.19) will be sought in the form

$$\vec{q} = \sum_{n=1}^{\infty} \vec{\Phi}_n(x,y,z)\, \xi_n(t) \qquad\qquad (3.31)$$

where $\xi_n(t)$ are the functions of t to be determined, and $\vec{\Phi}_n(x,y,z)$
are the characteristic functions of the nonrotating body. Substituting

Eq. (3.31) into Eq. (3.19), we obtain the equations of Galerkin's method:

$$M_{nn} \ddot{\xi}_n + \left[(\omega_{NR})_n^2 - \Omega_o^2 \right] M_{nn} \xi_n + 2 \sum_{\substack{r=1 \\ (\text{Skip } r=n)}}^{\infty'} \dot{\xi}_r \vec{\Omega}_o \cdot \vec{m}_{rn}$$

$$- \sum_{r=1}^{\infty} \xi_r \vec{\Omega}_o \cdot \tilde{M}_{nr} \cdot \vec{\Omega}_o$$

$$+ \sum_{r=1}^{\infty} \xi_r \tilde{\sigma}_o : \vec{\nabla} \vec{\Phi}_r \cdot \vec{\nabla} \vec{\Phi}_n = 0 \qquad (3.32)$$

where

$$\left. \begin{aligned} M_{nr} &= \iiint_V (\vec{\Phi}_n \cdot \vec{\Phi}_r) \, \rho dV \\[2em] \vec{m}_{rn} &= \iiint_V (\vec{\Phi}_r \times \vec{\Phi}_n) \, \rho dV \end{aligned} \right\} \qquad (3.33)$$

$$(n = 1, 2, \ldots)$$

Comparing the above Eq. (3.32) with the corresponding one, Eq. (59) of Ref. 3.7, shows that they differ at two places. First, is the addition of the last term in Eq. (3.32), which is missing in Eq. (59) of Ref. 3.7, since potential energy due to centrifugal force was not considered. The other one is the sign before Ω_o^2 in Eq. (59), which should read as positive. Comparing Eq. (3.19) with the corresponding one, Eq. (8) of Ref. 3.1, reveals that the second term of Eq. (8)

should be a vector cross product $[2\vec{\Omega}_o \times \iiint_V (\delta \vec{q}/\partial t) \cdot \vec{p} \, \Delta m]$ instead of a dot product before the integral sign. Also, Milne replaced the gradient operator of the last term of Eq. (3.32) by its antisymmetric part, assuming that the effects of rotations of the elements of the body are larger than the strains.

3.3 STABILITY THEORY

Stability theory is a subject which is of importance in all branches of physics. Many questions concerning this theory are still unanswered. Some of the controversial issues are: the definition of stability, linearization of the equations, correlation between the problem to be studied and the methods of stability analysis to be used, the role of internal and external damping in gyroscopic systems, the use of normal modes of a nonrotating structure for the rotating one, and the effect of model truncation. A review of the entire theory is out of place in this section, the main purpose of which is to find correlations between the problems to be studied and the methods to be used in order to identify some common features of rapidly rotating, deformable bodies of engineering interest. However, extensive discussions can be found on the concepts of stability in Ziegler [3.9], Leipholz [3.10], Stoker [3.11], Bolotin [3.4], Hermann [3.12], Bryan [3.13], and Meirovitch [3.14] in addition to several others. In this section we shall focus our discussion on two main points: 1) choice of axis system, and 2) shortcomings of kinetic and static methods of stability as applied to gyroscopic systems.

Basically the available approaches to dynamic stability analysis are known as the Liapunov direct method or Liapunov's second method, the dynamic or vibration or kinetic method, and the static methods (imperfection, equilibrium and energy). The word dynamic stability encompasses all the stability problems analyzed with the aid of Newton's equations of motion or by any equivalent method. The idea behind Liapunov's approach is to answer the stability question by utilizing the differential equations of the system without solving them. The method involves devising a suitable scalar function known as the Liapunov function in the phase space or motion space and using this function along with the motion equations to test the system stability. This method is valid for both linear and nonlinear systems. The main problem with this method is the construction of the Liapunov function, which is not unique, and indeed there is a large degree of flexibility in its selection. In the early stages, its applicability was restricted to systems governed by ordinary differential equations. In recent years, however, this method was extended to elastic and aeroelastic systems governed by partial differential equations by Wang [3.15], and Parks [3.16], and to systems governed by hybrid (both ordinary and partial) equations by Meirovitch [3.17,3.18].

The kinetic instability approach involves an examination of the roots of the characteristic equation if the system is governed by ordinary differential equations [for instance, Eq. (3.32)]; and an examination of the eigenvalues of the boundary-value problem if the system is governed by partial differential equations [for example,

Eqs. (3.24) and (3.25)]. Also, damping forces, either viscous type or structural type, can be included in these equations as shown in our following examples. The eigenvalues may be real or complex.

According to Eq. (3.23), if μ is negative and $\omega \neq 0$, the motion is damped simple harmonic; if λ is entirely real and negative, the disturbed motion settles back to steady motion. In either case it is stable. If μ is positive with $\omega \neq 0$ or λ is entirely real and positive, the displacements increase exponentially with time. Hence, the motion is unstable. If $\lambda = 0$, the displacements linearly increase with time in the case of nongyroscopic systems, and a static divergence boundary is defined. This is the approach used by aeroelasticians, such as Bisplinghoff and Ashley [3.3], Fung [3.19], Garrick [3.20], Bolotin [3.4] and others. More recently, Herrman and Bungay [3.21] followed this usage for structural instability problems. When applied to nongyroscopic systems, the kinetic method is characterized by the question: What is the value of the load for which the general motion of the perfect system in the vicinity of equilibrium ceases to be bounded? This method supplies all the instabilities of the linear nongyroscopic system.

When this approach is used for problems with gyroscopic forces, such as the rapidly rotating and deformable body, under certain conditions, one should be careful with regard to the condition that some of the eigenvalues are zero. A typical example is a rotating concentrated mass on a symmetric massless shaft, when analyzed with respect to a body fixed rotating coordinate system. When $\lambda = 0$, the amplitudes are

bounded if the imperfections are not considered. Any sort of imperfec-
tions with respect to body fixed rotating coordinates leads to insta-
bility of forced vibration motion. When the same system is considered
in a space fixed coordinate system, there is no possibility for λ to
be zero, implying thereby, tentatively, no static divergence. However,
experiments indicate such kinds of instability do exist [Ref. 3.9].
This was again attributed to the presence of imperfections (mass un-
balance) and was explained through the familiar resonance phenomenon.
Thus, when this kinetic method is applied to gyroscopic systems, one
must include certain imperfections in the system. The detection of
these instabilities associated with the imperfections is relatively
easier in the rotating coordinate system, since they appear as $\lambda = 0$
and require additional efforts in the fixed system. It implies that it
is always better to use a body fixed rotating coordinate system to de-
scribe the motion. With respect to this rotating coordinate system the
kinetic method is characterized by the question: What is the value of
the load or angular velocity for which the most general motion of the
imperfect system in the vicinity of steady-state equilibrium ceases to
be bounded? Then, this method supplies all the instabilities of the
linear gyroscopic system. At times, the solution of the characteristic
equation may prove to be a formidable task, particularly for higher
order systems. In such cases the Routh-Hurwitz criterion for stability
[3.22] provides certain conditions on the coefficients of the charac-
teristic equation.

The classical static approaches are the deflections of the imperfection method, the nontrivial equilibrium method, and the potential energy method. In linear stability problems of conservative nongyroscopic systems, all the critical loads are supplied by all these methods. With the addition of gyroscopic forces, the equilibrium method and the imperfection method supply the first critical load or the angular speed and give no indication concerning other instabilities. Actually, there are cases where the equilibrium may be stable although the potential energy is not positive definite. This effect was studied by Thomson and Tait [3.23], who referred to it as stability due to gyroscopic forces. Further, adding a little internal damping of the viscous type causes a loss of stability due to gyroscopic forces. Again, the system was shown to be stabilized under certain conditions by introducing external damping (air friction in the case of an unconstrained body; or friction at the bearings in the case of a constrained body) by Ziegler [3.9] and Bolotin [3.4]. If the system is also subjected to circulatory (velocity independent) forces, the static methods cannot be used. All these cases clearly reveal that static stability methods have shortcomings, particularly as applied to gyroscopic systems. For the problems considered in this dissertation, we shall assume the system is linear and imperfect and use the kinetic method of stability analysis. Whenever a simpler analysis is available, its results will be added to those of the kinetic method.

3.4 DAMPING MODELS

As mentioned in Section 3.3, damping forces may be divided into
two categories in consideration of the questions associated with sta-
bility of the rapidly rotating systems. The first one includes forces
caused by frictional forces from the surrounding medium, which can be
considered stationary, and by contact of the rotating body with the
adjacent fixed components. The second category includes frictional
forces set up by the hysteresis in the material of the body, as well
as certain other forces resulting from the relative motion between ro-
tating parts (for example, the frictional force at the flapping hinge
of a helicopter rotor). Damping forces belonging to the first cate-
gory are called external damping forces and those of the second cate-
gory internal damping forces. The internal forces must be included in
a body fixed rotating coordinate system, and the external forces must
be included in an inertial coordinate system.

A precise mathematical model of damping characteristics is not
possible due to the complex nature of the mechanism. Consequently,
there are many models. The most common types are the linear viscous
damping and the hysteretic or structural damping. According to the
first model, the damping is represented by a force proportional in
magnitude to the velocity and acting in the direction of the velocity.
This is commonly used in vibration studies. Structural damping is
associated with internal energy dissipation due to a hysteresis effect
in cyclic stress. The energy dissipation for a cycle is assumed to be

proportional to the square of the amplitude and independent of the frequency. Thus, this model is valid only for harmonic motion. This damping produces a force proportional to the elastic restoring force and in phase with the velocity of oscillation. Aeroelasticians dealing with fixed wing flutter, Theoderson and Garrick [3.25], Bisplinghoff, Ashley and Halfman [3.26], Fung [3.19], and Scanlan and Rosenbaum [3.27] among several others, commonly employed this structural damping model. Whirl flutter specialists who considered only external damping, Houbolt and Reed [3.28], Reed and Bland [3.29], used both the models; Richardson, McKillip and Naylor [3.30], Young and Lytwyn [3.31] adapted a viscous model. So also Bolotin [3.4] used both the models while discussing shaft problems with both external and internal damping included. Confining our attention to the rotating systems, the message from the corresponding references is that damping in gyroscopic systems has a strong influence on stability, unlike in fixed wing flutter. The comparative study of Ref. 3.29 using both the models indicated that viscous damping is not as effective as structural damping in the prevention of instability. However, the overall effect of damping on the stability boundary does not depend on the damping model used except for a slight quantitative shift in the boundary. This shift was attributed to the assumption that the damping coefficients of these two models are related by equivalent energy dissipation criterion. According to Ref. 3.4, the relative effect of internal and external damping does not depend on the type of damping model used. So in the investigations of this dissertation the viscous damping model is chosen arbitrarily.

Up to now we have derived the equations of motion of a rotating body and discussed the concept of stability and damping. In the following sections we shall illustrate the need for nonlinear elasticity theory, the phenomenon of frequency splitting, the advantages of using a rotating coordinate system, the role of internal and external damping, and the use of the kinetic method of stability with imperfections, by considering simple examples involving rotation.

3.5 VIBRATION OF A ROTATING SHAFT

It is well known that there seems to be a very practical limit on the use of a continuum model to extract meaningful conclusions particularly in the presence of rapid rotation. However, to gain useful insight into rotational effects, some simple examples, though most of them are not new, are considered to accomplish our stated objectives. The first example is a heavy uniform shaft having equal flexural rigidities in the principal directions and mounted in rigid axially symmetric bearings. It rotates with a constant angular velocity Ω_o about the horizontal centerline of the bearings. Let us fix the origin o of the inertial coordinate system $x'y'z'$ with the x' axis parallel to the center line of the bearings. The coordinate system xyzo rotates with the shaft with a constant angular velocity Ω_o about ox'. This body is constrained, and hence only the elemental equilibrium Eq. (3.19) has to be considered. For this kind of body the mean axes and the principal axes coincide (see Ref. 3.32). We shall fix directions oy and oz parallel to the principal or mean

axes of the shaft and initially coincident with oy' and oz' . The mass and elastic centers of the cross sections are assumed to lie on the axis of the shaft. Let v and w be the components of deflection of the shaft parallel to the directions oy and oz , and v' and w' be the components parallel to oy' and oz' (see Fig. 3.1).

The equations of motion of this shaft can be formulated either in an inertial coordinate system or in a body fixed coordinate system. First, we shall formulate them in a body fixed rotating coordinate system, and then transform them into an inertial coordinate system.

For this shaft, we have the displacement vector

$$\vec{q} = v\vec{j} + w\vec{R} - \left(\zeta \frac{\partial w}{\partial x} + \eta \frac{\partial v}{\partial x} \right) \vec{i} \qquad (3.34)$$

$$\vec{\Omega}_o = \Omega_o \vec{i} \qquad (3.35)$$

Substituting Eqs. (3.34) and (3.35) into Eq. (3.19); using beam theory of bending; and neglecting rotary inertia, shear deformations, and gravitational forces, we obtain

$$m \left(\frac{\partial^2 v}{\partial t^2} - 2\Omega_o \frac{\partial w}{\partial t} - v\Omega_o^2 \right) + EI \frac{\partial^4 v}{\partial x^4} = 0 \qquad (3.36)$$

$$m \left(\frac{\partial^2 w}{\partial t^2} + 2 \frac{\partial v}{\partial t} \Omega_o - w\Omega_o^2 \right) + EI \frac{\partial^4 w}{\partial x^4} = 0 \qquad (3.37)$$
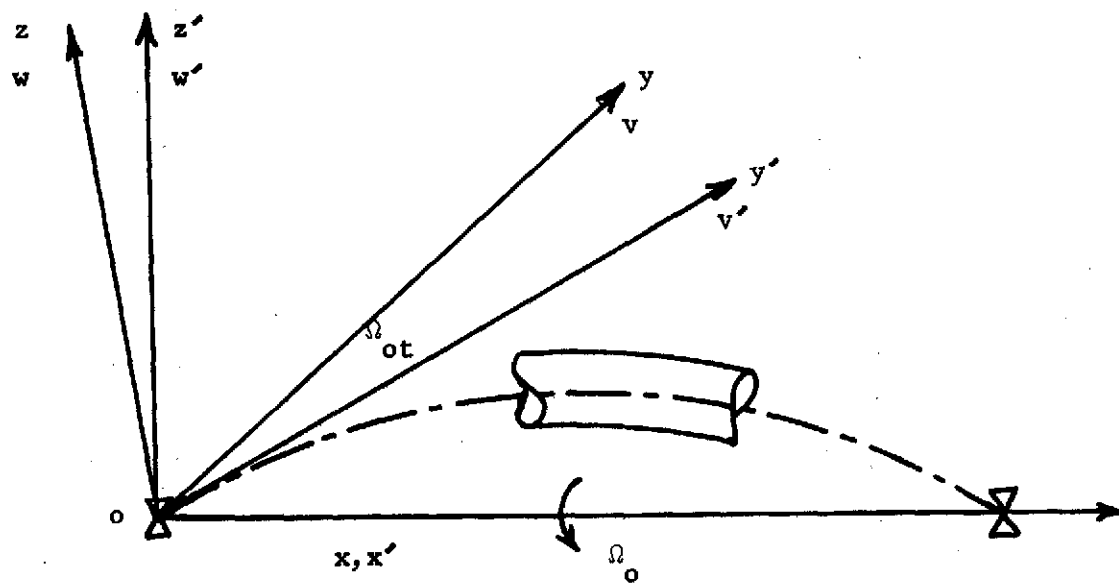
FIG. 3.1--Rotating elastic shaft.

and the following boundary conditions:

For a pinned-pinned shaft

$$v(0) \ = \ w(0) \ = \ EI \ \frac{\partial^2 v(0)}{\partial x^2} \ = \ EI \ \frac{\partial^2 w(0)}{\partial x^2} \ = \ 0$$

$$v(L) \ = \ w(L) \ = \ EI \ \frac{\partial^2 v(L)}{\partial x^2} \ = \ EI \ \frac{\partial^2 w(L)}{\partial x^2} \ = \ 0$$

For a pinned-free shaft

$$v(0) \ = \ w(0) \ = \ EI \ \frac{\partial^2 v(0)}{\partial x^2} \ = \ EI \ \frac{\partial^2 w(0)}{\partial x^2} \ = \ 0$$

$$EI \ \frac{\partial^2 v(L)}{\partial x^2} \ = \ EI \ \frac{\partial^2 w(L)}{\partial x^2} \ = \ EI \ \frac{\partial^3 v(L)}{\partial x^3} \ = \ EI \ \frac{\partial^3 w(L)}{\partial x^3} \ = \ 0$$

For a cantilever shaft

$$v(0) \ = \ w(0) \ = \ \frac{\partial v(0)}{\partial x} \ = \ \frac{\partial w(0)}{\partial x} \ = \ 0$$

$$EI \ \frac{\partial^2 v(L)}{\partial x^2} \ = \ EI \ \frac{\partial^2 w(L)}{\partial x^2} \ = \ EI \ \frac{\partial^3 v(L)}{\partial x^3} \ = \ EI \ \frac{\partial^3 w(L)}{\partial x^3} \ = \ 0$$

$$\left. \vphantom{\begin{array}{c} a \\ a \\ a \\ a \\ a \\ a \\ a \\ a \\ a \\ a \\ a \\ a \\ a \end{array}} \right\} \quad (3.38)$$

We can set $\eta = v + iw$ and write Eqs. (3.36)-(3.38) as

$$\frac{\partial^2 \eta}{\partial t^2} + (EI/m) \ \frac{\partial^4 \eta}{\partial x^4} - \Omega_o^2 \eta + 2i\Omega_o \ \frac{\partial \eta}{\partial t} \ = \ 0 \qquad (3.39)$$

- 40 -

and the boundary conditions become:

For a pinned-pinned shaft

$$\eta(0) \;=\; EI\,\frac{\partial^2 \eta(0)}{\partial x^2} \;=\; 0$$

$$\eta(L) \;=\; EI\,\frac{\partial^2 \eta(L)}{\partial x^2} \;=\; 0$$

For a pinned-free shaft

$$\eta(0) \;=\; EI\,\frac{\partial^2 \eta(0)}{\partial x^2} \;=\; 0$$

$$EI\,\frac{\partial^2 \eta(L)}{\partial x^2} \;=\; EI\,\frac{\partial^3 \eta(L)}{\partial x^3} \;=\; 0$$

For a cantilever shaft

$$\eta(0) \;=\; \frac{\partial \eta(0)}{\partial x} \;=\; 0$$

$$EI\,\frac{\partial^2 \eta(L)}{\partial x^2} \;=\; EI\,\frac{\partial^3 \eta(L)}{\partial x^3} \;=\; 0$$

$$\left.\vphantom{\begin{array}{c}1\\2\\3\\4\\5\\6\\7\\8\\9\end{array}}\right\} \quad (3.40)$$

Seeking a solution in the form

$$\eta(x,t) \;=\; \Phi(x)\,\xi(t) \qquad\qquad (3.41)$$

we obtain after some algebra

$$v(x,t) = \sum_{n=1}^{\infty} \Phi_n(x) \left\{ A_n \cos\left[(\omega_R)_{1n}t + \epsilon_{1n}\right] \right.$$
$$\left. + B_n \cos\left[(\omega_R)_{2n}t + \epsilon_{2n}\right] \right\} \tag{3.42}$$

$$w(x,t) = \sum_{n=1}^{\infty} \Phi_n(x) \left\{ A_n \cos\left[(\omega_R)_{1n}t + \epsilon_{1n} + \frac{\pi}{2}\right] \right.$$
$$\left. + B_n \cos\left[(\omega_R)_{2n}t + \epsilon_{2n} - \frac{\pi}{2}\right] \right\} \tag{3.43}$$

where

$$(\omega_R)_{1n} = \Omega_o + (\omega_{NR})_n$$
$$(\omega_R)_{2n} = -\Omega_o + (\omega_{NR})_n \tag{3.44}$$

and A_n , B_n , ϵ_{1n} and ϵ_{2n} are constants to be determined from initial conditions. The coordinate functions, $\Phi_n(x)$, and the non-rotating frequencies, $(\omega_{NR})_n$, depend on the type of boundary conditions, and they can be found in Ref. 3.24. Equations (3.44) are plotted for the first mode in Fig. 3.2(a). It shows that each non-rotating frequency, $(\omega_{NR})_n$, is split into two frequencies, $(\omega_R)_{1n}$ and $(\omega_R)_{2n}$. This phenomenon is referred to as frequency splitting in Ref. 3.6. In the mode with the frequency $(\omega_R)_{1n}$, a point on the shaft traces a path in a direction opposite to that of rotation, and

- 42 -
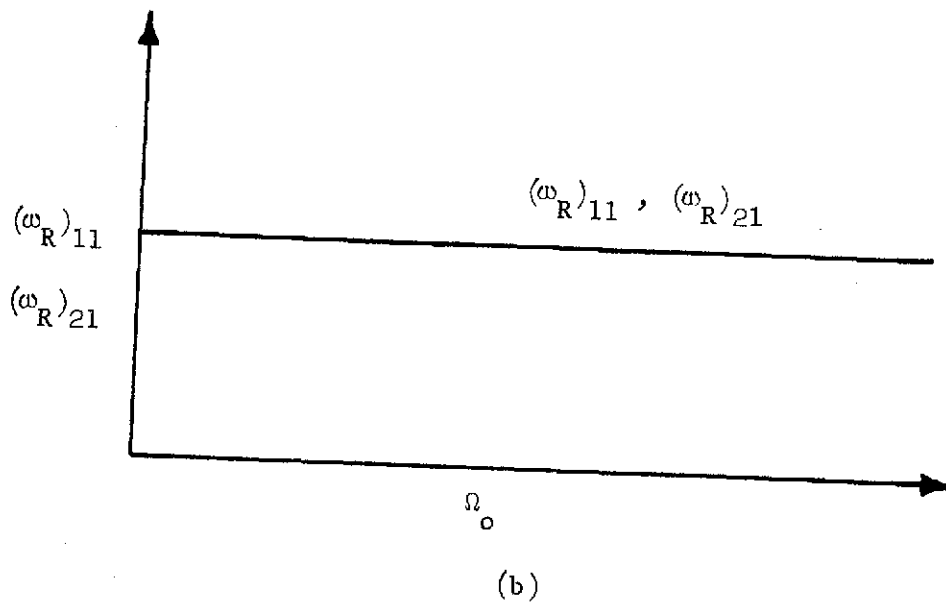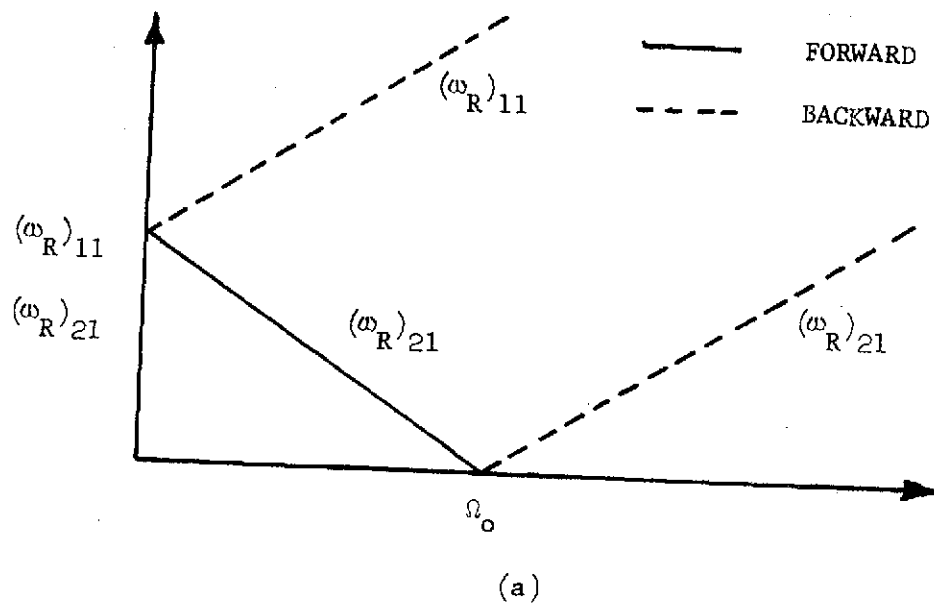
FIG. 3.2--Variation of frequencies with rotation of a symmetric shaft: (a) rotating observer, (b) inertial observer.

in the other mode the point moves in the same direction. The former is called backward whirl or precession and the latter forward whirl or precession. When $\Omega_o > (\omega_{NR})_n$, both the modes are backward; and when $\Omega_o = (\omega_{NR})_n$, Eqs. (3.42) and (3.43) show that the displacements v and w are bounded. Hence, the kinetic method of stability without imperfections fails to predict the practically observed instability at this condition. As stated earlier, we must introduce imperfections to extract all the instabilities of the gyroscopic system. These imperfections, such as initial lack of straightness, will lead to some constant terms on the right-hand sides of Eqs. (3.36) and (3.37). Then at $\Omega_o = (\omega_{NR})_n$ the steady forced motion is unbounded.

The same problem in inertial coordinates leads to

$$ m \frac{\partial^2 v'}{\partial t^2} + EI \frac{\partial^4 v'}{\partial x^4} = 0 \tag{3.45} $$

$$ m \frac{\partial^2 w'}{\partial t^2} + EI \frac{\partial^4 w'}{\partial x^4} = 0 \tag{3.46} $$

which are the same as those of a nonrotating shaft. The frequency is the same in any plane passing through the ox' axis, and the motion is independent of Ω_o . Here also, if the system is perfect, there is no possibility for instability. However, the presence of imperfections, like rotating unbalance mass, will lead to harmonic exciting force terms on the right-hand sides of Eqs. (3.45) and (3.46). Then the forced motion is unbounded at $\Omega_o = (\omega_{NR})_n$. This is the well known resonance phenomenon used to explain the critical speeds. The

frequencies of the shaft are unaffected by the rotation. For comparison, the variation of frequency in any plane passing through ox' with Ω_o is shown in Fig. 3.2(b). It is clear that there is no possibility for frequency splitting.

Now let us introduce both internal and external damping to the system. We assume that these damping coefficients are equal in all the planes passing through ox' . If mc_e is the external viscous damping, the damping forces in y and z directions are given by $mc_e(\partial v'/\partial t)$ and $mc_e(\partial w'/\partial t)$. Using the transformation between inertial and rotating coordinates

$$
\begin{bmatrix} \vec{j} \\ \vec{k} \end{bmatrix} = \begin{bmatrix} \cos \Omega_o t & \sin \Omega_o t \\ -\sin \Omega_o t & \cos \Omega_o t \end{bmatrix} \begin{bmatrix} \vec{j'} \\ \vec{k'} \end{bmatrix} \tag{3.47}
$$

the damping forces in the y and z directions are $mc_e(\frac{\partial v}{\partial t} - \Omega_o w)$ and $mc_e(\frac{\partial w}{\partial t} + \Omega_o v)$ respectively. If mc_i is the internal damping coefficient, $mc_i \frac{\partial v}{\partial t}$ and $mc_i \frac{\partial w}{\partial t}$ are the damping forces in the y and z directions. Adding these additional forces to Eqs. (3.36) and (3.37), we obtain

$$
\frac{\partial^2 v}{\partial t^2} - 2\Omega_o \frac{\partial w}{\partial t} - v\Omega_o^2 + c_i \frac{\partial v}{\partial t} + c_e \left(\frac{\partial v}{\partial t} - \Omega_o w \right)
$$

$$
+ (EI/m) \frac{\partial^4 v}{\partial x^4} = 0 \tag{3.48}
$$

and

$$\frac{\partial^2 w}{\partial t^2} + 2\Omega_o \frac{\partial v}{\partial t} - w\Omega_o^2 + c_i \frac{\partial w}{\partial t} + c_e \left(\frac{\partial w}{\partial t} + \Omega_o v \right)$$

$$+ (EI/m) \frac{\partial^4 w}{\partial x^4} = 0 \qquad (3.49)$$

To demonstrate the role of damping we shall seek a solution in the form

$$\left. \begin{aligned} v &= \sum_{n=1}^{\infty} p_n(t)\, \Phi_n(x) \\[2em] w &= \sum_{n=1}^{\infty} q_n(t)\, \Phi_n(x) \end{aligned} \right\} \qquad (3.50)$$

where the $\Phi_n(x)$ are the characteristic functions of the nonrotating shaft, and p_n and q_n are the functions to be determined. Substituting Eq. (3.50) into Eqs. (3.48) and (3.49), we obtain the following equations of Galerkin's method:

$$\frac{\partial^2 \xi_n}{\partial t^2} + \left[(\omega_{NR})_n^2 - \Omega_o^2 + c_e i\Omega_o \right] \xi_n$$

$$+ (c_i + c_e + 2i\Omega_o) \frac{\partial \xi_n}{\partial t} = 0 \qquad (3.51)$$

- 46 -

where $\xi_n = p_n + iq_n$. The solution of Eq. (3.51) is given by

$$
\xi_n = F e^{\left\{-\left(\frac{c_e + c_i}{2} + s_n\right)(\omega_{NR})_n - i\left[\Omega_o + (\omega_{NR})_n r_n\right] t\right\}}
$$

$$
+ G e^{\left\{-\left(\frac{c_e + c_i}{2} - s_n\right)(\omega_{NR})_n - i\left[\Omega_o - (\omega_{NR})_n r_n\right] t\right\}} \tag{3.52}
$$

where

$$
- r_n + is_n = \left\{1 - \frac{(c_i + c_e)^2}{4} - i\left[\Omega/(\omega_{NR})_n\right] c_i\right\}^{\frac{1}{2}} \tag{3.53}
$$

Here r_n and s_n are real constants, and F and G are complex constants.

The stability of the free motion can be studied by Routh's method, and it is shown in Ref. 3.4 (Page 158) that the condition for stability is

$$
\Omega_o < \left(1 + \frac{c_e}{c_i}\right)(\omega_{NR})_n \tag{3.54}
$$

The F term in Eq. (3.52) represents the backward mode, the path of which is an inward spiral. However, the G term represents an inward spiral motion until the condition of Eq. (3.54) is met, and an outward one if it is not. The direction of the spiral is forward if $\Omega_o < (\omega_{NR})_n$ and backward if $\Omega_o > (\omega_{NR})_n$. The same conclusions could be drawn if the analysis is made with respect to an inertial

coordinate system (see Ref. 3.9, Page 101). In both the coordinate systems we need to introduce imperfections to explain static instabilities. But, as said earlier, the job is relatively easier in the rotating coordinate system.

If the external damping is large compared to the internal damping, the shaft is stable for $\Omega_o > (\omega_{NR})_n$; whereas, if the internal damping is very large compared to the external damping, the shaft is unstable for $\Omega_o > (\omega_{NR})_n$. This indicates that the internal damping has a marked influence on stability in gyroscopic systems.

3.6 VIBRATION OF A ROTATING UNSYMMETRIC SHAFT

In this section we shall consider an unsymmetric uniform shaft mounted in rigid axially symmetric bearings. The lack of rotational symmetry leads to time dependent coefficients in the equations of motion if formulated in an inertial coordinate system. So, a body fixed rotating coordinate system is ideal for the analysis. However, the unsymmetry in stiffness precludes the use of complex variable technique. This problem was studied by Ariaratnam [3.33]. Without going into the details, the principal findings that are relevant to our study are summarized. The internal damping plays a key role in the stability of the shaft. There is no question of frequency splitting since the shaft is not symmetric. The kinetic method of stability predicts all the instabilities without considering any imperfections in the system, unlike the case of a symmetric shaft. Finally, there is no need for

nonlinear theory of elasticity, since the shaft does not experience any
steady-state equilibrium loads.

3.7 VIBRATION OF A ROTATING BEAM

When a deformable beam rotates about an axis perpendicular to its
own axis, it experiences equilibrium stresses in the steady-state con-
dition. A common approach to the derivation of the vibrational equa-
tions of motion is to treat the centrifugal loads at the steady-state
condition as an applied load. Consequently, the need for nonlinear
theory of elasticity was not mentioned in Refs. 3.24, 3.26, 3.34 and
3.35 among several others. Now, we shall derive these equations using
our general theory employing nonlinear elasticity and discuss vibration
and stability of this beam.

Let us assume that the beam is torsionally rigid without any ini-
tial pretwist. We shall fix the origin o of the inertial coordinate
system $x'y'z'$ at one end of the beam with x' along the axis of the
beam in the initial condition. This beam rotates with a constant angu-
lar velocity Ω_o about the z' axis. Initially, the x axis of the
beam-fixed rotating coordinate system xyzo coincides with the x'
axis. We shall fix the directions oy and oz parallel to the prin-
cipal or mean axes (both are coincident for this case). It is also
assumed that the mass center and the elastic axis lie on the axis of

the beam. Then, we have

$$\vec{r}_u = \vec{i}\,x + \vec{j}\,y + \vec{k}\,z$$

$$\vec{q} = -\vec{i}\left(\zeta\,\frac{\partial w}{\partial x} + \eta\,\frac{\partial v}{\partial x}\right) + \vec{j}\,v + \vec{k}\,w$$

$$\vec{\Omega}_o = \vec{k}\,\Omega$$

$$(3.55)$$

From Eq. (3.13) the equilibrium stress field is given by

$$(\sigma_o)_{xx}\,\vec{i}\,\vec{i} = \frac{1}{A(x)}\int_L^x m(x)\,\Omega_o^2\,dx\,\vec{i}\,\vec{i} \qquad (3.56)$$

where $A(x)$ is the cross-sectional area of the beam. Substitution of Eqs. (3.55) and (3.56) into Eq. (3.19) and routine execution of the integrals after neglecting shear deformations, rotary inertia terms and gravitational terms produces the equations of motion for flapwise and chordwise vibrations as

$$\frac{\partial}{\partial x^2}\left(EI_{yy}\,\frac{\partial^2 w}{\partial x^2}\right) - \Omega_o^2\,\frac{\partial}{\partial x}\left(T\,\frac{\partial w}{\partial x}\right) + m\,\frac{\partial^2 w}{\partial t^2} = 0 \qquad (3.57)$$

$$\frac{\partial^2}{\partial x^2}\left(EI_{zz}\,\frac{\partial^2 v}{\partial x^2}\right) - \Omega_o^2\,\frac{\partial}{\partial x}\left(T\,\frac{\partial v}{\partial x}\right) + m\left(\frac{\partial^2 v}{\partial t^2} - v\Omega_o^2\right) = 0 \quad (3.58)$$

and the boundary conditions become:

For a pinned-free beam

$$v(0) = w(0) = EI_{zz}\frac{\partial^2 v(0)}{\partial x^2} = EI_{yy}\frac{\partial^2 w(0)}{\partial x^2} = 0$$

$$EI_{zz}\frac{\partial^2 v(L)}{\partial x^2} = EI_{yy}\frac{\partial^2 w(L)}{\partial x^2} = EI_{zz}\frac{\partial^3 v(L)}{\partial x^3}$$

$$= EI_{yy}\frac{\partial^3 w(L)}{\partial x^3} = 0$$

$$(3.59)$$

For a cantilever beam

$$v(0) = w(0) = \frac{\partial v(0)}{\partial x} = \frac{\partial w(0)}{\partial x} = 0$$

$$EI_{zz}\frac{\partial^2 v(L)}{\partial x^2} = EI_{yy}\frac{\partial^2 w(L)}{\partial x^2} = EI_{zz}\frac{\partial^3 v(L)}{\partial x^3}$$

$$= EI_{yy}\frac{\partial^3 w(L)}{\partial x^3} = 0$$

$$(3.60)$$

where

$$T = \int_x^L m(x)\, x dx \qquad (3.61)$$

EI_{yy} and EI_{zz} are the flexural rigidities of the beam in two principal planes; m is the mass per unit length; and L is the length of the beam. The Eqs. (3.57)-(3.61) are self-adjoint and they are uncoupled. Consequently, we can find normal coordinates in each principal

plane. No coriolis forces are present, and hence the problem is non-gyroscopic. The centrifugal inertia forces enter only in the equation representing vibration in the oxy plane. As a result, the frequencies with rotation in two principal planes, even for a symmetric circular beam, differ, being higher in the flapping plane ozx and lower in the edgewise plane oxy . This can be interpreted as frequency splitting due to centrifugal inertia forces, if the beam is symmetric. However, there is no possibility for instability of this elastic beam. But, when rigid body motions $[v = xp(t)$, $w = xq(t)]$ for a pinned-free beam are considered, from Eqs. (3.57) and (3.58) it is seen that the frequencies with rotation are $(\omega_R)_w = \Omega_o$ and $(\omega_R)_v = 0$, which clearly indicates that the beam is statically unstable in the chordwise direction. Loosely, this instability is analogous to that of the symmetric shaft when $\Omega_o = (\omega_R)_n$. It can be seen that the kinetic method of stability without imperfections can predict the present instability because the system in nongyroscopic. Though the system of Eqs. (3.57)-(3.61) is self-adjoint, no exact solutions are possible, even for a uniform symmetric beam. However, approximate solutions by Galerkin and Raleigh-Ritz methods are given in Ref. 3.34 and 3.36. Numerically, exact solutions will be given in Chapter IV for a cantilever beam.

3.8   VIBRATION AND STABILITY OF A ROTATING BEAM WITH CONING ANGLE

The problems discussed in Sections 3.5 - 3.6 turn out to be special cases of a broader problem, whose analysis throws more light on both of them and elucidates the nature of the coupling in such systems

generally. This model, as shown in Fig. 3.3, consists of a slender beam capable of bending in two planes perpendicular to its neutral axis and spinning about an inertial fixed z' axis, which makes an arbitrary angle $\left(\frac{\pi}{2} - \beta_o\right)$ with the axis of the beam. β_o is called the coning angle of the beam. Due to this angle, there enter coriolis, centrifugal and steady-state equilibrium forces into the equations of vibration. From the academic point of view, this problem gives an opportunity to study the effect of all these forces on vibration and stability; and from the practical point of view, these results can be profitably used for a better understanding of whirl flutter in proprotors, wherein the blades of certain rotors have built-in precone in order to reduce the out-of-plane bending moments and feathering bearing loads.

Referring to Fig. 3.3, we have

$$\vec{q} = \vec{i} \left(- \eta \frac{\partial v}{\partial x} - \zeta \frac{\partial w}{\partial x} \right) + \vec{j} \, v + \vec{k} \, w \qquad (3.62)$$

$$\vec{\Omega}_o = \vec{i} \, \Omega_o \, \sin \beta_o + \vec{k} \, \Omega_o \, \cos \beta_o \qquad (3.63)$$

$$\tilde{\sigma}_o = [1/A(x)] \int_o^L \Omega_o^2 \, \cos^2 \beta_o \, m(x) \, dx \, \vec{i} \, \vec{i} \qquad (3.64)$$

where $A(x)$ is the area of cross section of the beam. We have neglected longitudinal deformation in addition to shear deformations. Substituting Eqs. (3.62)-(3.63) into Eq. (3.19), after neglecting rotary inertia and assuming that the rotations are larger than the
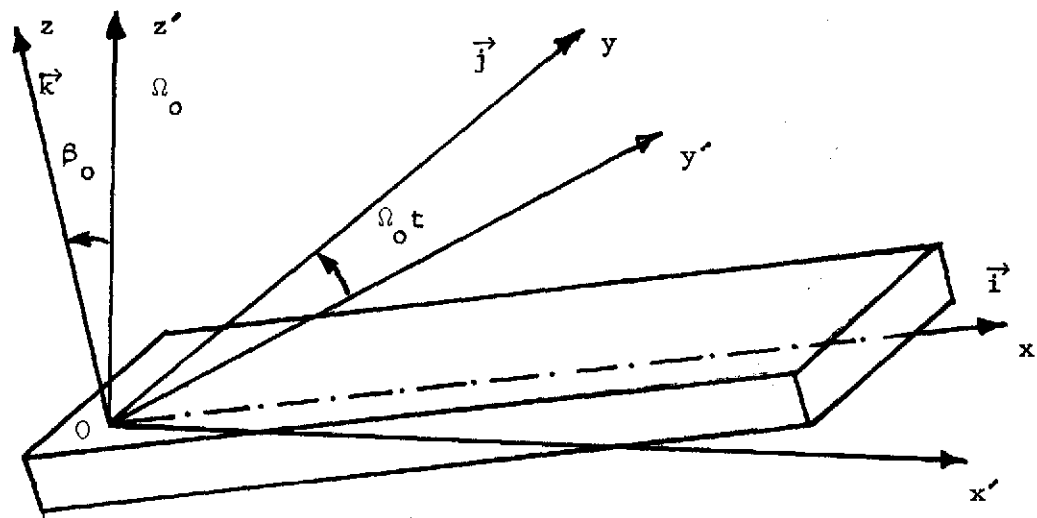
FIG. 3.3--Rotating beam inclined at an arbitrary
angle with the axis of rotation.

strains, we obtain the following:

$$m \left(\frac{\partial^2 v}{\partial t^2} - 2 \frac{\partial w}{\partial t} \Omega_o \sin \beta_o - v \Omega_o^2 \right) - \Omega_o^2 \cos^2 \beta_o \left[T(x) \frac{\partial v}{\partial x} \right]$$

$$+ \frac{\partial^2}{\partial x^2} \left(EI_{zz} \frac{\partial^2 v}{\partial x^2} \right) = 0 \qquad (3.65)$$

$$m \left(\frac{\partial^2 w}{\partial t^2} + 2 \frac{\partial v}{\partial t} \Omega_o \sin \beta_o - w \Omega_o^2 \sin^2 \beta_o \right)$$

$$- \Omega_o^2 \cos^2 \beta_o \frac{\partial}{\partial x} \left[T(x) \frac{\partial v}{\partial x} \right] + \frac{\partial^2}{\partial x^2} \left(EI_{yy} \frac{\partial^2 w}{\partial x^2} \right)$$

$$= - x \Omega_o^2 m \sin \beta_o \cos \beta_o \qquad (3.66)$$

where

$$T(x) = \int_x^L m(x) \, x dx \qquad (3.67)$$

The boundary conditions for a pinned-free and a cantilever beam are given by Eqs. (3.59) and (3.60), respectively.

The above Eqs. (3.65) and (3.66) and the appropriate boundary conditions can also be obtained by equilibrium considerations for an element of the beam considering the equilibrium centrifugal load as an applied one. The present method explicitly demonstrates the need for nonlinear theory of elasticity when the system is subjected to

equilibrium steady-state loads. Now, one can safely conclude that any general theory of vibration of a rotating deformable body must include nonlinear theory of elasticity. In some simple cases, for example, in the case of a rotating shaft, the terms associated with the nonlinear theory may be dropped, since it experiences no steady-state centrifugal loads. The right-hand side in Eq. (3.66) is constant, and hence for the study of vibration this can be dropped. An exact solution of these equations in closed form appears to be not possible. However, we shall concentrate on approximate solutions in this section and shall present a numerical solution in Chapter IV.

First, we shall show that the approximate frequencies of a uniform coned beam with rotation can be deduced from the information on approximate frequencies of the same beam without coning presented in Ref. 3.34. Second, the stability of the uniform symmetric coned beam for a range of values of β_o and Ω_o will be discussed. We assume a solution of Eqs. (3.65), (3.66), (3.59), and (3.60) of the form

$$v = \sum_{n=1}^{\infty} \Phi_n(x) \, p_n(t) \tag{3.68}$$

$$w = \sum_{n=1}^{\infty} \Phi_n(x) \, q_n(t) \tag{3.69}$$

where $\Phi_n(x)$ are the characteristic functions of the self-adjoint boundary-value problem

$$EI_{zz} \frac{\partial^4 \Phi_n}{\partial x^4} - \frac{\partial}{\partial x} \left(T \frac{\partial \Phi_n}{\partial x} \right) \Omega_o^2 \cos^2 \beta_o - m \, (\omega_{R\eta})_n^2 \, \Phi_n = 0 \tag{3.70}$$

and the boundary conditions become:

For a pinned-free beam

$$\Phi_n(0) \; = \; \frac{\partial^2 \Phi_n(0)}{\partial x^2} \; = \; 0$$

$$\frac{\partial^2 \Phi_n(L)}{\partial x^2} \; = \; \frac{\partial^3 \Phi_n(L)}{\partial x^3} \; = \; 0$$

For a cantilever beam   (3.71)

$$\Phi_n(0) \; = \; \frac{\partial \Phi_n(0)}{\partial x} \; = \; 0$$

$$\frac{\partial^2 \Phi_n(L)}{\partial x^2} \; = \; \frac{\partial^3 \Phi_n(L)}{\partial x^3} \; = \; 0$$

We then obtain

$$\ddot{p}_n - 2\dot{q}_n \Omega_0 \sin \beta_0 + \left[(\omega_{R\eta})_n^2 - \Omega_0^2 \cos^2 \beta_0 - \Omega_0^2 \sin^2 \beta_0 \right] p_n = 0$$

$$\ddot{q}_n + 2\dot{p}_n \Omega_0 \sin \beta_0 + \left[(\omega_{R\zeta})_n^2 - \Omega_0^2 \sin^2 \beta_0 \right] q_n \; = \; 0 \qquad (3.72)$$

where the $(\omega_{R\zeta})_n$ are the frequencies of the corresponding boundary-value problems (3.70) and (3.71) with EI_{yy} distribution instead of EI_{zz}. Though the frequencies are different, the characteristic functions are the same. The values $(\omega_{R\eta})_n$ and $(\omega_{R\zeta})_n$, which are equal

- 57 -

if the beam is symmetric, can be obtained from the charts of Ref. 3.34 just by considering the rotation as $\Omega_o \cos \beta_o$ instead of Ω_o . It can be seen from Eqs. (3.72) that, even for a symmetric beam, we cannot use the complex variable technique to solve the equations as in Section 3.5. Seeking a solution of the form

$$p_n = P\, e^{\lambda t}$$

$$q_n = Q\, e^{\lambda t} \tag{3.73}$$

where λ , P , Q are constants, we find that the exponent λ is given by the characteristic equation

$$\lambda^4 + \left[(\omega_{R\eta})_n^2 + (\omega_{R\zeta})_n^2 - \Omega_o^2 + 3\Omega_o^2 \sin^2 \beta_o \right] \lambda^2$$

$$+ \left[(\omega_{R\eta})_n^2 - \Omega_o^2 \right] \left[(\omega_{R\zeta})_n^2 - \Omega_o^2 \sin^2 \beta_o \right] = 0 \tag{3.74}$$

which leads to

$$(\lambda_{1n})^2 , \; (\lambda_{2n})^2 = -\frac{1}{2} \left[(\omega_{R\eta})_n^2 + (\omega_{R\zeta})_n^2 - \Omega_o^2 \cos^2 \beta_o + 2\Omega_o^2 \sin^2 \beta_o \right]$$

$$\pm \left\{ \Omega_o^2 \sin^2 \beta_o \left[(\omega_{R\eta})_n^2 - \Omega_o^2 \cos^2 \beta_o + (\omega_{R\zeta})_n^2 \right] \right.$$

$$\left. + \frac{1}{4} \left[(\omega_{R\eta})_n^2 - (\omega_{R\zeta})_n^2 - \Omega_o^2 \cos^2 \beta_o \right]^2 \right\}^{\frac{1}{2}} \tag{3.75}$$

The general solution is bounded if $(\lambda_{1n})^2$, $(\lambda_{2n})^2$ are both negative. This condition is satisfied when $\Omega_o \sin \beta_o$ lies outside the intervals

$$\left[(\omega_{R\eta})^2_n - \Omega^2_o \cos^2 \beta_o\right] \leq \Omega^2_o \sin^2 \beta_o \leq (\omega_{R\zeta})^2_n \qquad (3.76)$$

This inequality imposes certain restrictions on Ω_o and β_o for stability to prevail. Let $(\beta_o)_{vn}$ be the minimum value of β_o for which $[(\omega_{R\eta})^2_n - \Omega^2_o \cos \beta_o] = \Omega^2_o \sin^2 \beta_o$, and the corresponding value of Ω_o be $(\Omega_o)_{vn}$, and let $(\beta_o)_{wn}$ and $(\Omega_o)_{wn}$ be the corresponding values at which $(\omega_{R\zeta})^2_n = \Omega^2_o \sin^2 \beta_o$. To illustrate the stability we consider a uniform symmetric beam and also divide the interval 0 to $\pi/2$ of β_o into several subintervals. Further we assume the beam is such that $(\beta_o)_{v1} < (\beta_o)_{v2} < (\beta_o)_{v3} < \dots$, and $(\Omega_o)_{v1} < (\Omega_o)_{v2} < \dots$, with the same inequalities assumed valid for $(\beta_o)_{wn}$ and $(\Omega_o)_{wn}$. The first subinterval of β_o is $0 \leq \beta_o < (\beta_o)_{v1}$. In this interval both $[(\omega_{R\eta})^2_n - \Omega^2_o \cos^2 \beta_o]$ and $(\omega_{R\zeta})^2_n$ are greater than $\Omega^2_o \sin^2 \beta_o$, and hence the beam is stable for all the values of Ω_o . At $\beta_o = (\beta_o)_{v1}$, and $\Omega_o = (\Omega_o)_{v1}$ the eigenvalue $\lambda = 0$ is a double root of Eq. (3.74). This corresponds to a solution of the form

$$p_1 = P_1 + P_2 t$$

$$q_1 = Q_1 \qquad (3.77)$$

which shows p_1 is unbounded. With $(\beta_o)_{v1}$ constant and $\Omega_o > (\Omega_o)_{v1}$,
the value of $\Omega_o \sin \beta_o$ lies inside the interval given by Eq. (3.76),
and hence the beam is unstable. This is illustrated in Fig. 3.4(a).

In the second subinterval $(\beta_o)_{v1} < \beta_o < (\beta_o)_{w1}$, an increase in
β_o from $(\beta_o)_{v1}$ reduces the angular velocity Ω_o at which instability
sets in first and the bandwidth of instability continues to be infinity
until $\beta_o = (\beta_o)_{w1}$ and $\Omega_o = (\Omega_o)_{w1}$ at which point the solution is

$$p_1 = P_1$$

$$q_1 = Q_1 + Q_2 t \qquad (3.78)$$

It shows q_1 is unbounded. With further increase in Ω_o and
$\beta_o = (\beta_o)_{w1}$, the value of $\Omega_o \sin \beta_o$ lies outside the interval,
Eq. (3.76), and hence the beam is stable. Thus, for $\beta_o = (\beta_o)_{w1}$
the infinite bandwidth of instability of the mode begins to change
to a finite one. The variations of frequencies of the first two modes
with Ω_o for this range of β_o are shown in Fig. 3.4(b).

Next, subinterval $(\beta_o)_{w1} < \beta_o < (\beta_o)_{v2}$ is considered. For each
β_o, there are two values of Ω_o: namely, $(\Omega_o)_{11}$ and $(\Omega_o)_{21}$
between which the shaft is unstable. The range between $(\Omega_o)_{11}$ and
$(\Omega_o)_{21}$ is called the bandwidth of instability of the first mode. An
increase in β_o reduces the bandwidth of instability of the first mode
and the beam is stable for all speeds $\Omega_o > (\Omega_o)_{21}$. When $\beta_o = (\beta_o)_{v2}$
and $(\Omega_o)_{w1} < (\Omega_o)_{v2}$, the beam is again unstable statically at
$\Omega_o = (\Omega_o)_{v2}$. Thus, the beam has finite bandwidth of instability in

$0 \leq \beta_o < (\beta_o)_{v1}$

$(\omega_R)_{12}$

$(\omega_R)_{22}$

$(\omega_R)_{11}$

$(\omega_R)_{1n}$

$(\omega_R)_{2n}$

$(\omega_R)_{21}$

$(\beta_o)_{v1} < \beta_o < (\beta_o)_{w1}$

$(\omega_R)_{12}$

$(\omega_R)_{22}$

$(\omega_R)_{11}$

$(\omega_R)_{1n}$

$(\omega_R)_{2n}$

$(\omega_R)_{21}$

UNSTABLE

$\beta_o = (\beta_o)_{v1}$

$(\omega_R)_{12}$

$(\omega_R)_{22}$

$(\omega_R)_{11}$

$(\omega_R)_{1n}$

$(\omega_R)_{2n}$

$(\omega_R)_{21}$

UNSTABLE

$(\Omega_o)_{v1}$

Ω_o

(a)

$\beta_o = (\beta_o)_{w1}$

$(\omega_R)_{12}$

$(\omega_R)_{22}$

$(\omega_R)_{1n}$

$(\omega_R)_{2n}$

$(\omega_R)_{11}$

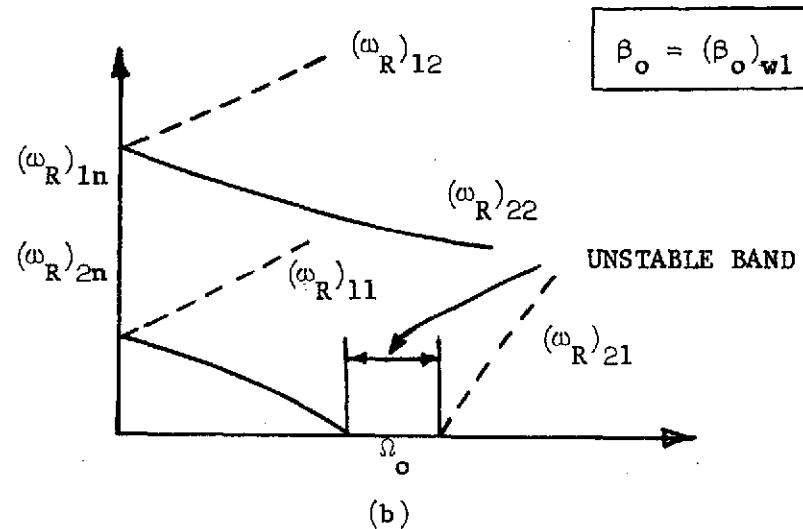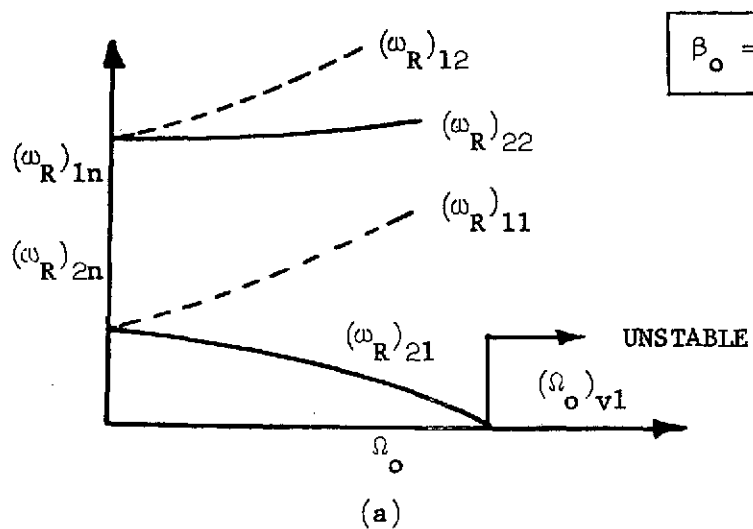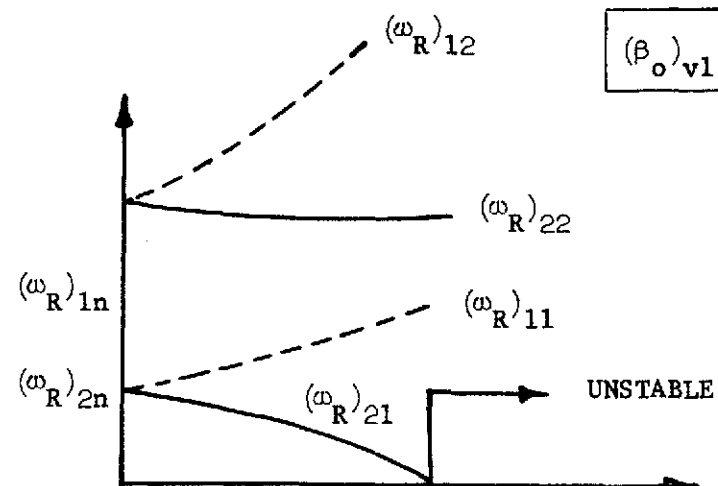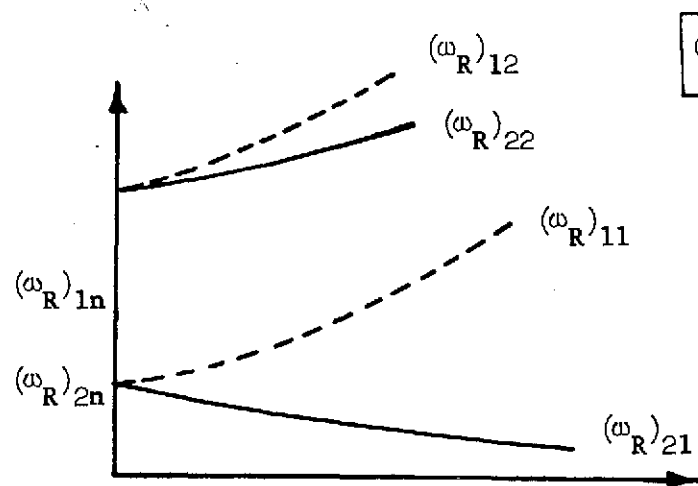UNSTABLE BAND

$(\omega_R)_{21}$

Ω_o

(b)

FIG. 3.4--Vibration frequencies with rotation of a uniform symmetric
beam at different values of β_o .

the first mode and an infinite one in the second mode, as shown in Fig. 4.3(c).

In the fourth subinterval $(\beta_o)_{v2} < \beta_o < (\beta_o)_{w2}$, the first mode has a finite bandwidth of instability, whereas the second mode has an infinite bandwidth until $\beta_o = (\beta_o)_{w2}$ at which the infinite bandwidth of the second mode begins to change to a finite one. At this point for any $\Omega_o > (\Omega_o)_{w2}$ the beam is stable. This process repeats as we increase β_o . Eventually, at a given β_o and for all values of $n_o > n$, where n_o is the value of n for which $(\Omega_o)_{1n_o+1} \leq (\Omega_o)_{2n_o}$, these bandwidths of instability overlap ones immediately preceding them, and hence for all the speeds $\Omega_o \geq (\Omega_o)_{1n_o}$ the beam is unstable. This is shown in Fig. 3.4(e).

Finally, when $\beta_o = \pi/2$, these bandwidths shrink to points whenever $\Omega_o = (\omega_{NR})_n$, $(n = 1 , 2 , \dots)$, which is the familiar shaft problem. As pointed out earlier, the amplitudes p_n and q_n are bounded if imperfections are ignored. This case is shown in Fig. 3.4(f).

The next problem is to define the symmetric beam model by considering rotary inertia and shear deformations. This problem with $\beta_o = 0$ was studied by Pederson (Ref. 3.37), who also introduced both internal and external damping, and anisotropic elastic restraints at the bearings. Here, there is no need for nonlinear theory of elasticity, since the equilibrium stresses are absent. A space fixed coordinate system was used because of the anisotropic bearings. Therefore, the instabilities of the system were brought out through the resonance phenomenon by considering imperfections. Instead of going through all the
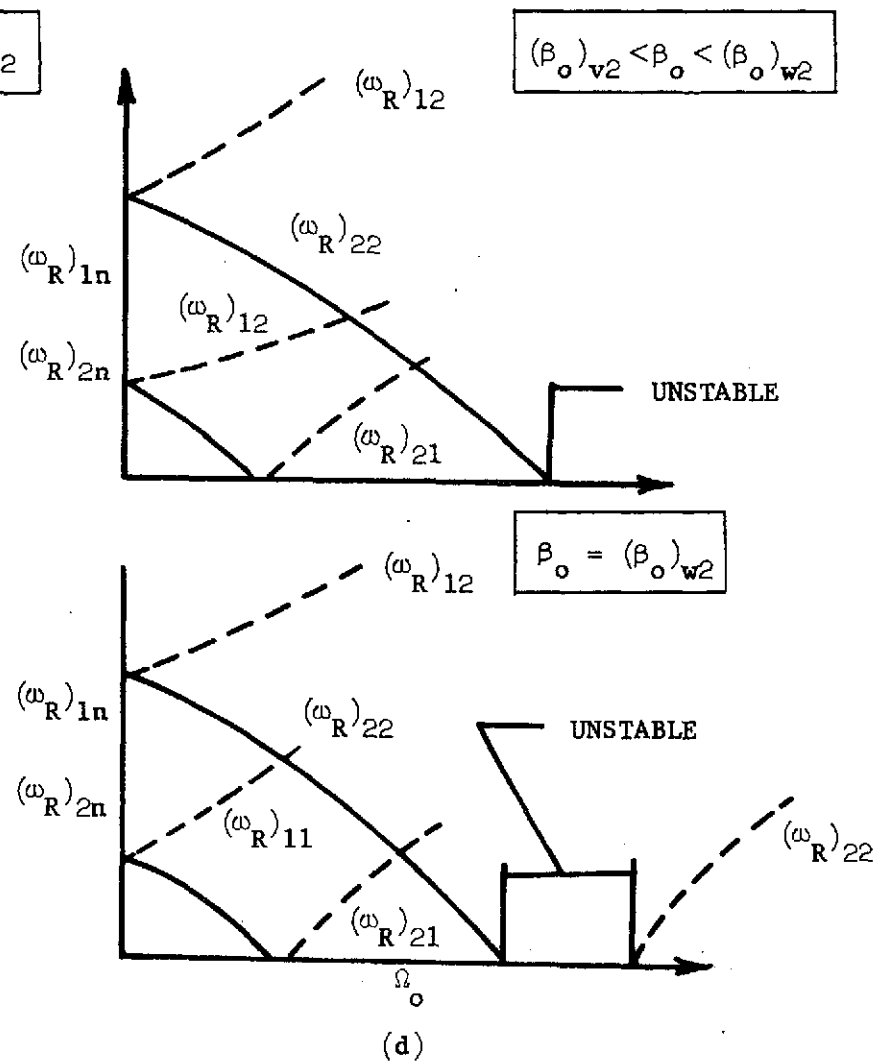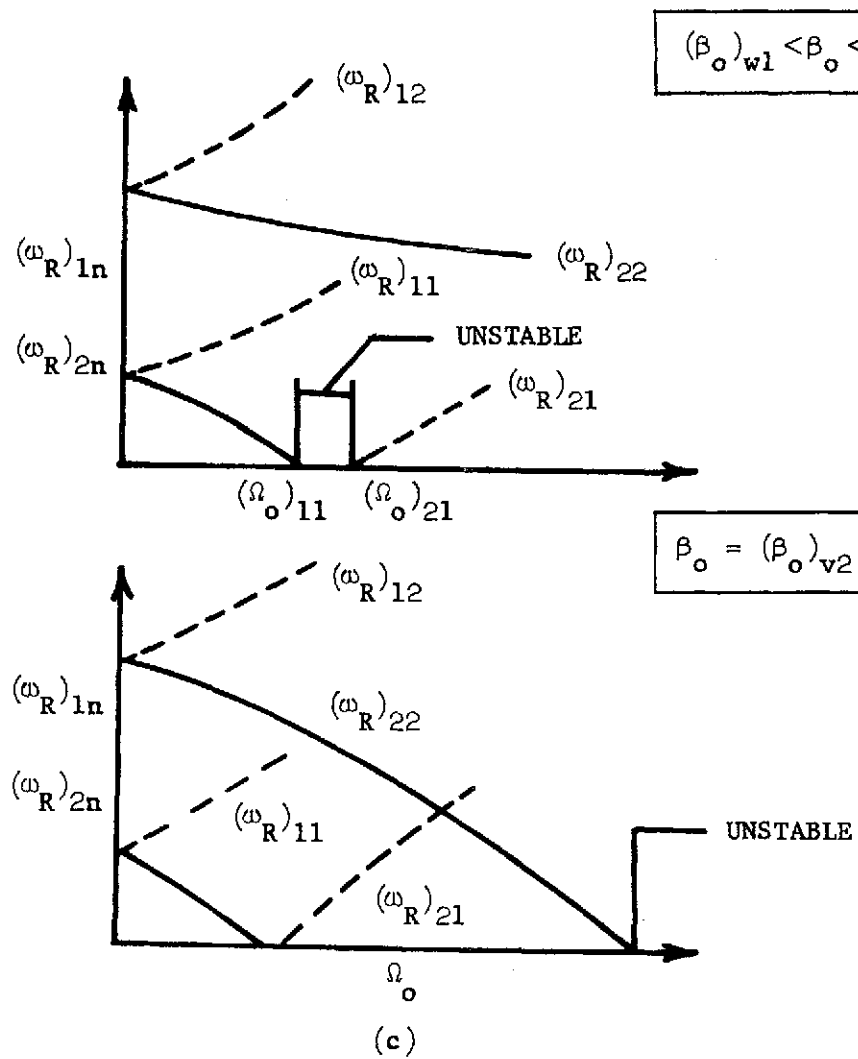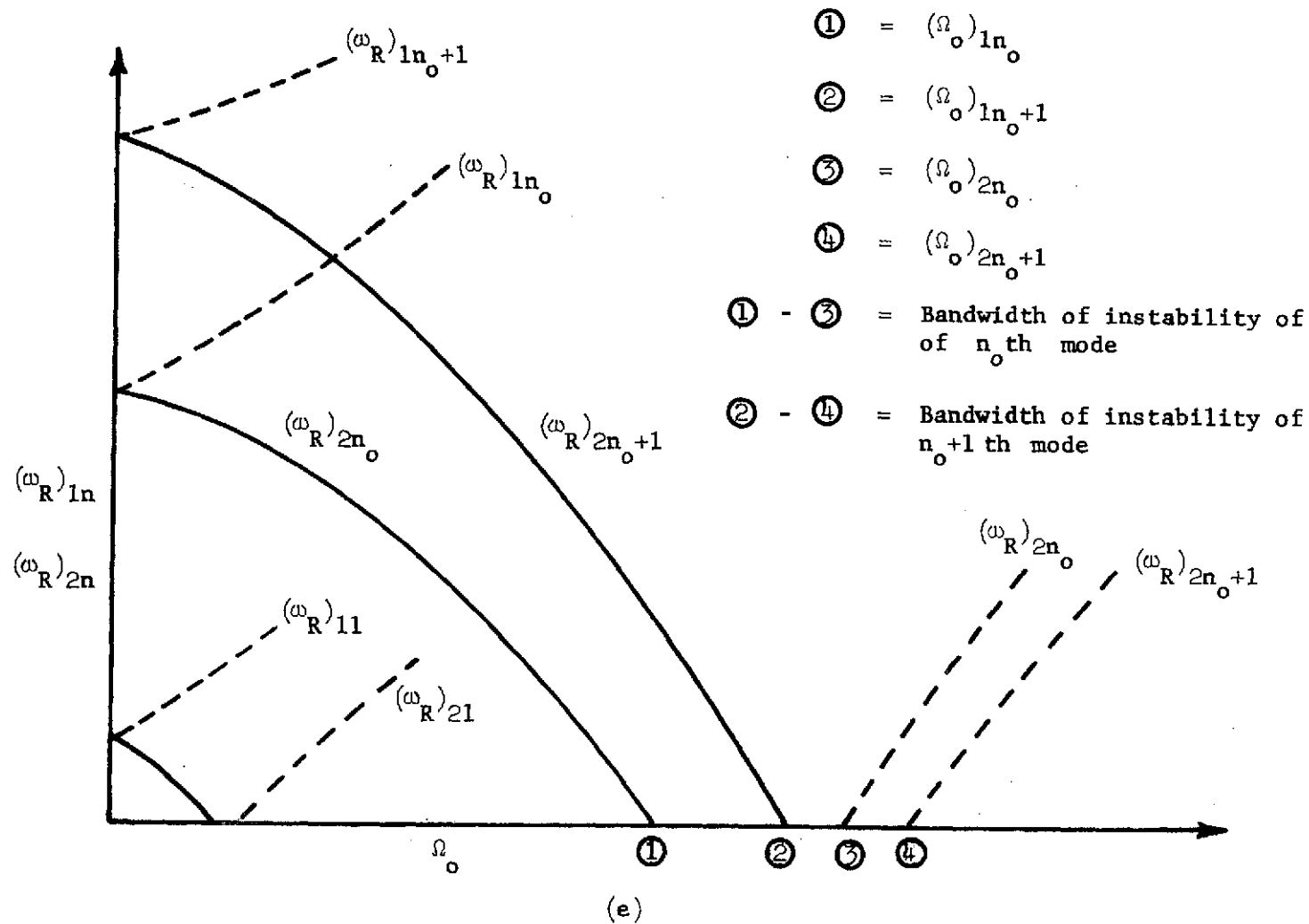
- 62 -

FIG. 3.4--Continued.

FIG. 3.4--Continued.

$$\beta_o = \frac{\pi}{2}$$

(f)
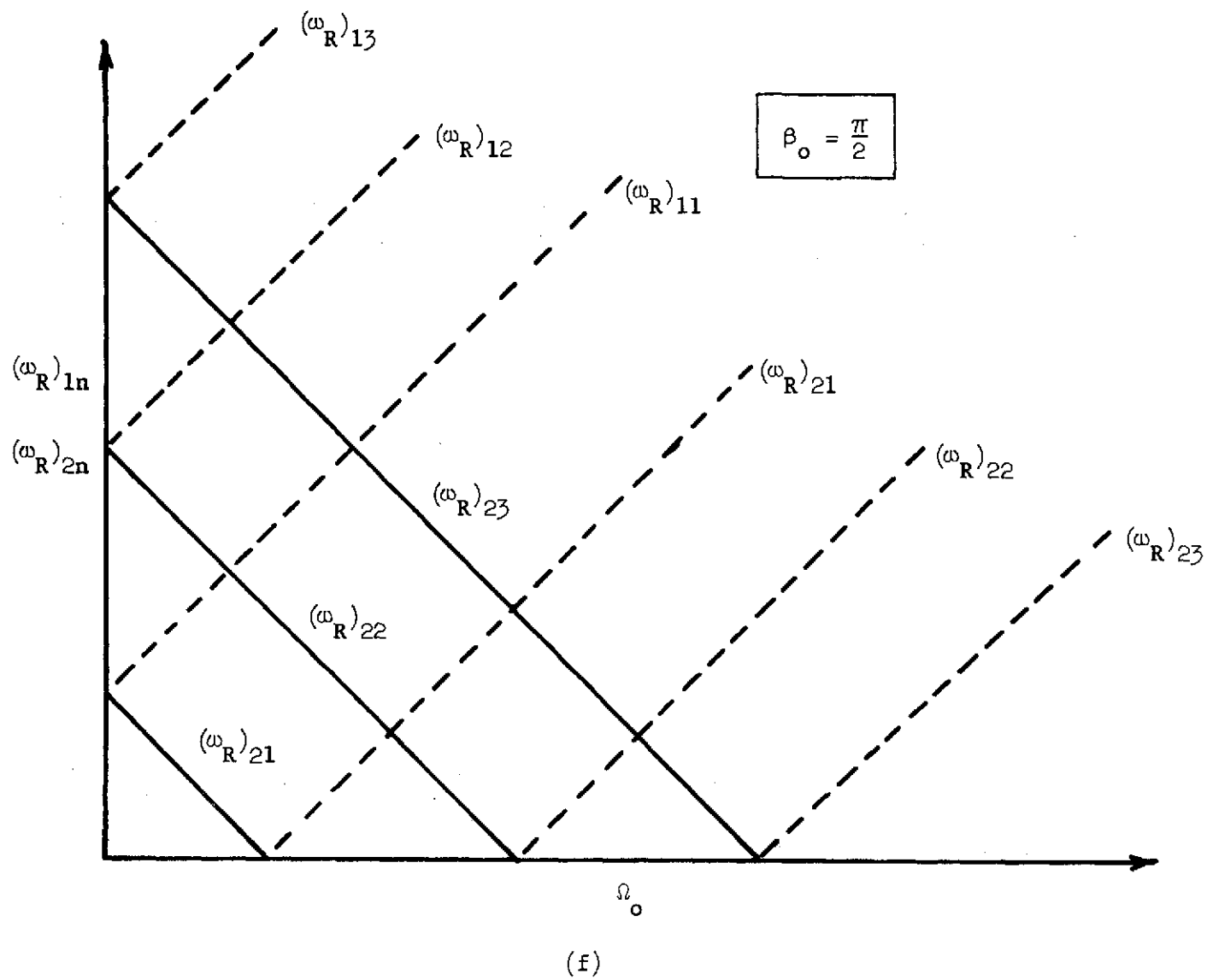
FIG. 3.4--Concluded.

details, we shall summarize the principal findings that are relevant to our study.

When rotation speed Ω_0 is zero, the system frequencies can be divided into two groups. One corresponds to the slender beam group, and the other to the rotor group. These two groups are coupled even in the absence of rotation. Therefore, the system has an infinite number of frequencies. When this symmetric shaft with isotropic bearing restraint is spun at a speed Ω_0, each frequency is split into two frequencies; the higher one with respect to inertial observer is called forward whirl; and the lower one, backward whirl. Thus, at any speed Ω_0, there are an infinite number of forward and an infinite number of backward frequencies. So, the frequency splitting takes place even when the system is studied with respect to an inertial coordinate system. This splitting is due to gyroscopic moments. If the imperfections are ignored, the system is stable at all speeds which is a typical characteristic of gyroscopic systems under certain conditions.

When forced vibration of the shaft due to static unbalance was considered through modal analysis, it was shown that if the bearings of the rotor have anisotropy, the amplitudes of both forward and backward whirl modes are unbounded. Another interesting observation is the role of both internal and external damping. With the introduction of these dampings (internal/external = 0.2), the amplitudes of the backward whirl modes are reduced more than those corresponding to forward whirl modes. However, for the isometric bearing case the amplitudes of the backward whirl modes are always bounded both with and without damping.

3.9 OTHER RELATED EXAMPLES

The other problems of interest with a continuum mathematical model are the transverse vibrations of a spinning circular disk, Refs. 3.38 and 3.39; in plane vibrations of a thin uniform spinning ring, Refs. 3.40 and 3.41; and the stability of a spinning body containing elastic parts, Refs. 3.18, 3.41, and 3.42. In the disk problem, the motions of all its points are perpendicular to the plane of the disk so far as first-order terms are concerned, equilibrium centrifugal loads are present, and hence there will be some increase in vibration frequencies with rotational speed. But there is no frequency splitting as there are neither centrifugal inertia nor coriolis forces. The disk is stable for all speeds. In the ring problem, the equilibrium centrifugal loads increase the frequencies, and the coriolis forces cause the nodes not to remain fixed in the ring. The effects of rotation on the third problem depend on the orientation of elastic members in the body. A comparative study of stability methods based on the Liapunov direct method is described in Ref. 3.43.

3.10 SUMMARY

For a general theory of vibration of a rapidly rotating deformable body, it is always safe to include the nonlinear theory of elasticity. Though this fact was not explicitly mentioned in the literature dealing with rotation, the additional terms in the equations due to nonlinear theory are brought in through an effective applied load concept which

cannot be easily implemented for a general elastic body. It is clear from the examples that the frequency splitting phenomenon depends on the axis system considered, the geometry, and the orientation of the body with respect to the rotation vector. In general for this phenomenon to take place, the body must have different modes with equal frequencies in the absence of rotation, and the rotation must add either centrifugal or coriolis terms to the equations of motion. The boundary-value problem governing the vibrational motion about the steady-state condition is not in general self-adjoint, and hence the modes are not orthogonal. With regard to stability criteria, the kinetic method when applied to a rotating elastic body fails in some cases if imperfections are not considered. Therefore, it is always safe to include imperfections in the system and apply the kinetic method. Another stability method, if possible, is the Liapunov direct method. The instabilities associated with imperfections are relatively easier to detect in the body fixed rotating coordinate system, if one is suitable, rather than in the inertial coordinate system since they appear as $\lambda = 0$ in the rotating system. The last feature is the role of internal and external damping. It was seen that internal damping, when it exceeds external damping, has a destabilizing effect on stability in gyroscopic systems under certain conditions. Finally, the existence of several interesting bands of instabilities of a rotating beam with coning angle as a parameter is established. This analysis is believed to be new. Chapter VI will examine the effects of coning of the blades of a prop-rotor, and of internal damping at the blade flapping hinges on whirl flutter stability.

IV. NUMERICAL CALCULATION OF BENDING FREQUENCIES

OF A ROTATING BEAM WITH CONING ANGLE

4.1 INTRODUCTION

The governing equations of bending vibration of a rotating beam with coning angle were derived in Section 3.7, and it was also shown that the approximate frequencies can be deduced from the information presented in Refs. 4.1 and 4.2 for a class of rotating beams without coning. In this chapter we shall present an exact method (within the accuracy of the numerical calculations) to calculate the frequencies of the coned beam with rotation, and these values will be compared with those of the approximate Galerkin's method.

4.2 THEORETICAL CONSIDERATIONS

It can be seen from Eqs. (3.65), (3.66), (3.59), and (3.60) that the eigenvalue problem governing the vibration of the beam considered is a two-point boundary value problem since all the boundary values at the root are not known. So a solution of these equations for a set of arbitrarily chosen unknown boundary conditions and the frequency are first obtained at a given rotational speed by the Runge-Kutta numerical integration process [4.3] after transformation of these equations into a set of simultaneous linear first-order

differential equations. The actual solution of the equations is a linear combination of all these arbitrary solutions. So imposing the condition that the actual solution must satisfy the known boundary conditions at the tip of a cantilever beam results in a set of homogeneous equations. The vanishing of the determinant of their coefficients gives the frequency at the preselected rotational speed, and the mode shapes along the beam can be obtained from the linear combination of these solutions at this frequency. The steps involved in this process are as follows:

    (a) Transformation of Eqs. (3.65) and (3.66) into state vector form; these are given by

$$
\frac{d}{dx}
\begin{bmatrix} y_1 \\ y_2 \\ y_3 \\ y_4 \\ y_5 \\ y_6 \\ y_7 \\ y_8 \end{bmatrix}
=
\begin{bmatrix}
0 & 1 & 0 & 0 & 0 & 0 & 0 & 0 \\
0 & 0 & 1/I_{yy} & 0 & 0 & 0 & 0 & 0 \\
0 & 0 & 0 & 1 & 0 & 0 & 0 & 0 \\
(\ )^1 & (\ )^2 & (\ )^3 & 0 & (\ )^4 & 0 & 0 & 0 \\
0 & 0 & 0 & 0 & 0 & 1 & 0 & 0 \\
0 & 0 & 0 & 0 & 0 & 0 & 1/I_{zz} & 0 \\
0 & 0 & 0 & 0 & 0 & 0 & 0 & 1 \\
M_r(\ )^4 & 0 & 0 & 0 & (\ )^5 & M_r(\ )^2 & M_r(\ )^3 & 0
\end{bmatrix}
\begin{bmatrix} y_1 \\ y_2 \\ y_3 \\ y_4 \\ y_5 \\ y_6 \\ y_7 \\ y_8 \end{bmatrix}
$$

(4.1)

where

$$(\ )^1 \ = \ mc^4 \ (\nu_R^2 + \nu_1^2 \sin^2 \beta_o)$$

$$(\ )^2 \ = \ - mc^4 \times \nu_1^2 \cos^2 \beta_o$$

$$(\ )^3 \ = \ c^4 \nu_1^2 \cos^2 \beta_o \ y_9/I_{yy}$$

$$(\ )^4 \ = \ mc^4 2\nu_1 \nu_R \sin \beta_o$$

$$(\ )^5 \ = \ M_r mc^4 \ (\nu_1^2 + \nu_R^2)$$

$$y_1 \ = \ w$$

$$y_2 \ = \ w'$$

$$y_3 \ = \ I_{yy} w''$$

$$y_4 \ = \ (I_{yy} w'')'$$

$$y_5 \ = \ v$$

$$y_6 \ = \ v'$$

$$y_7 \ = \ I_{zz} v''$$

$$y_8 \ = \ (I_{zz} v'')'$$

(Cont'd)

and

$$y_9 = \int_x^1 m(x)\, dx$$

$$w(x,t) = y_1(x)\, \sin \omega_R t$$

$$v(x,t) = y_5(x)\, \cos \omega_R t$$

$$\nu_1 = \Omega_o/(\omega_{NR})_1$$

$$\nu_R = \omega_R/(\omega_{NR})_1$$

$$(\omega_{NR})_1^2 = c^4 EI_{yyo}/(m_o L^4)$$

$$M_r = I_{yyo}/I_{zzo} \tag{4.2}$$

The parameters m, I_{yy}, etc. are nondimensionalized with respect to their corresponding values at the origin, and the variable x is non-dimensionalized with the length L of the beam. The boundary conditions are given by

$$y_1 = y_2 = y_5 = y_6 = 0 \quad \text{at} \quad x = 0 \tag{4.3}$$

$$y_3 = y_4 = y_7 = y_8 = y_9 = 0 \quad \text{at} \quad x = 1 \tag{4.4}$$

(b) Values of the rotational parameter ν_1 and the frequency

parameter ν_R are assumed.

(c) Starting at $x = 1$, the uncoupled differential equation

$y_9' = - mx$ is integrated by the Runge-Kutta step-by-step

numerical integration process.

(d) The four known boundary conditions at the root are set

to their respective values, and the remaining boundary

conditions are assigned arbitrarily as

set 1 $y_3 = 1$, $y_4 = y_7 = y_8 = 0$

set 2 $y_4 = 1$, $y_3 = y_7 = y_8 = 0$

set 3 $y_7 = 1$, $y_3 = y_4 = y_8 = 0$

set 4 $y_8 = 1$, $y_3 = y_4 = y_7 = 0$ (4.5)

Starting from $x = 0$, four sets of solutions of Eqs. (4.1) are ob-
tained by the Runge-Kutta numerical integration process. At the tip,
we shall write

$$y_{i,j}(1) = E(i,j)$$

$$i = 1, 2, \ldots, 8$$

$$j = 1, 2, 3, 4 \qquad (4.6)$$

where suffix j indicates the solution of the equations with the jth set of boundary conditions [Eq. (4.5)].

Since Eqs. (4.1) are linear, the actual solutions at the tip are given by

$$y_i(1) \ = \ \sum_{j=1}^{4} a_j \ E(i,j) \tag{4.7}$$

So also

$$y_i(x) \ = \ \sum_{j=1}^{4} a_j \ y_{i,j}(x) \tag{4.8}$$

where the a_j (j = 1, 2, 3, 4) are constant coefficients.

The known boundary conditions at x = 1 represented by Eq. (4.4) require that

$$\sum_{j=1}^{4} a_j \ E(i,j) \ = \ 0$$

$$(i = 5, 6, 7, 8) \tag{4.9}$$

and hence we must have

$$|E(i,j)| \ = \ 0$$

$$(i = 5, 6, 7, 8)$$

$$(j = 1, 2, 3, 4) \tag{4.10}$$

The value of the determinant is zero if and only if the assumed frequency ν_R is a correct one. So the value of the determinant is calculated for a range of values of ν_R at a preselected value of ν_1, and it is plotted against ν_R. The points of intersection on the frequency axis give the frequencies of the system. For each value of ν_1, there are two values of $(\nu_R)_n$, $[(\nu_R)_{1n}$, $(\nu_R)_{2n}]$ for each mode because of the frequency splitting due to rotation. Both of these frequencies can be extracted from Eqs. (4.2). However, to determine the type of whirl, we must also solve Eqs. (4.1) by writing

$$w = y_1(x) \cos \omega_R t \tag{4.11}$$

$$v = y_5(x) \sin \omega_R t \tag{4.12}$$

Then we obtain the same frequencies with different mode shapes. Guided by the experience from Eqs. (3.42) and (3.43), if we write the solutions of Eqs. (3.65)-(3.68) in the form

$$v = \sum_{n=1}^{\infty} \Phi_n(x) \left[g_n \cos (\omega_R)_{1n} t + h_n \sin (\omega_R)_{1n} t \right.$$

$$\left. + c_n \cos (\omega_R)_{2n} t + d_n \sin (\omega_R)_{2n} t \right] \tag{4.13}$$

$$w = \sum_{n=1}^{\infty} \psi_n(x) \left[G_n \cos (\omega_R)_{1n} t + H_n \sin (\omega_R)_{1n} t \right.$$

$$\left. + C_n \cos (\omega_R)_{2n} t + D_n \sin (\omega_R)_{2n} t \right] \tag{4.14}$$

- 75 -

the coefficients g_n , h_n , G_n and H_n determine the direction of whirl of the mode with frequency $(\omega_R)_{1n}$, and the coefficients c_n , d_n , C_n and D_n determine the direction of the other mode. If the beam is symmetric $\Phi_n(x)$ and $\psi_n(x)$ are identical.

Knowing the frequency, the coefficients a_2 , a_3 and a_4 are determined from Eqs. (4.9) for an arbitrary value of a_1 , say 1 , and the mode shapes are obtained from Eq. (4.8).

These equations are programmed on an IBM 360/67, and the exact frequencies and mode shapes of a uniform, symmetric beam are obtained for different values of the parameters ν_1 and β_0 .

The assumption of the parameter ν_R in step (b) above is guided by an approximate one-term Galerkin solution. In this method, the frequencies of each mode of a uniform beam are calculated by using the corresponding nonrotating mode shape. These frequencies are also included in Figs. 4.1 and 4.2.

4.3 RESULTS AND DISCUSSION

Both the exact and the approximate one-term Galerkin solutions are plotted in Figs. 4.1-4.3 for a uniform symmetric beam. Also included in Fig. 4.1(a) is a five-term Galerkin solution from Ref. 4.1. It is seen that the approximate one-term results are in good agreement with the exact results for the second mode. For the first mode, however, the maximum error with one mode is larger, about 7% in the frequency, and that with the five mode is less than 5%. From these results it appears that a one-term Galerkin method can be used for a
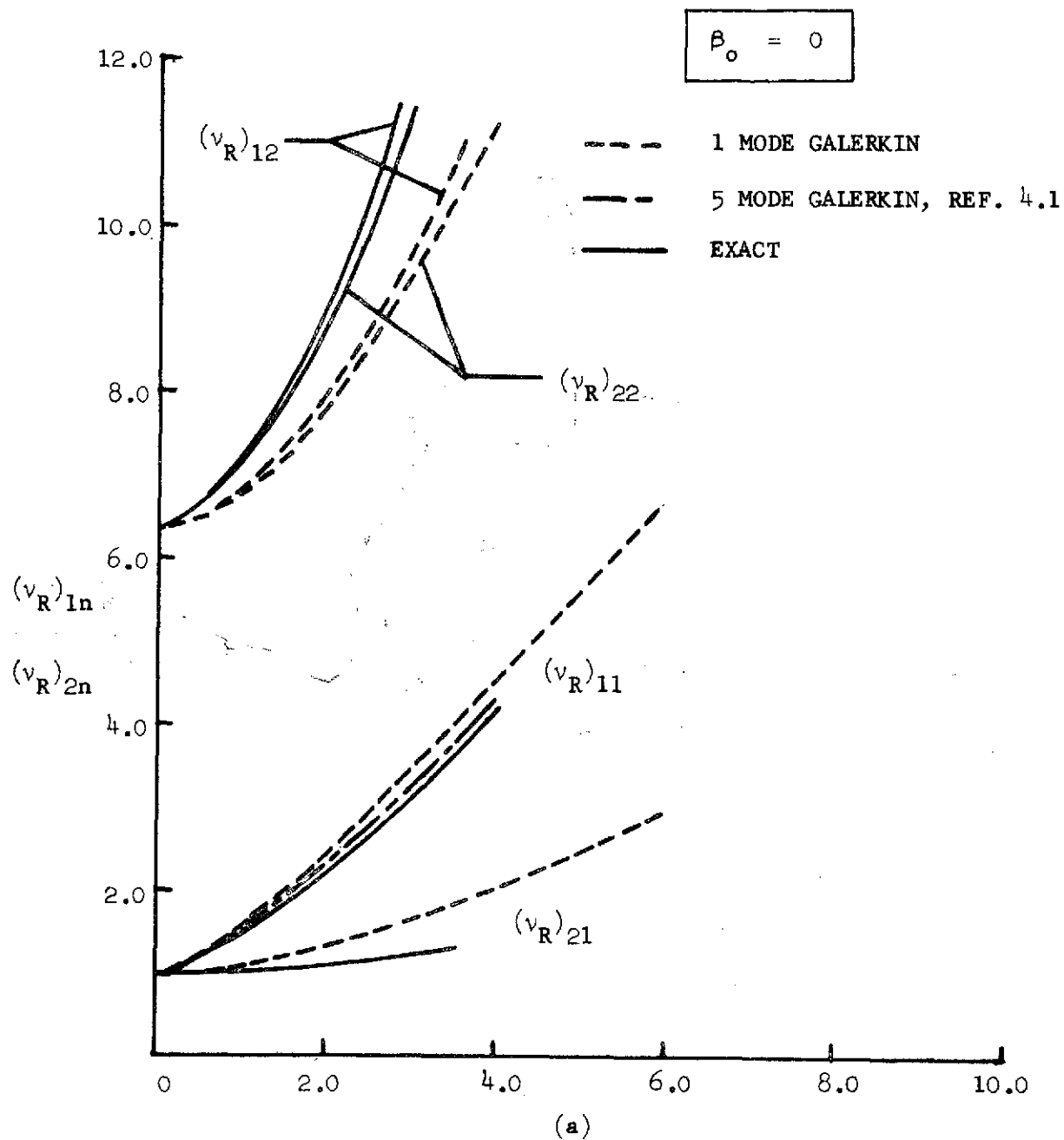
FIG. 4.1--Effect of rotation on the bending frequencies
of uniform cantilever beam.
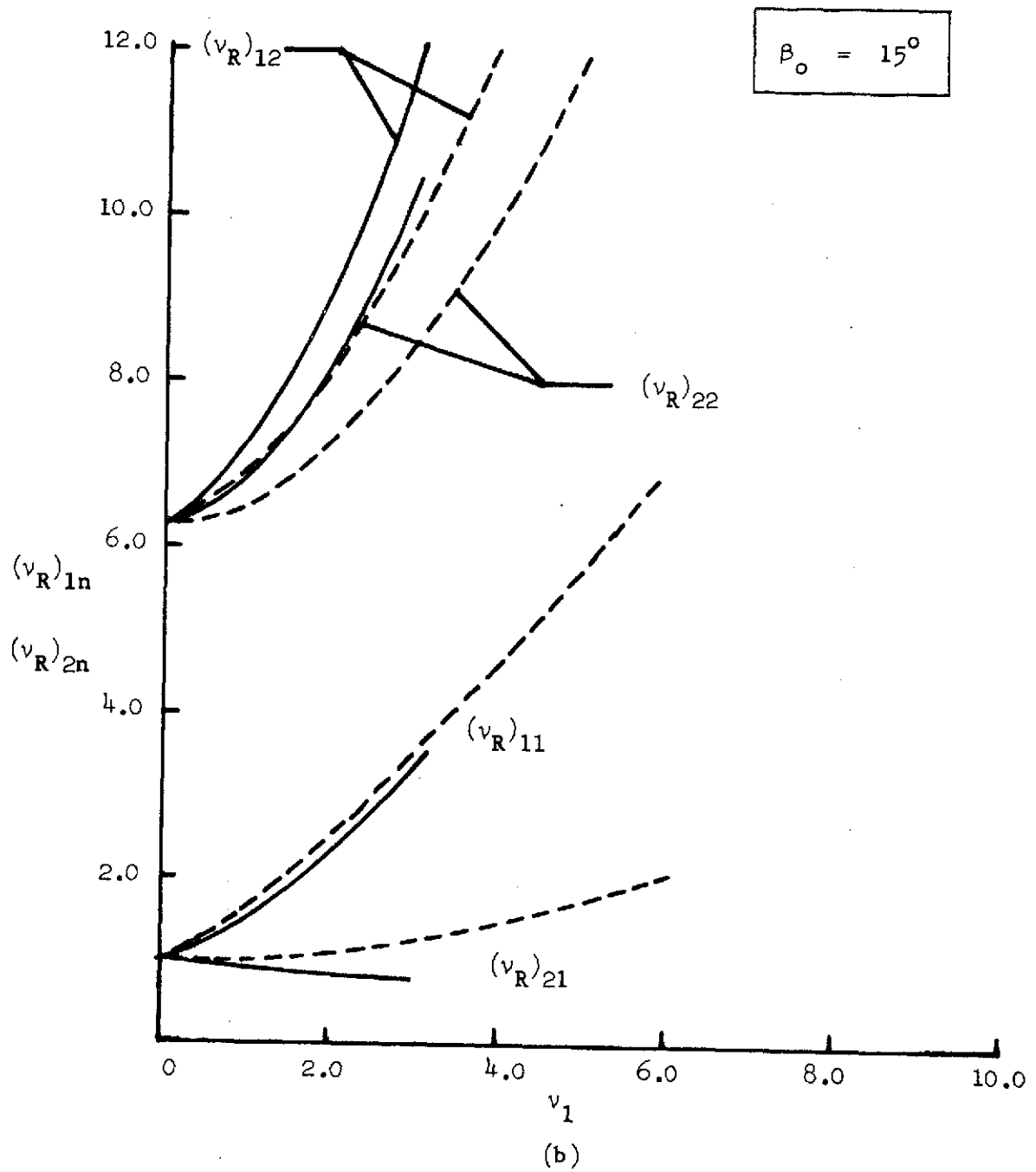
FIG. 4.1--Continued.
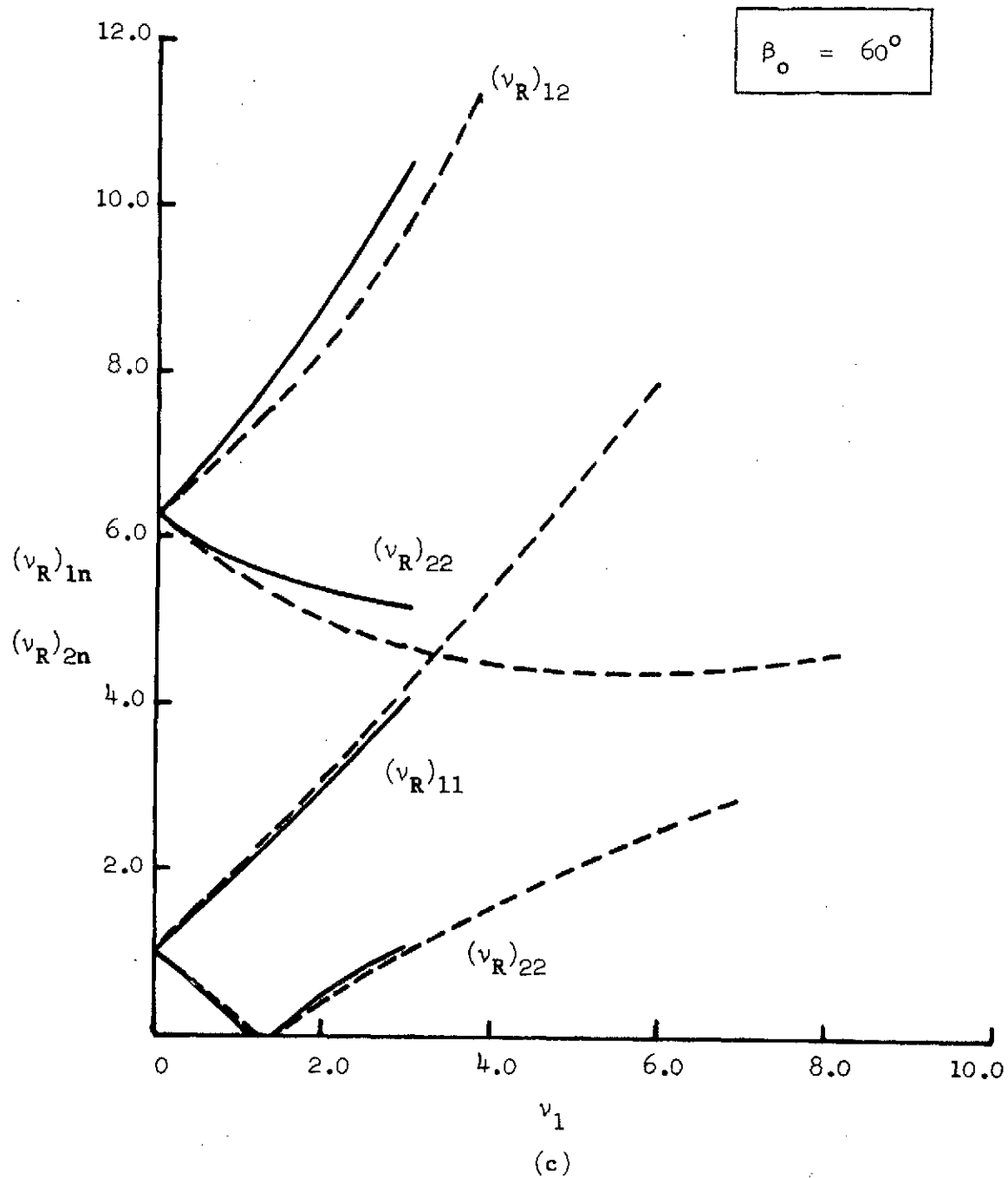
FIG. 4.1--Concluded.
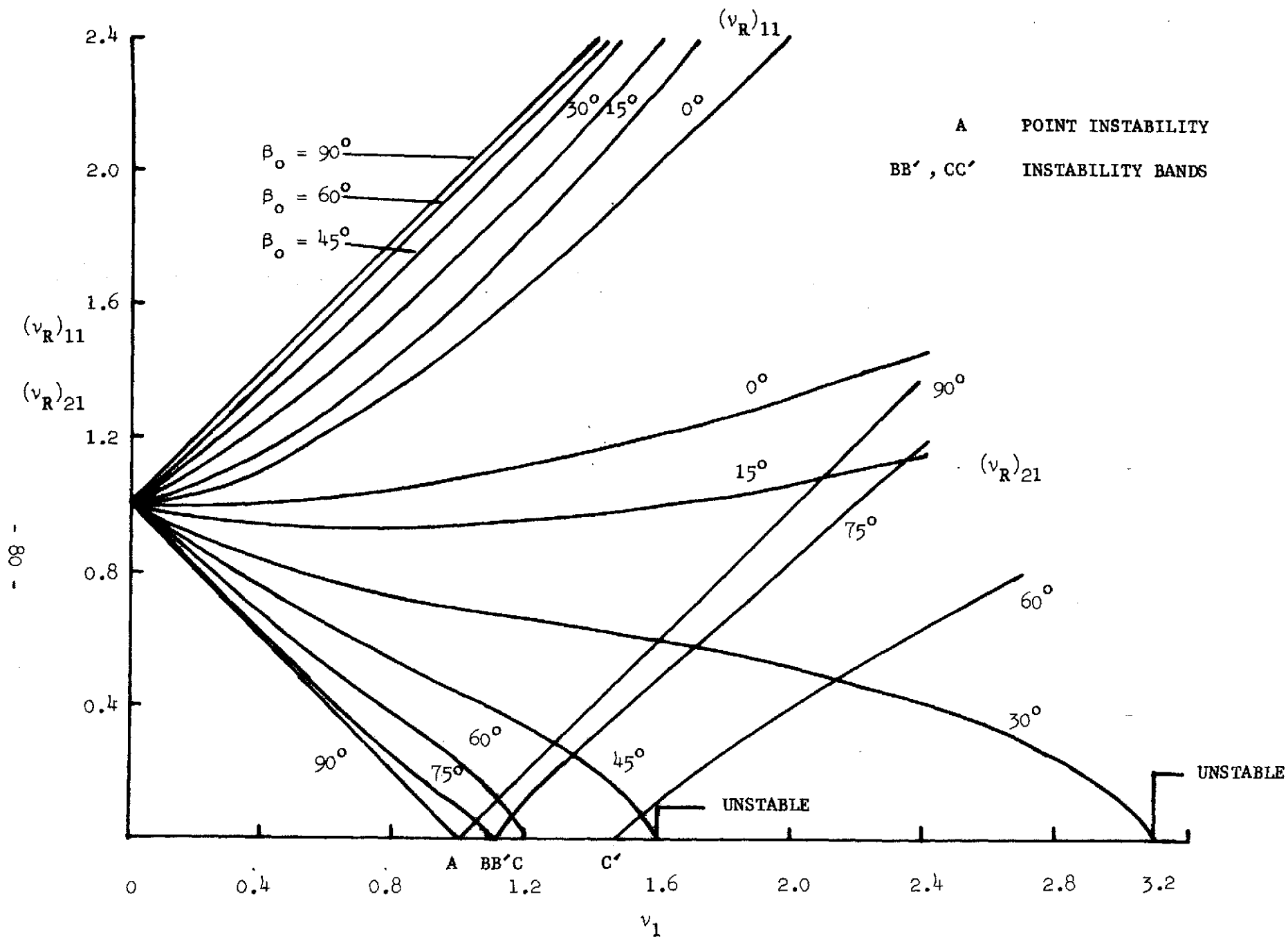
FIG. 4.2—Influence of rotation on the first bending frequency of a
uniform beam with β_o as parameter.
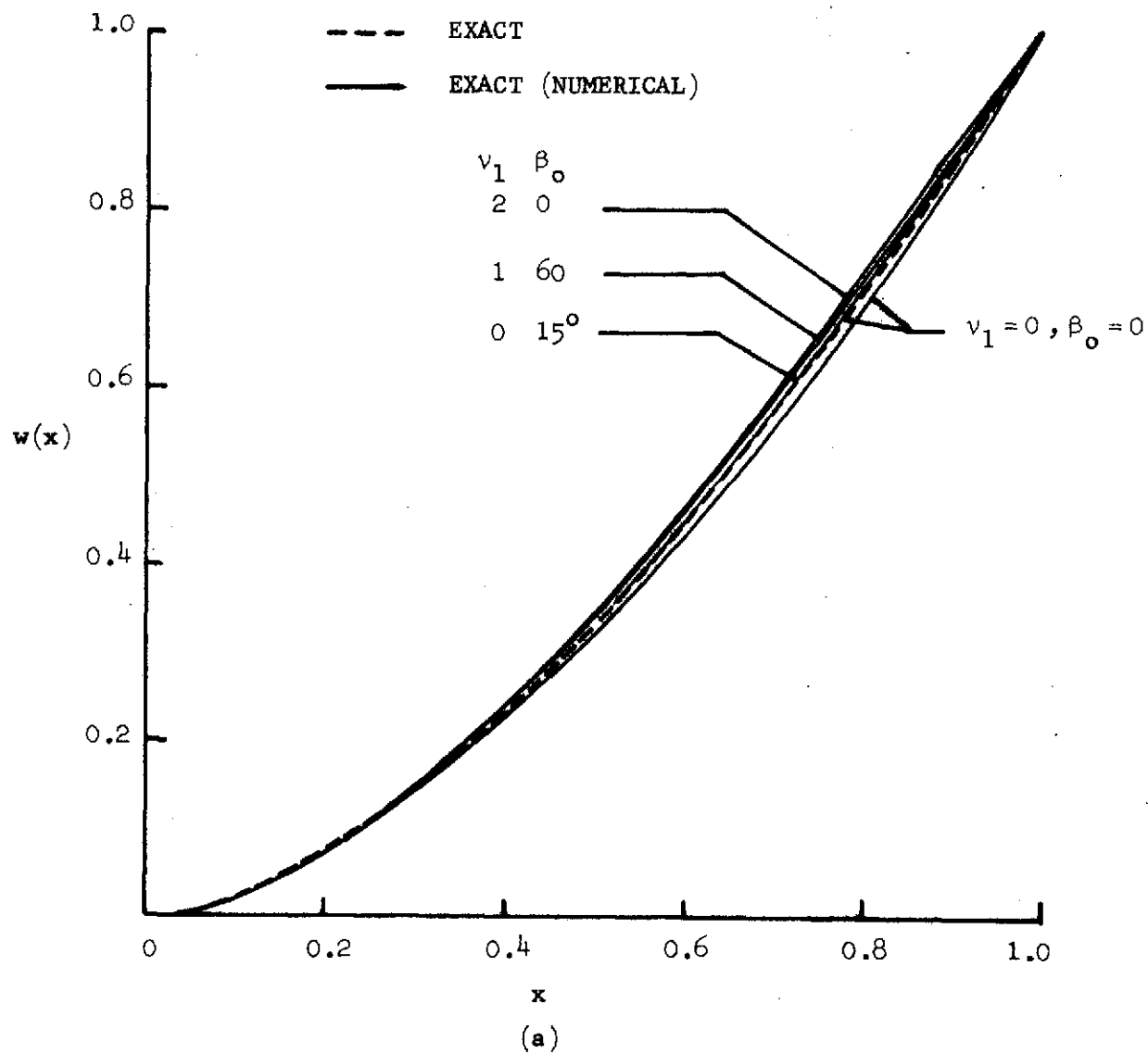
FIG. 4.3--Effect of rotation on the bending mode
shapes of a uniform cantilever beam.
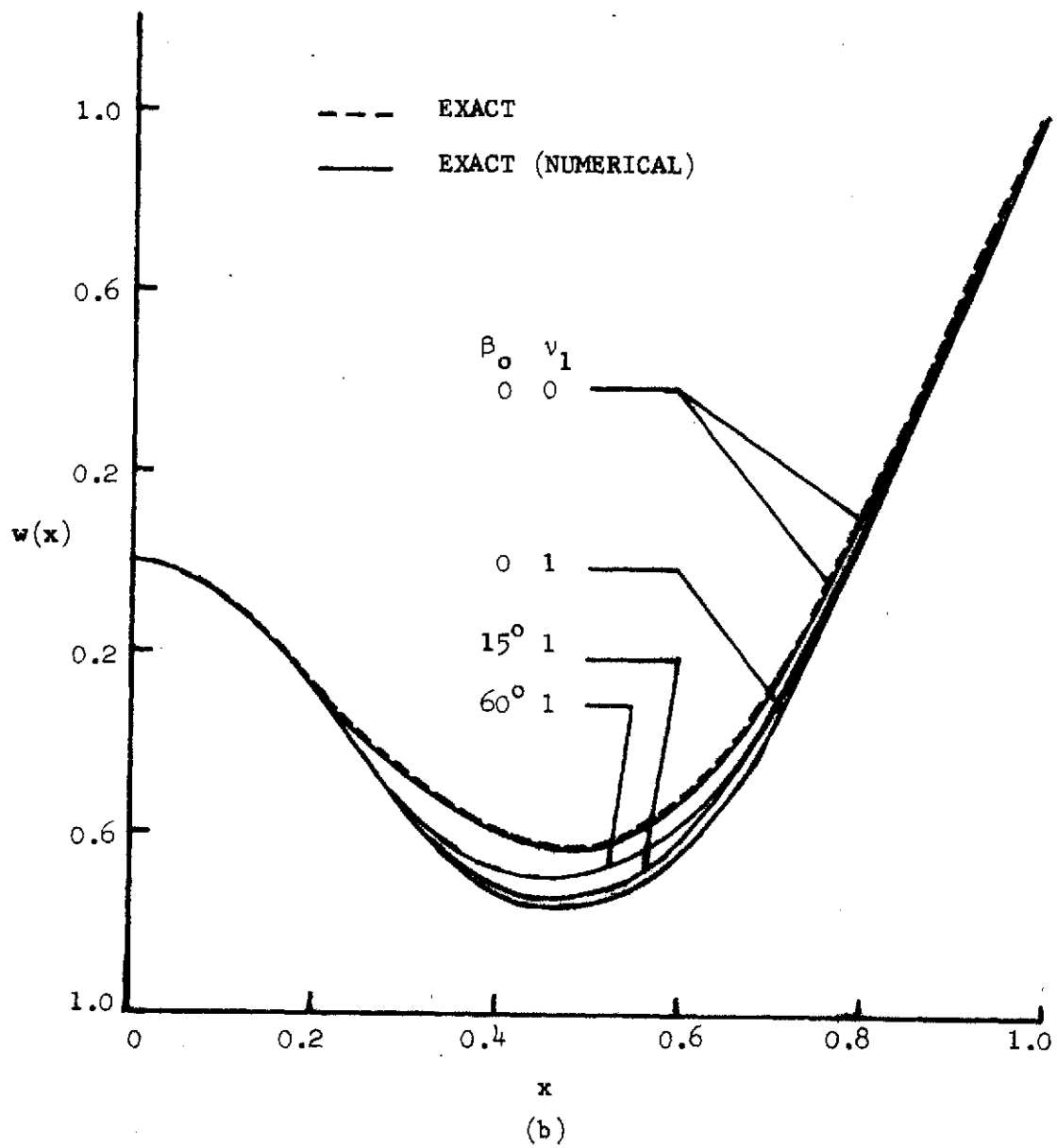
FIG. 4.3--Concluded.

rapid estimation of the frequencies of a rotating coned beam.

At any β_o , the effect of rotation is to split each frequency of a nonrotating symmetric beam into two and alter them with ν_1 . In fact, the rotational parameter ν_1 , depending on the value of β_o , may cause one of the frequency parameters $[(\nu_R)_{2n}]$ to be zero or imaginary. If $(\nu_R)_{2n}$ is imaginary, then the beam is dynamically unstable; and if it is zero, the beam is statically unstable. Both of these instabilities associated with the nonrotating first mode are shown in Fig. 4.2 with β_o as a parameter. It is clear from the figure that the type of instability or stability, as discussed in Section 3.7, depends on the range of β_o .

The effect of rotation at different values of β_o on the vibration mode shapes is shown in Fig. 4.3. An examination of these shapes indicates that, although some differences between the modes exist, they are relatively small, particularly for the second mode. We shall use the exact flapping frequencies of the rotating uniform beam in the following chapter.

V. LEAST WEIGHT DESIGN OF A ROTATING CANTILEVER

BEAM WITH ONE FIXED FLAPPING FREQUENCY

5.1 INTRODUCTION

The main object of structural optimization is to achieve minimum weight designs subjected to certain design requirements. These requirements may be termed constraints on the optimization process. More emphasis is placed on the minimization of weight because of the overwhelming importance of this parameter, particularly in aerospace applications.

For optimization studies there are two mathematical models for representing the structure. One is the elastic continuum model, and the other is the distributed mass finite element model. The former one is suitable for simple, continuous structures and the latter for all types of structures. Once the problem, the type of constraint, and the mathematical model of the structure are known, the next step is to find a suitable optimization technique which accomplishes our stated objective. In the literature there exist several kinds of such techniques depending on the problem and the tastes of the investigator.

When the mathematical model of the structure is of a continuum type with differential equations as constraint, one method of optimization is to use control theory techniques, which are themselves

ramifications of the calculus of variations. The constraint equation

is an ordinary differential equation with one independent spatial var-

iable if the structure is one-dimensional like a beam, and it is a

partial differential equation for a two-dimensional structure such as

a plate. Many simple problems can be described by differential equa-

tions, particularly in the field of optimal control theory. In the

case of a discrete model, mathematical programming techniques have

been used. Both of these approaches have been developed, and they

represent two complementary methods of solution.

The first model is adapted for the problem of interest in this

chapter. This model was widely used by earlier investigators, Turner

[5.1], Keller and Niordson [5.2], Niordson [5.3], Olhoff [5.4], Sheu

and Prager [5.5], Prager and Taylor [5.6], Ashley and McIntosy [5.7],

Armand and Vitte [5.8], Weisshaar [5.9], Armand [5.10] and Vepa [5.11],

to name only a few. The literature on the second model, which is not

our concern here, can be found in Refs. 5.12 to 5.16 among others.

In this chapter the constraint equations and boundary conditions

of the stated problem are deduced from those of the coning beam of

Section 3.7, and then a set of nonlinear differential equations and

boundary conditions, which are necessary for the optimal depth distribu-

tion, are derived using optimal control theory techniques. Finally, a

numerical solution of these equations is obtained using the "transi-

tion matrix" method described by Bryson and Ho [5.17], and a physical

interpretation of the optimality condition is given.

5.2 STATEMENT OF THE PROBLEM

The problem considered is a beam rotating at a constant speed with its axis perpendicular to the axis of rotation. The beam has a fixed width and length with a solid rectangular cross-section. Our objective is to find a distribution of depth along the span such that the weight is optimum and the fundamental flapping frequency with rotation is the same as that of the uniform depth beam with the same rotational speed and geometry. Two sets of boundary conditions can be considered for this rotating beam. One set of boundary conditions will be those due to clamping at one end of the beam while allowing the other end to be free. The second set of boundary conditions will be due to fixing the beam with freedom to rotate at one end while allowing the other end to be free. This set of end conditions is referred to as "pinned-free". However, the optimum depth distributions will be obtained only for clamped-free boundary conditions.

The equilibrium equations governing the flapping vibrational motion are given by Eqs. (3.57), (3.59), (3.60), and (3.61) with the chordwise elastic displacement v being zero. Setting

$$w(x,t) = w(x) \, e^{i(\omega_R)_{1n} t} \qquad (5.1)$$

Eqs. (3.57), (3.59), (3.60), and (3.61) can be written in nondimensional

form as

$$[t^3(x) \; w''(x)]'' + \nu_1^2 c^4 \; [xt(x) \; w'(x) - w''(x) \; u(x)]$$

$$- (\nu_R)_{11}^2 \; c^4 t(x) \; w(x) \; = \; 0 \qquad (5.2)$$

$$u'(x) \; = \; - xt(x) \qquad (5.3)$$

where

$$w(x) \; = \; w/L$$

$$x \; = \; x/L$$

$$t(x) \; = \; T_\ell(x)/T_o \; = \; \text{local depth/depth at the root}$$

$$m(x) \; = \; m_o t(x)$$

$$I_{yy}(x)/I_{yyo} \; = \; t^3(x)$$

$$\nu_1 \; = \; \Omega_o/(\omega_{NR})_1$$

$$(\nu_R)_{11} \; = \; (\omega_R)_{11}/(\omega_{NR})_1$$

$$(\omega_{NR})_1^2 \; = \; c^4 EI_{yyo}/(m_o L^4) \qquad (5.4)$$

$$w(0) \; = \; w'(0) \; = \; t^3(1) \; w''(1) \; = \; [t^3(1) \; w''(1)]' \; = \; 0$$

$$u(1) \; = \; 0 \qquad (5.5)$$

A closed form analytical solution of the boundary-value problem [Eqs. (5.2), (5.3), and (5.5)] is not possible even for a uniform beam. However, the frequency $(\nu_R)_{11}$ at a selected ν_1 is obtained from Fig. 4.1.

Now we are in a position to state the optimization problem. We want to minimize the integral

$$J = \int_0^1 t(x)dx \qquad (5.6)$$

representing the dimensionless mass of the beam. J is also called a performance index or merit function. The depth function is subjected to the additional conditions represented by Eqs. (5.2), (5.3), and (5.5). This is a problem of the calculus of variations and may be viewed as one of the Bolza type (Ref. 5.18). This problem can be reduced to a more conventional type by converting Eq. (5.2) into first-order equations. Let us introduce the new variables

$$p = w'$$

$$q = t^3 w''$$

$$r = (t^3 w'')' \qquad (5.7)$$

Then

$$r' = -\nu_1^2 c^4 \left(x\,t\,p - \frac{uq}{t^3} \right) + c^4 (\nu_R)_{11}^2 \, tw$$

$$q' = r$$

$$w' = p$$

$$p' = q/t^3$$

$$u' = -xt \qquad\qquad (5.8)$$

with boundary conditions

$$w(0) = p(0) = r(1) = u(1) = q(1) = 0 \qquad (5.9)$$

The problem represented by Eqs. (5.6), (5.8), and (5.9) is a kind often encountered in optimal control theory (Refs. 5.17). However, here the role of time is being played by the dimensionless coordinate x . The control function here is $t(x)$, and the state variables are r , q , w , p , and u .

5.3 REVIEW OF OPTIMAL CONTROL THEORY TECHNIQUES AS APPLIED TO THE PROBLEM CONSIDERED

The general problem is to choose a control function $t(x)$ and the state variables $y_1(x)$, $y_2(x)$, ... , $y_n(x)$ which satisfy the

conditions

$$\tilde{y}'(x) = \tilde{f}(t,\tilde{y},x)$$

$$y_i(0) = 0 \qquad\qquad i = 1,2,3,\ldots,m$$

$$y_j(1) = 0 \qquad\qquad j = m+1,\ldots,n \qquad (5.10)$$

and which also minimize

$$J = \int_0^1 t(x)dx \qquad\qquad (5.11)$$

The function $\tilde{f}$ is required to be differentiable with respect to $\tilde{y}$ and t, but may be piecewise continuous with respect to x. The functions $\tilde{y}$ are required to be piecewise continuously differentiable, but t may be only piecewise continuous.

The classical approach to the solution of the problem is to obtain a list of additional conditions which the solution of the problem must satisfy and then construct a set of functions which satisfy all these necessary conditions. Since all the functions satisfy only necessary conditions, they are merely candidates for an extremal, rather than extremals themselves. So the one among the functions which yields the smallest value of J is the solution of the problem. The lack of sufficient conditions for this kind of problem forces the designer to make decisions on the basis of his experience and engineering knowledge rather than rigorous mathematics. However, the

distinction between necessary and sufficient conditions is not of great importance in problems of classical mechanics where equilibrium problems require stationarity of the functional rather than its extremal. Some discussion on the necessity of certain conditions for optimization problems were discussed by Caratheodory [5.19].

A very general principle, which furnishes the tools for the above optimal design problem, was hypothesized by Pontryagin [5.20] on the basis of the work by him and his associates. This principle is called the "maximum principle". In this principle Pontryagin introduced the Hamiltonian in a more direct manner as opposed to an indirect manner in classical mechanics as a Legendre transformation of the Lagrangian density. The Hamiltonian is defined as

$$H[\tilde{y}(x),t(x),x] = t(x) + \tilde{\lambda}^T(x)\tilde{f}[y(x),t(x),x] \qquad (5.12)$$

where $\tilde{\lambda}$ is a vector of Lagrange multipliers. According to this principle, to find the control function $t(x)$ that gives a stationary value of J , the following set of additional equations constitute the necessary conditions for an extremal:

$$\tilde{\lambda}' = -\left(\frac{\partial H}{\partial \tilde{y}}\right)^T \qquad (5.13)$$

$$\frac{\partial H}{\partial t} = 0 \qquad (5.14)$$

and

$$\lambda_i(1) = 0 \qquad i = 1, 2, 3, \ldots, m$$

$$\lambda_j(0) = 0 \qquad j = m + 1, \ldots, n \tag{5.15}$$

The multipliers $\tilde{\lambda}$ are continuous and have piecewise continuous derivatives. These are also called adjoint variables, and the conditions, Eqs. (5.15), are also often referred to as transversality conditions. The Hamiltonian function H serves only as a device for conveniently displaying necessary conditions for the Bolza problem. Out of all the possible controls, one which yields the maximum H is the optimum one.

5.4 APPLICATION OF OPTIMAL CONTROL THEORY TO THE PROBLEM CONSIDERED

For the problem of Section 5.2, the Hamiltonian function

$$H = t(x) - \lambda_u t(x)x + \lambda_w p + \lambda_p q/t^3 + \lambda_q r$$

$$+ \lambda_r [- c^4 v_1^2 (ptx - uq/t^3) + (v_R)_{11}^2 c^4 tw] \tag{5.16}$$

leads to the following necessary conditions for an extremal:

$$\lambda_p' = - \lambda_w + \lambda_r v_1^2 c^4 tx$$

$$\lambda_w' = - \lambda_r (v_R)_{11}^2 c^4 t \tag{Cont'd}$$

and

$$\lambda'_u = -\lambda_r v_1^2 c^4 q/t^3$$

$$\lambda'_q = -\lambda_p/t^3 - c^4 v_1^2 \lambda_r u/t^3$$

$$\lambda'_r = -\lambda_q \qquad (5.17)$$

$$t = \left\{ \frac{3\lambda_p q + 3\lambda_r c^4 v_1^2 qu}{1 - \lambda_u x - \lambda_r c^4 [v_1^2 px - (v_R)_{11}^2 w]} \right\}^{1/4} \qquad (5.18)$$

$$\lambda_u(0) = \lambda_p(1) = \lambda_w(1) = \lambda_q(0) = \lambda_r(0) = 0 \qquad (5.19)$$

Finally, we end up with a system of ten nonlinear, first-order differential equations represented by Eqs. (5.8) and (5.17), optimality condition, Eq. (5.18), and the boundary conditions, Eqs. (5.9) and (5.19), for eleven unknowns r , q , w , p , u , λ_r , λ_q , λ_w , λ_p , λ_u , and t . Since half the boundary conditions at the root $x = 0$ and the other half at the tip $x = 1$ are specified, this problem is referred to as a two-point boundary value problem. An examination of these equations reveals no possibility for an analytical solution and hence a numerical solution is given in the next section.

5.5 NUMERICAL SOLUTION

The transition matrix approach developed and described by Bryson [5.17] has been successfully applied for some problems of this nature by the earlier investigators Armand [5.8] and Weisshaar [5.9]. Since this method has become a common approach, we will not review it here. However, we shall present the steps involved in applying this method to our particular problem.

(a) To obtain the transition matrix, the perturbed equations of Eqs. (5.8) and (5.17) are required, and these are given by

$$(\delta u)' = - x\delta t$$

$$(\delta \lambda_p)' = - \delta \lambda_w + x v_1^2 c^4 (t\delta \lambda_r + \lambda_r \delta t)$$

$$(\delta \lambda_w)' = - (v_R)_{11}^2 c^4 (t\delta \lambda_r + \lambda_r \delta t)$$

$$(\delta q)' = \delta r$$

$$(\delta r)' = v_1^2 c^4 (\delta u q/t^3 + \delta q u/t^3 - 3\delta t u q/t^4$$

$$\qquad - \delta p x t - x p \delta t) + (v_R)_{11}^2 c^4 (t\delta w + w\delta t)$$

$$(\delta w)' = \delta p$$

$$(\delta \lambda_u)' = - v_1^2 c^4 (\delta \lambda_r q/t^3 + \lambda_r \delta q/t^3 - 3\lambda_r q\delta t/t^4)$$

(Cont'd)

- 94 -

and

$$(\delta\lambda_q)' = -\delta\lambda_p/t^3 + 3\lambda_p\delta t/t^4 - \nu_1^2 c^4\,(\delta\lambda_r u/t^3$$

$$+ \lambda_r\delta u/t^3 - 3\lambda_r u\delta t/t^4)$$

$$(\delta\lambda_r)' = -\delta\lambda_q$$

$$(\delta_p)' = -3q\delta t/t^4 + \delta q/t^3 \tag{5.20}$$

$$\delta t = \left\{ [\delta\lambda_p q + \lambda_p\delta q + \nu_1^2 c^4\,(\lambda_r u\delta q + uq\delta\lambda_r \right.$$

$$+ \lambda_r q\delta u)]\quad \{1 - \lambda_u x - \lambda_r c^4\,[\nu_1^2 px$$

$$- (\nu_R)_{11}^2 w]\} + (\lambda_p q + \lambda_r\nu_1^2 c^4 uq)\quad \{x\delta\lambda_u$$

$$+ \delta\lambda_r c^4\,[x\nu_1^2 p - (\nu_R)_{11}^2 w] + \lambda_r x\nu_1^2 c^4\delta p$$

$$\left. - \lambda_r\,(\nu_R)_{11}^2\,c^4\delta w\} \right\}$$

$$\div \left\{ (4t^3/3)\,\{1 - \lambda_u x - \lambda_r c^4\,[\nu_1^2 px \right.$$

$$\left. - (\nu_R)_{11}^2 w]\}^2 \right\}$$

(b) We express all the Eqs. (5.8), (5.17), and (5.20) in a

compact and convenient state vector form as

$$\tilde{y}' = \tilde{f}(\tilde{y}, x, t) \tag{5.21}$$

and

$$\tilde{y}_1 = \{0\} \quad \text{at} \quad x = 1$$

$$\tilde{y}_2 = \{0\} \quad \text{at} \quad x = 0$$

$$\tilde{y}_3 = \{0\} \quad \text{at} \quad x = 1$$

$$\tilde{y}_4 = \{0\} \quad \text{at} \quad x = 0 \tag{5.22}$$

where

$$\tilde{y}_1 = (u\lambda_p \lambda_w qr)^T$$

$$\tilde{y}_2 = (wp\lambda_u \lambda_q \lambda_r)^T$$

$$\tilde{y}_3 = \delta\tilde{y}_1^T$$

$$\tilde{y}_4 = \delta\tilde{y}_2^T \tag{5.23}$$

(c) We now guess the unspecified conditions $y_1(0)$.

(d) Integrate Eqs. (5.21) for 5 different values of $y_3(0)$,
each time taking one of the perturbation quantities of
$y_3(0)$ as unity and the other values of $y_3(0)$ as zero,
with the values $y_1(0)$, $y_2(0)$, and $y_4(0)$ being un-
changed. Each time one column of the transition matrix
$\tilde{T}$ (5×5) is filled up by the values of $\tilde{y}_3$ at $x = 1$.

(e) Then, calculate a change $\tilde{\Delta y}_1$ in $\tilde{y}_1$ at $x = 0$ such

that the error in $\tilde{y}_1$ at $x = 1$ is reduced by an amount

ϵ ; it is given by

$$\tilde{\Delta y}_1 \;\; = \;\; - \, \epsilon \, \tilde{T}^{-1} \, \tilde{y}_1$$

$$(\text{at} \;\; x \;\; = \;\; 0) \qquad (\text{at} \;\; x \;\; = \;\; 1) \tag{5.24}$$

(f) Calculate the new initial conditions

$$\tilde{y}_1 \;\; = \;\; \tilde{y}_1 \;\; + \, \tilde{\Delta y}_1 \tag{5.25}$$

$$(\text{new}) \qquad (\text{old})$$

other values being the same. The same process is re-
peated until $\tilde{y}_1 = \{0\}$ at $x = 1$ to the required ac-
curacy.

The main problem in this iterative integration process is to guess
the initial values for a rotating beam. Presently, this is overcome by
a sort of perturbation on the rotational frequency parameter. First,
the optimum solution of a nonrotating cantilever beam is obtained by
estimating the required initial values from the eigenfunction solutions
of a uniform depth beam. Since the eigenvalue problem of the nonrota-
ting cantilever beam is self-adjoint, the adjoint variables are linear

functions of the state variables. That is,

$$
\begin{bmatrix} w' \\ p' \\ q' \\ r' \end{bmatrix}
=
\begin{bmatrix}
0 & 1 & 0 & 0 \\
0 & 0 & 1/t^3 & 0 \\
0 & 0 & 0 & 1 \\
c^4 (v_R)_{11}^2 t & 0 & 0 & 0
\end{bmatrix}
\begin{bmatrix} w \\ p \\ q \\ r \end{bmatrix}
\tag{5.26}
$$

$$
\begin{bmatrix} \lambda_w' \\ \lambda_p' \\ \lambda_q' \\ \lambda_r' \end{bmatrix}
=
\begin{bmatrix}
0 & 0 & 0 & -(v_R)_{11}^2 c^4 t \\
-1 & 0 & 0 & 0 \\
0 & -1/t^3 & 0 & 0 \\
0 & 0 & -1 & 0
\end{bmatrix}
\begin{bmatrix} \lambda_w \\ \lambda_p \\ \lambda_q \\ \lambda_r \end{bmatrix}
\tag{5.27}
$$

and the boundary conditions associated with these variables lead to

$$
\begin{bmatrix} w \\ p \\ q \\ r \end{bmatrix}
= A
\begin{bmatrix}
0 & 0 & 0 & 1 \\
0 & 0 & -1 & 0 \\
0 & 1 & 0 & 0 \\
-1 & 0 & 0 & 0
\end{bmatrix}
\begin{bmatrix} \lambda_w \\ \lambda_p \\ \lambda_q \\ \lambda_r \end{bmatrix}
\tag{5.28}
$$

where A is an arbitrary constant. The above result was reasoned by Turner [5.1]. Making use of this relation and the eigenfunctions of the nonrotating beam, the ratio of $r(0)/q(0) = -1.37734$, was estimated by Weisshaar [5.9]. An estimate of $q(0)$ for a uniform depth beam can be obtained from Eq. (5.18) as

$$t^4(0) = 3\lambda_q(0) \, q(0) \tag{5.29}$$

Assuming $\lambda_p = q$ and $t(0) = 1$, a likely initial value of $q(0)$ is 0.5773. Thus the starting values for the nonrotating cantilever beam are

$$\begin{bmatrix} u \\ \lambda_p \\ \lambda_w \\ q \\ r \end{bmatrix} = \begin{bmatrix} 0.00 \\ 0.5773 \\ 0.7952 \\ 0.5773 \\ -0.7952 \end{bmatrix} \tag{5.30}$$

and $v_1 = 0$, $(v_R)_{11}^2 c^4 = 12.36$. The value $u(0)$ is arbitrarily set to zero since it does not matter for a nonrotating beam. Further, the control Eq. (5.18) and the boundary conditions at $x = 1$ make $t = 0$ at $x = 1$, a fact causing numerical problems. This is handled by introducing an end constraint on depth. For the constraint $t \geq t_{min}$ $(0 \leq x \leq 1)$, logic is introduced into the program such that in the calculation process whenever t is less than

or equal to t_{min} , then $t(x)$ is set equal to t_{min} and δt is set to zero. The value of δt must be zero because no variation of depth is permitted. Again, the integration process continues with these new values of t and δt . Initially, a large value of t_{min} is used, and subsequently it is reduced step-by-step until it is $t_{min} = 0.01$. This algorithm is designed to reduce ϵ by one-half every time until the depth distribution is zero somewhere between $x = 0$ and $x = 1$, and starts again from the preceding step with a little higher value of this ϵ . After establishing the likely value of ϵ , convergence is obtained within 4 to 6 iterations. The differential equations are integrated using the Runge-Kutta numerical scheme. The actual depth distribution for the nonrotating cantilever beam is shown in Fig. 5.1.

Next, a small amount of rotation is introduced, and the corresponding $(v_R)_{11}$ is estimated from Fig. 4.1. Keeping the two parameters v_1 and $(v_R)_{11}$ fixed, and using the stationary cantilever results corresponding to the optimum depth distribution as starting data, the iterative process is repeated to determine the optimum depth distribution. This process is continued with a step-by-step increase in v_1 . Figure 5.2 shows the optimum depth distributions with v_1 as a parameter.

5.6 PHYSICAL INTERPRETATION OF THE OPTIMALITY CONDITION

Even in the presence of rotation Eq. (5.2) is self-adjoint, and hence the relation [Eq. (5.28)] between the state variables w , p ,
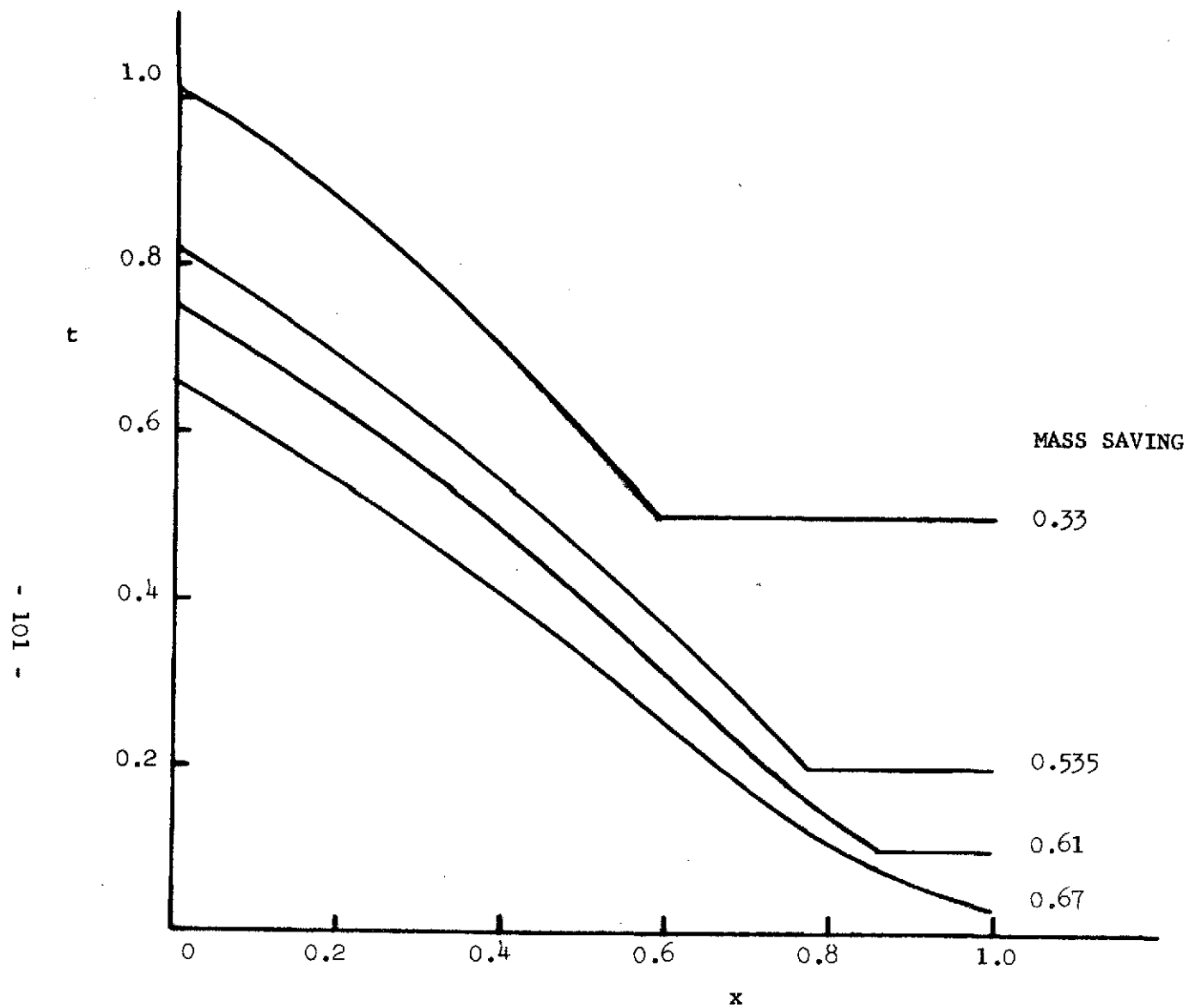
FIG. 5.1--Nondimensional depth distributions for minimum weight solid cantilever beam.
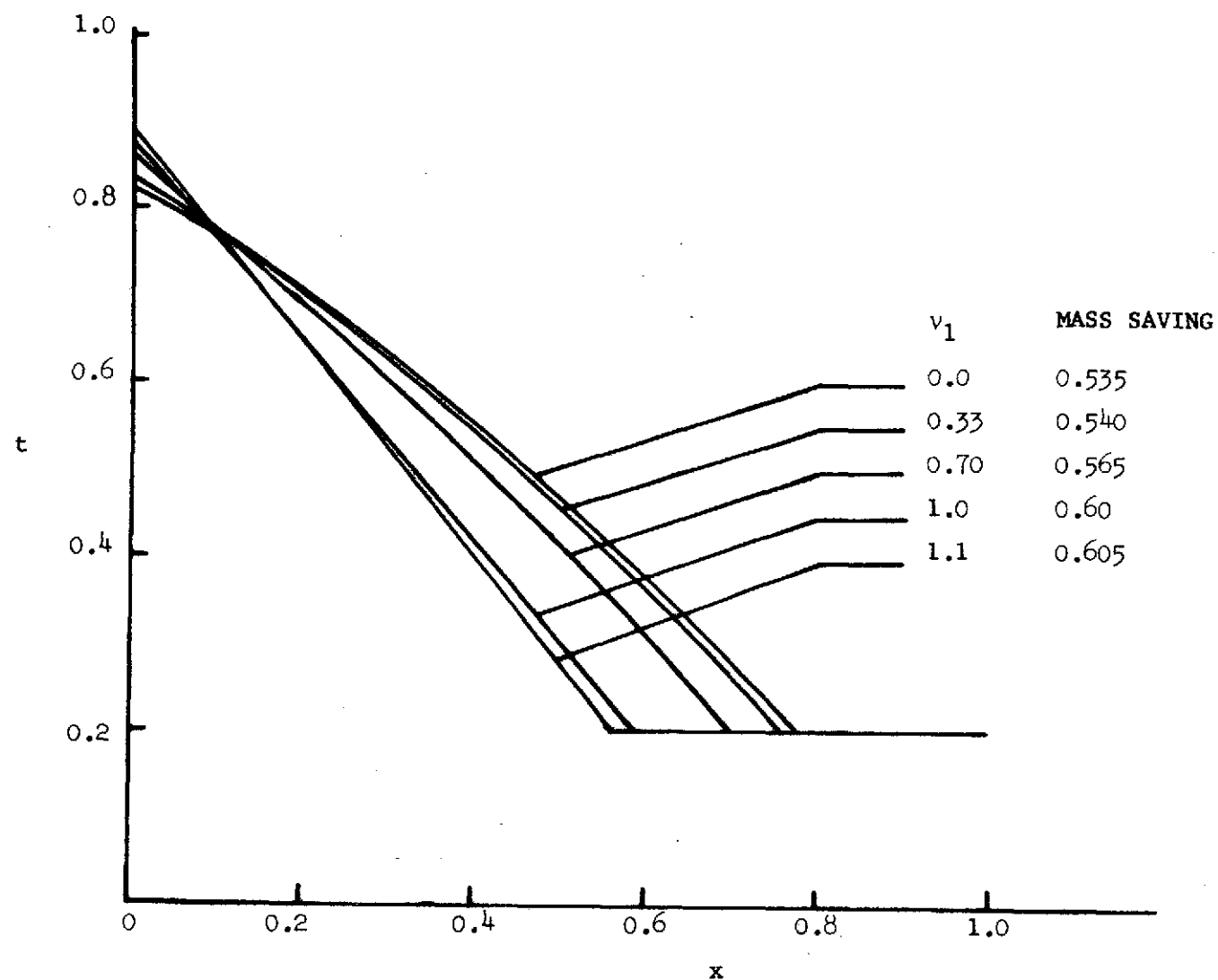
FIG. 5.2--Nondimensional depth distributions for minimum weight
rotating solid cantilever beam.

q , r and the adjoint variables λ_w , λ_p , λ_q , λ_r is valid. In fact, it can be easily verified from Eqs. (5.8), (5.9), (5.17), and (5.19). However, this relation is not possible if we include the equations

$$u' = -tx$$

$$\lambda_u' = -\lambda_r v_1^2 c^4 q / t^3 \tag{5.31}$$

in the above sets [Eqs. (5.26) and (5.27)] in addition to the terms due to rotation. Nevertheless, the equality [Eq. (5.28)] is valid. Therefore, we can write

$$\lambda_r = w/c_1^2 \tag{5.32}$$

where c_1 is a constant. Now, combining Eqs. (5.18) and (5.32), the optimality condition can be simplified as

$$3w''^2 t^2 - w^2 (v_R)_{11}^2 c^4 = c_1^2 (1 - \lambda_u x) - c^4 v_1^2 ww'x \tag{5.33}$$

Integrating the second equation of Eqs. (5.31), we obtain

$$\lambda_u x = -(v_R)_1^2 c^4 ww'x/c_1^2 + \frac{v_1^2 c^4 x}{c_1^2} \int_0^x w'^2 dx \tag{5.34}$$

- 103 -

Substitution of Eq. (5.34) into Eq. (5.33) leads to

$$3w''^2 t^2 - w^2 (\nu_R)^2_{11} c^4 = c_1^2 - \nu_1^2 c^4 x \int_0^x w'^2 dx \qquad (5.35)$$

Multiplying by t and integrating between 0 and 1 , we obtain

$$\int_0^1 3t^3 w''^2 dx - (\nu_R)^2_{11} c^4 \int_0^1 tw^2 dx$$

$$+ \nu_1^2 c^4 \int_0^1 \left(\int_x^1 \xi t d\xi \right) w'^2 dx = \int_0^1 c_1^2 t dx \qquad (5.36)$$

where ξ is a dummy variable. One can easily recognize that the first term is peak strain energy, the second term is peak kinetic energy, and the last term is peak potential energy of the equilibrium centrifugal forces.

Thus, the optimality condition [Eq. (5.35)] means that the optimal structure is characterized by the property that a linear combination of the peak kinetic energy density, the peak strain energy density, and the peak potential energy density of the equilibrium centrifugal forces is proportional to the design or optimization variable.

5.7 DISCUSSION OF RESULTS

The mass saving for a nonrotating cantilever beam is 0.67 at a minimum depth constraint of 0.01; on extrapolating for zero minimum constraint, the mass saving is 0.68. This number appears repeatedly

in these sorts of optimizations; indeed, it is interesting to compare it with the results reported for a sandwich beam with 50% structural mass in Fig. 4.4 of Ref. 5.9. The mass saving for this beam is 0.34. A linear extrapolation of this for a solid beam (100% structural mass) gives a mass saving of 0.68, which surprisingly coincides with the presently obtained value.

An increase in rotational speed increases the slope of the depth distribution as well as mass savings. Hence, quite sizable mass savings can be realized when only one vibration frequency is held constant. This is of particular engineering interest since this type of beam is used in some helicopter rotor configurations. Thus, if there are no constraints such as strength, aerodynamic shape, and blade flutter speed, great savings can be realized.

VI. THE EFFECT OF ROTATION IN AEROELASTICITY: THE WHIRL FLUTTER PROBLEM IN PROP-ROTORS

6.1 INTRODUCTION

The present chapter extends the study of the effects of rotation to aeroelastic problems. Virtually every VTOL aircraft configuration, and its base configurations (the helicopter, the propeller aircraft, and the turbo-prop aircraft) make use of propellers or rotors for thrust or lift. All these configurations present a rich source of problems involving the effects of rotation. One potential problem that demands careful attention is prop-rotor whirl flutter, which can occur in a flexibly supported aircraft-engine-prop-rotor combination. It involves coupling of elastic, inertial, gyroscopic, centrifugal, damping, and aerodynamic forces.

First the whirl flutter problem is briefly reviewed, and then, guided by the experience of the studies in the earlier chapters, the effects of two additional parameters — steady-state coning angle of the blades, and internal damping at the blade flapping hinges — are considered. The engine-nacelle-prop-rotor combination is represented by a concentrated mass and stiffness mathematical model. Although the continuum mathematical model is appropriate for the blades, the concentrated mass model is used in order to gain quick engineering

insight into this complex problem without extensive computation. With this model, all three types of rotors — the first, in which the blades are attached to the hub by hinges, free to flap up and down; the second, in which the blades are rigidly interconnected to a hub, but with the hub free to tilt with respect to the shaft; and the third, in which the blades are connected rigidly to the shaft — can be considered. The hinges of the freely flapping rotor may be located at varying distances from the axis of rotation.

The governing equations of motion with these two additional parameters included are derived in Appendix A by the Lagrangian approach using quasi-steady blade element theory for aerodynamic forces. The linearized analysis of these equations is applied to two wind tunnel models of previous investigations, and the effects of these new parameters on whirl flutter stability boundary are studied. The present results are compared with the earlier ones. It is shown that internal damping at the flapping hinges may help to resolve the disagreement between theory and experiment in some earlier investigations, and to explain why some investigations show good correlation between theory and experiment and some do not.

6.2 DISCUSSION OF THE PREVIOUS WORK

Reed [6.1] covered the early history, the mechanism, and the state-of-the-art of the whirl flutter problem and showed the existence of some gaps, particularly in correlating theory and experiment in the case of a flapped blade prop-rotor in the propeller mode of

operation. Comparing analytical and experimental results for two flap-
ping hinge offset cases, one 13% and the other 8%, with isotropic pylon
stiffnesses, he found that theory and experiment are in good agreement
for the 13% hinge offset case. However, the experimental model for the
8% hinge offset case fluttered in a forward whirl mode, and this forward
whirl flutter was not predicted by his analysis in spite of introducing
aerodynamic lag effects as high as 45°. Earlier to this work, a simi-
lar type of disagreement between theory and experiment was reported by
Richardson and Naylor [6.2]. This work was followed by an article by
Young and Lytwyn [6.3], who studied analytically the influence of flap-
ping restraint on the whirl flutter of a fully flapped rotor (a rotor
with only flapping hinges without any offset). They established the
existence of an optimum flapping frequency parameter $\omega_{\beta1}/\Omega_o$ between
1.1 and 1.2, depending on the ratio of the nacelle (pylon) stiffnesses
in the pitch and yaw directions, and that at the optimum condition
nacelle stiffness requirements for neutral stability are at a minimum.
Further, it was shown that forward whirl type instability is possible
if the pylon mounting is anisotropic, or the flapping frequency param-
eter is less than the optimum value.

Almost at the same time as Ref. 6.3, motivated by experience in
conducting an exploratory investigation of whirl flutter in high by-
pass ratio fan jet engines (Refs. 6.4 and 6.5), Kaza [6.6] studied
both analytically and experimentally the whirl flutter problem in
prop-rotors for two hinge offset positions (10% and 13.6%). Both
theory and experiment predicted backward whirl type instability for

both the hinge offset cases with isotropic pylon mounting, and the quantitative agreement is reasonably good. Also it was shown that an optimum flapping frequency parameter, similar to that of Ref. 6.3, exists through a combination of hinge offset and flapping spring restraint parameters. The possibility of both backward and forward whirl flutter is established when the pylon mounting is isotropic and the flapping frequency parameter is less than approximately 1.05. Moreover, the dominant mode is backward whirl in the range 1.05 to 0.95, and forward whirl in the range 0.95 and less, of the flapping frequency parameter for isotropic pylon mounting. Thus, this study indicates the possibility of forward whirl even when the system is mounted isotropically. However, both this study and that of Ref. 6.3 are unable to defend the experimental observations of Ref. 6.1 for the 8% hinge offset case and those of Ref. 6.2.

In attempting to explain the disagreement between theory and experiment for the 8% hinge offset case, Gaffey [6.7] assumed that the flapping hinge also acts as a lead-lag hinge. This assumption opened the room for the possibility of forward whirl instability for both the 8% and the 13% hinge offset cases, and surprisingly the theory and experiment for the 8% case compare well. However, the forward whirl instability due to the lead-lag motion for the 13% case was not at all encountered in the wind tunnel. Evidently, the disagreement was still unresolved. Recently, Baird, Bauer, and Kohn [6.8] presented results of a parametric study on whirl flutter. This study includes variations of blade pitch-flap coupling, flap hinge offset, pylon damping,

and pylon stiffness. A good agreement between theory and experiment was reported for both the 5% and the 13% hinge offset cases.

More recently, almost at the same time as the present work, Kvaternik [6.9] presented results of experimental studies on whirl flutter, those of joint NASA/Bell Helicopter investigations of a 0.133-scale, semispan, dynamic, aeroelastic model in the NASA-Langley Transonic Dynamic Tunnel, and a comparison with theoretical results. Analytical results were shown to be in good agreement with measured dynamic characteristics. Kvaternik also covered the mechanism of whirl flutter in proprotors and gave a comprehensive list of references on the subject. His study also included a small steady-state coning angle of the blades and a small damping at the flapping hinges. Confining his model to within the covered range of these parameters, Kvaternik reported that an increase in coning angle has a destabilizing effect, and an increase in flap damping has a stabilizing effect on whirl flutter. Though this study shows good correlation between theory and experiment, apparently it does not aid in resolving the disagreement between theory and experiment noticed in Refs. 6.1 and 6.2.

6.3 STATEMENT OF THE PRESENT PROBLEM

The problems considered in the previous chapters suggest that damping may be a factor for the disagreement between theory and experiment. Also, the results of Ref. 6.6 show the possibility for predominant forward whirl flutter if the flapping frequency parameter is less than approximately 0.95, which is possible according to Section 3.7 if there

exists a steady-state coning angle of the blades. In fact, a small

coning angle results in practice from the balance between centrifugal,

gravity and aerodynamic forces at the unperturbed steady-state condi-

tion of the rotor in the case of flapped blade systems, or from the

steady flap bending in the case of rotors with flexible blades attached

rigidly to the hub. Therefore, in the present study this parameter is

also considered. Also, Loewy [6.10] pointed out that the coning angle

may be the source of error for the discrepancy between theory and ex-

periment.

The problem of this chapter is to study in depth the influence of

these new parameters on the whirl flutter boundary. The contents of

this chapter are summarized in a paper by Kaza [6.11].

6.4 MATHEMATICAL MODEL

The discretised mathematical model shown in Fig. 6.1 consists of

N $(N \geq 3)$ ideally rigid blades, restrained elastically with equal

spring constants at the flapping hinges. A viscous type of damping,

which may be due to friction at the flapping hinge in the case of

flapped rigid blade rotors, or may be due to hysteresis type damping

of the blade material in the case of rotors with flexible blades rig-

idly attached to the hub, is considered. This rotor system along with

an ideally rigid pylon or nacelle is restrained elastically in pitch

and yaw at a distance h from the rotor plane. A viscous type of

damping is also assumed in the pitch and yaw directions. This dy-

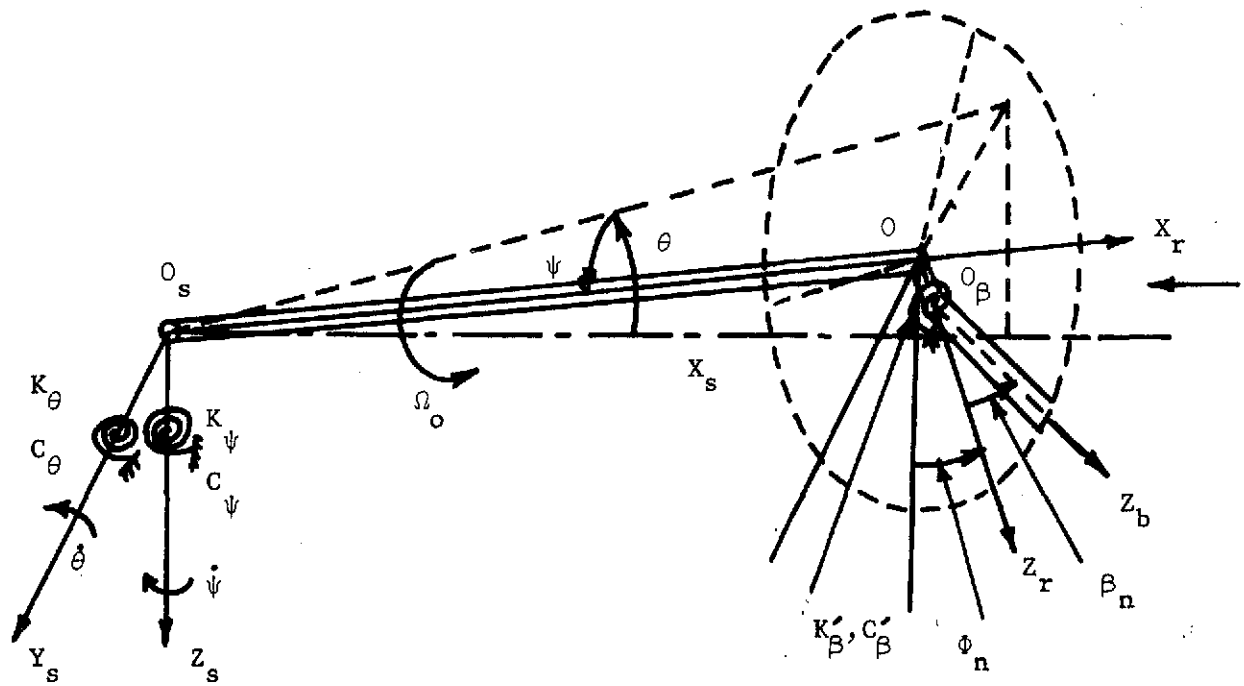namic system has $N + 2$ degrees of freedom with respect to a rotating

FIG. 6.1--Mathematical model of the system.

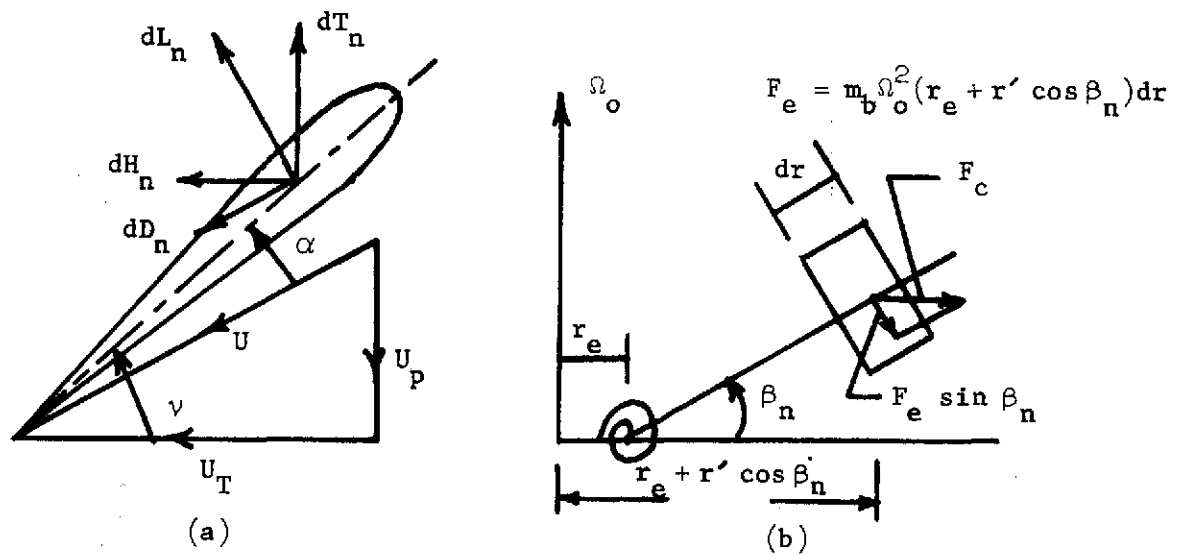$$F_e = m_b \Omega_o^2 (r_e + r' \cos \beta_n) dr$$

(a)

(b)

FIG. 6.2--A typical blade element.

observer. The rotor blades also have a steady-state coning angle β_o, which is due to the balance between centrifugal, gravity, and aerodynamic forces at the unperturbed steady-state position of the rotor in the case of flapped blade systems or due to a built-in angle, in the case of rotors with flexible blades attached rigidly to the hub. If $N \geq 3$, the rotor has rotational symmetry. Consequently, the N degrees of freedom of the rotor blades may conveniently be reduced to two degrees of freedom through quasi-coordinates, namely, the pitch flap angle β_θ and yaw flap angle β_ψ. Since attention is directed to the propeller mode of operation of the prop-rotor, the resulting equations of motion are free from time dependent coefficients.

Quasi-steady blade element theory is used to generate the aerodynamic coefficients. A typical blade element and velocities experienced by it are shown in Fig. 6.2. The quasi-steady blade element theory is justified mainly because the vorticity shed by the blades is carried away from the propeller plane at a much faster rate than that associated with the helicopter in forward flight. In addition to wake effects, several other assumptions, which are quite common in whirl flutter stability analysis, are made. They are: 1) no compressibility effects; 2) no aerodynamic forces on pylon and spinner; 3) the blade airfoil is symmetric with constant chord along the span; 4) lift coefficient is 2π and profile drag coefficient is a quadratic function of angle of attack; and 5) no induced velocity due to thrust. All these assumptions are self-explanatory except the last one, which is justified since the disc loading in the propeller mode of airplane

- 113 -

mode of operation is less than that in the hover mode. No restriction is imposed on the value of the steady-state coning angle β_0 .

Finally, the governing equations of motion of this mathematical model are derived in Appendix A. They are a set of four simultaneous, ordinary, coupled second order differential equations with respect to a space fixed coordinate system.

6.5 MATHEMATICAL ANALYSIS

The system with the blade motion β_θ , and β_ψ fixed, and with the coning angle β_0 set equal to zero, is considered. This has two degrees of freedom, pitch and yaw. These are uncoupled in the absence of rotation. When the rotation is introduced, these two motions are coupled. The higher frequency one is called forward whirl and the lower frequency one backward whirl.

When the pitch and yaw freedoms of the pylon are locked, the rotor blade has an undamped flapping frequency $\omega_{\beta 1}$, and a damped frequency $\omega_{\beta 1 d} = \omega_{\beta 1} \sqrt{1 - \zeta_\beta^2}$ with respect to the rotating observer. In the absence of steady coning angle β_0 and damping ζ_β , the flapping frequency $\omega_{\beta 1 d}$ varies from Ω_0 to infinity. The lower limit corresponds to an ideally rigid blade without an elastic restraint at the flapping hinge, which is located on the axis of rotation, and the upper limit corresponds to an ideally rigid blade attached rigidly to the hub. But in the presence of the coning angle β_0 and the damping ζ_β , the lower limit of $\omega_{\beta 1 d}$ will be less than Ω_0 , depending on the value of β_0 . When the blade motions are expressed with respect to a space

fixed coordinate system, the flapping frequency $\omega_{\beta 1d}$ is split into

two frequencies, $-\Omega \pm \omega_{\beta 1d}$ and $\Omega \pm \omega_{\beta 1d}$. The frequencies occur

in pairs as expected from a gyroscopic system. The rotor tip path

plane has two types of motions, depending on the parameters, with re-

spect to a stationary observer. When $\Omega_o < \omega_{\beta 1d}$, the two positive

frequencies are $-\Omega + \omega_{\beta 1d}$ and $\Omega_o + \omega_{\beta 1d}$. The first one corres-

ponds to a backward whirl mode and the second one to a forward whirl

mode of the rotor tip path plane with respect to a stationary observer.

For the case $\Omega_o > \omega_{\beta 1d}$, the two positive frequencies are $\Omega_o + \omega_{\beta 1d}$

and $\Omega_o - \omega_{\beta 1d}$, both representing the forward whirl modes of the tip

path plane of the rotor. Thus the presence of the coning angle and

damping ζ_β may even change the rotor model characteristics, depending

on the other parameters.

The governing Eqs. (A.37) of motion of the model in a uniform, in-

compressible, and inviscid flow at a speed V are derived in Appendix

A.

Assuming

$$\{q\} = \{q_o\} e^{(\mu_o + i\gamma)\tau} = \{q_o\} e^{\mu\tau} \qquad (6.1)$$

Eqs. (A.37) can be written as

$$[D]\{Q\} = -\frac{1}{\mu}\{Q\} \qquad (6.2)$$

where

$$[D] = \begin{bmatrix} [D_0] & [D_1] \\ -[1] & [0] \end{bmatrix}$$

$$[D_1] = \Big[[SS] - [AS]\Big]^{-1} [AN]$$

$$[D_0] = \Big[[SS] - [AS]\Big]^{-1} \Big[[SD] - [AD]\Big]$$

$$\{Q\} = \begin{Bmatrix} q_o \\ \mu q_o \end{Bmatrix} \qquad\qquad (6.3)$$

This is a standard eigenvalue problem. The eigenvalues are four complex conjugate pairs, two pairs for the pylon and two pairs for the rotor. The general solution of the system will be obtained if we consider the eigenvalues only with positive imaginary parts. The associated eigenvectors will determine the direction of the whirl mode. When the flapping frequency $(\omega_{\beta 1d})$ of the blade with damping and aerodynamics included is greater than Ω_o , there are two backward whirl modes with frequencies $\omega_1 = \gamma_1 \Omega_o$ (pylon backward) and $\omega_3 = \gamma_3 \Omega_o$ (rotor backward), and two forward whirl modes with frequencies $\omega_2 = \gamma_2 \Omega_o$ (pylon forward) and $\omega_4 = \gamma_4 \Omega_o$ (rotor forward). But when $\omega_{\beta 1d} < \Omega_o$ the backward rotor mode changes to forward whirl, and there will be three forward whirl modes and one backward whirl mode. The system is critical when the real part (μ_o) of any one of the eigenvalues is zero. Keeping all the parameters, ϵ , β_o , ζ_β , ζ_θ , ζ_ψ , $\omega_\beta/\omega_\theta$, ℓ_h , $\omega_\psi/\omega_\theta$, λ , α_o and c as constants, Ω_o/ω_θ is varied

until the system is unstable in one or possibly more than one mode. The stability boundaries are obtained using the complex eigenvalue algorithm (Ref. 6.12).

As mentioned earlier, this analysis is applied to two models, the 8% and 13% model of Ref. 6.1, and a fully flapped ($\epsilon = 0$) version of the model of Ref. 6.6. Most of the parameters of these models are taken from the appropriate references. Some parameters for the 8% model of Ref. 6.1 were obtained through private communication from Reed. The additional parameters needed to consider the effect of coning angle are calculated from the available data. Finally, all these parameters are tabulated in Table 6.1.

6.6 RESULTS AND DISCUSSION

The main attention is focused on the effect of β_0 and ζ_β on an isometrically mounted pylon system, which is the most critical case from the flutter point of view. $\omega_\beta/\omega_\theta$ is also included since the effect of β_0 and ζ_β depends on it.

The effect of coning angle and flapping restraint stiffness on flutter speed is shown in Fig. 6.3 for the model of Ref. 6.6. Depending on the system parameters, either whirl flutter or static divergence may be possible in all except one of the modes, the rotor high frequency forward mode. However, which mode is predominant depends on the parameters β_0, $\omega_\beta/\omega_\theta$. The magnitude of the critical speed strongly depends on both β_0 and $\omega_\beta/\omega_\theta$. For each coning angle β_0, there exists an optimum flapping frequency ratio $\omega_\beta/\omega_\theta$ at which the flutter

- 117 -

TABLE 6.1

Parameters of the Models Used in Whirl Flutter Calculations

Parameter	Fully Flapped Model, Ref. 6.6	8% Case Ref. 6.1	13% Case Ref. 6.1
a	2π	2π	2π
c (at 3/4R), ft	0.167	0.0835	0.0835
J	1.27	1.10	1.10
I_θ slug-ft^2	385.0×10^{-4}	1.31×10^{-4}	1.31×10^{-4}
I_o slug-ft^2	0.0	0.037×10^{-4}	0.0495×10^{-4}
I_1 slug-ft^2	30.0×10^{-4}	0.3816×10^{-4}	0.3816×10^{-4}
I_2 slug-ft^2	30.0×10^{-4}	0.298×10^{-4}	0.2586×10^{-4}
I_β slug-ft^2	30.0×10^{-4}	0.261×10^{-4}	0.2090×10^{-4}
I_{ho} slug-ft^2	34.35×10^{-4}	0.2320×10^{-4}	0.2320×10^{-4}
1_h	0.4318	0.25	0.25
N	4	4	4
R, ft.	1.042	0.5	0.5
ϵ	0.0	0.08	0.137
$\zeta_\theta, \zeta_\psi, \zeta_\beta$	varied	varied	varied

TABLE 6.1 (Cont'd)

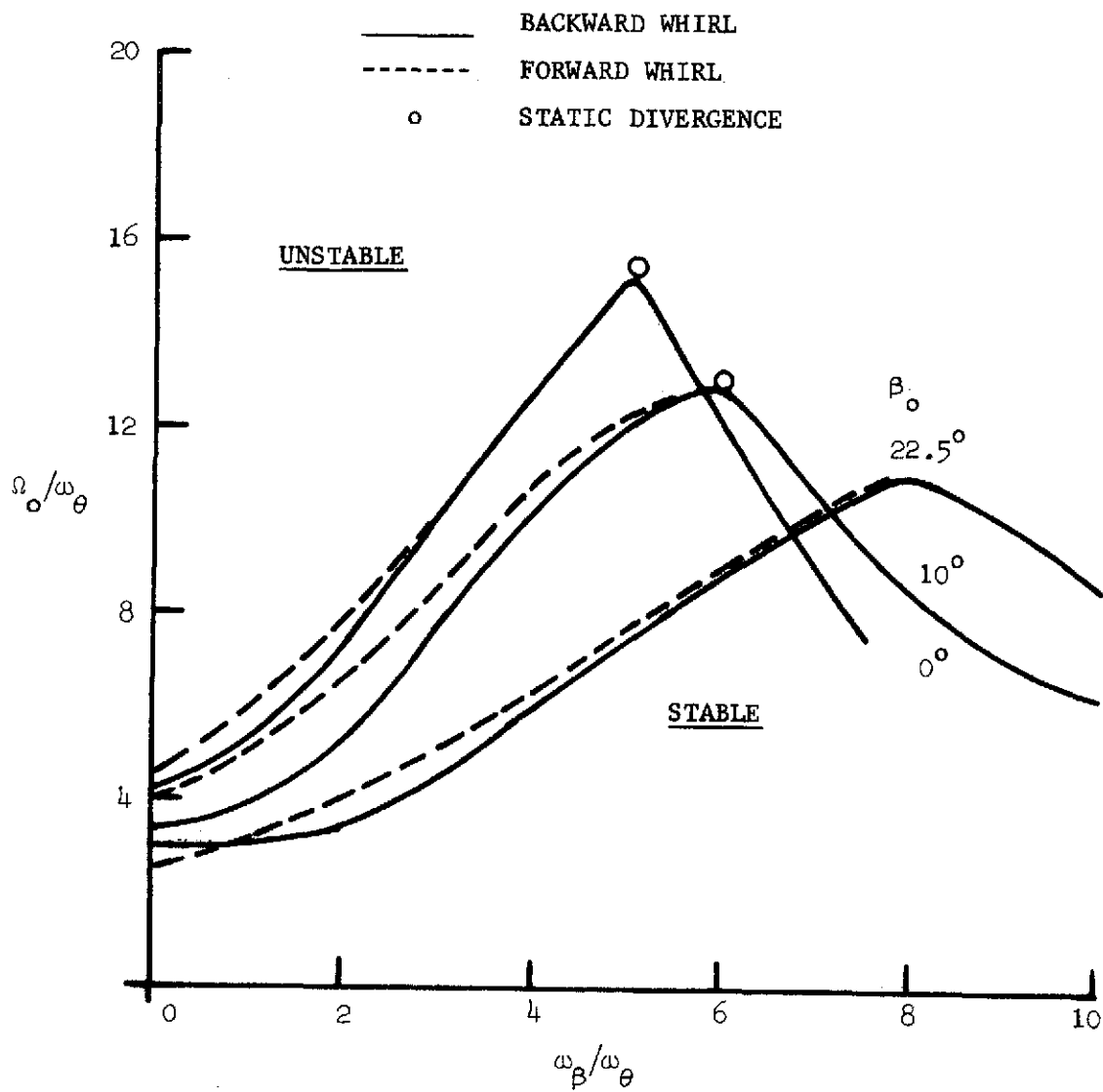| Parameter	Fully Flapped Model, Ref. 6.6	8% Case Ref. 6.1	13% Case Ref. 6.1
α_o	0.0	0.0	0.0
γ_θ	varied	varied	varied
β_o	varied	varied	varied
K_{DO}	0.0087	0.0087	0.0087
K_{D1}	-0.0216	-0.0246	-0.0216
K_{D2}	0.40	0.40	0.40

FIG. 6.3--Effect of flapping restraint and coning angle on
flutter speed -- $\epsilon = 0$; $\omega_\theta/\omega_\psi = 1$; $\zeta_\theta = \zeta_\psi = 0.02$;
$\zeta_\beta = 0$ (see Table 6.1).

speed is maximum, and below that value there is a possibility of forward type whirl flutter even when the system pylon mounting is isotropic. At the optimum condition, the flapping frequency of the rotor with respect to a rotating coordinate system is $\omega_{\beta 1} = \Omega_o [\cos 2\beta_o + (\omega_\beta/\omega_\theta)^2 (\omega_\theta/\Omega_o)^2]^{\frac{1}{2}}$, where Ω_o/ω_θ is the associated flutter speed. In the present case, this value is approximately $1.05 \, \Omega_o$ for all values of β_o considered, and it is in agreement with those of Refs. 6.3 and 6.6. Hence, it appears that the optimum condition can be achieved either by changing β_o or $\omega_\beta/\omega_\theta$. However, an increase in β_o causes a decrease in flutter speed when $\omega_{\beta 1}$ is less than $1.05 \, \Omega_o$, and an increase in flutter speed if $\omega_{\beta 1}$ is greater than $1.05 \, \Omega_o$. In view of the fact that both the flutter speed and its mode are very sensitive to $\omega_{\beta 1}$ in the range $1.00 \, \Omega_o$ to $1.1 \, \Omega_o$ which, in turn, depends on β_o , one must include β_o in the analysis, even for the windmilling case, where β_o is minimum. In fact, the models tested in Refs. 6.1, 6.2, and 6.6 have $\omega_{\beta 1}$ in the range $1.05 \, \Omega_o$ to $1.20 \, \Omega_o$ without any β_o effect. Figure 6.4 is a cross plot of Fig. 6.3, showing explicitly the effect of β_o on both flutter speed and mode for the case of a fully flapped rotor without an elastic restraint spring at the flapping hinge and with isotropic pylon mounting. Both pylon backward and forward modes flutter. The backward mode is predominant between 0° and 15° of coning and the forward mode takes the lead when the coning is more than 15°. The overall effect is a decrease in flutter speed with an increase in coning.

Next, the effect of coning for the case of a hinge offset blade rotor is considered. The parameters used are those of the 8% hinge
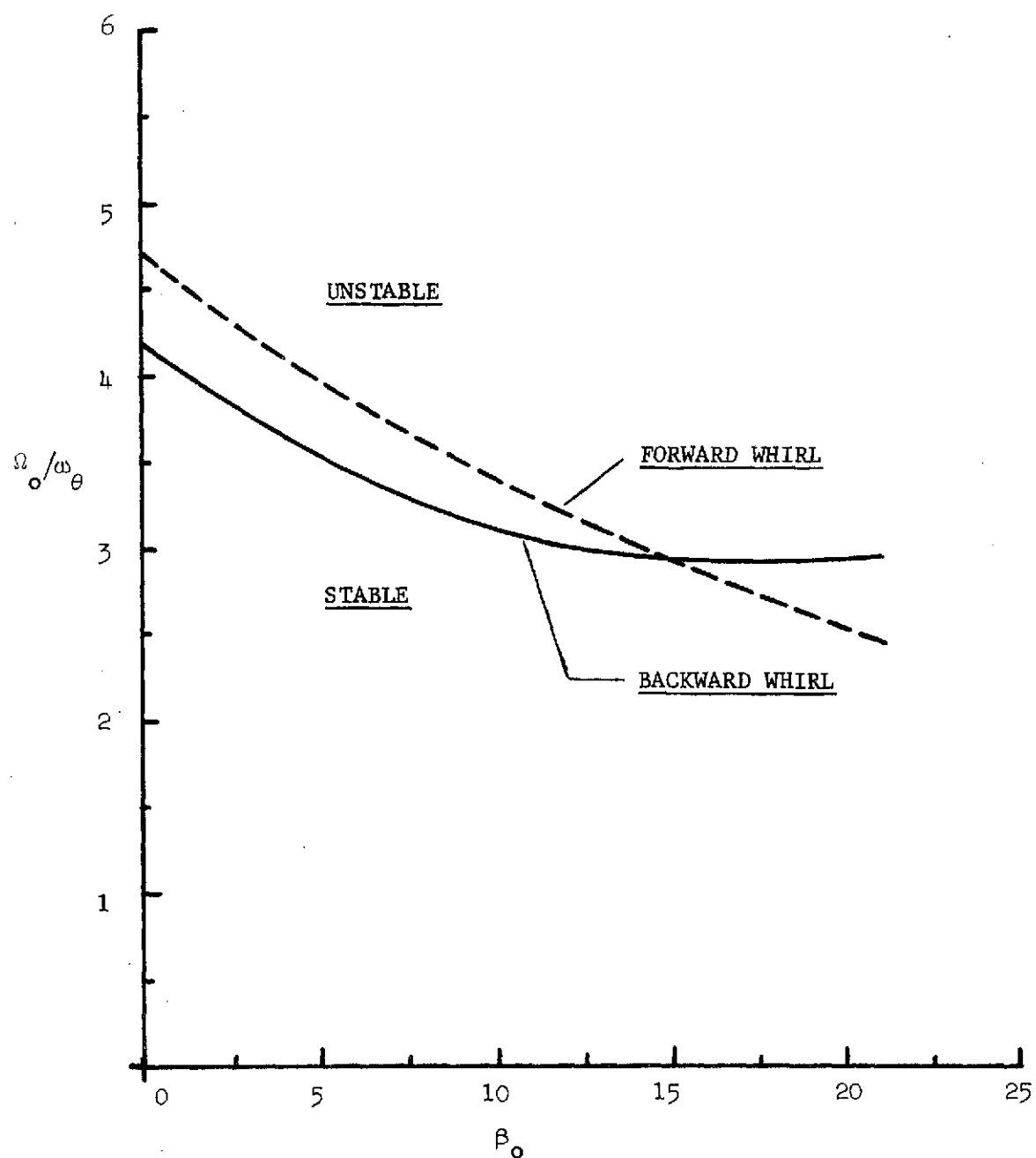
FIG. 6.4--Effect of coning angle on flutter speed — $\epsilon = 0$; $\omega_\theta/\omega_\psi = 1$; $\zeta_\theta = \zeta_\psi = 0.02$; $\zeta_\beta = 0$ (see Table 6.1).

offset model with windmilling blades of Ref. 6.1. The range of β_o is extended to the negative side in order to account for the windmilling case. The flapping frequency of the rotor with respect to a rotating observer is given by $\omega_{\beta 1} = \Omega_o [\cos 2\beta_o + \cos \beta_o \ I_o/I_\beta + (\omega_\beta/\omega_\theta)^2 (\omega_\theta/\Omega_o)^2]^{\frac{1}{2}}$. Figure 6.5 shows the effect of coning angle on the aforesaid model without elastic restraints at the blade hinges. An increase in β_o from -5° to about 7° causes an increase in flutter speed, and from there onwards it not only causes a decrease in flutter speed but also destabilizes the pylon forward mode in addition to the backward mode. However, the predominant flutter mode is backward except in the range 6° to 8°, which corresponds to $\omega_{\beta 1d} = 1.05 \ \Omega_o$. Studying closely Figs. 6.4 and 6.5, one can quickly conclude that the effects of β_o , ϵ , and $\omega_\beta/\omega_\theta$ can be integrated as the effect of $\omega_{\beta 1}$ if β_o is positive. But when the propeller is windmilling, β_o is negative, and hence its effect should be considered explicitly. At the optimum condition both divergence and flutter occur almost at the same speed, as in the case of a fully flapped rotor. This model exhibited a forward whirl instability in the wind tunnel. Both the analysis of Ref. 6.1 and the present one for $\beta_o = 0$ predicted a backward whirl flutter, and they are in good agreement. This model in the windmilling case might have a coning angle anywhere in between -5° and -2°. In this range there is no possibility for forward flutter as expected from experiment. However, a forward whirl flutter at a much higher speed than observed in the wind tunnel is possible when β_o is in the vicinity of 7.5^o. On further increasing β_o to 15°, the predominant flutter mode changed
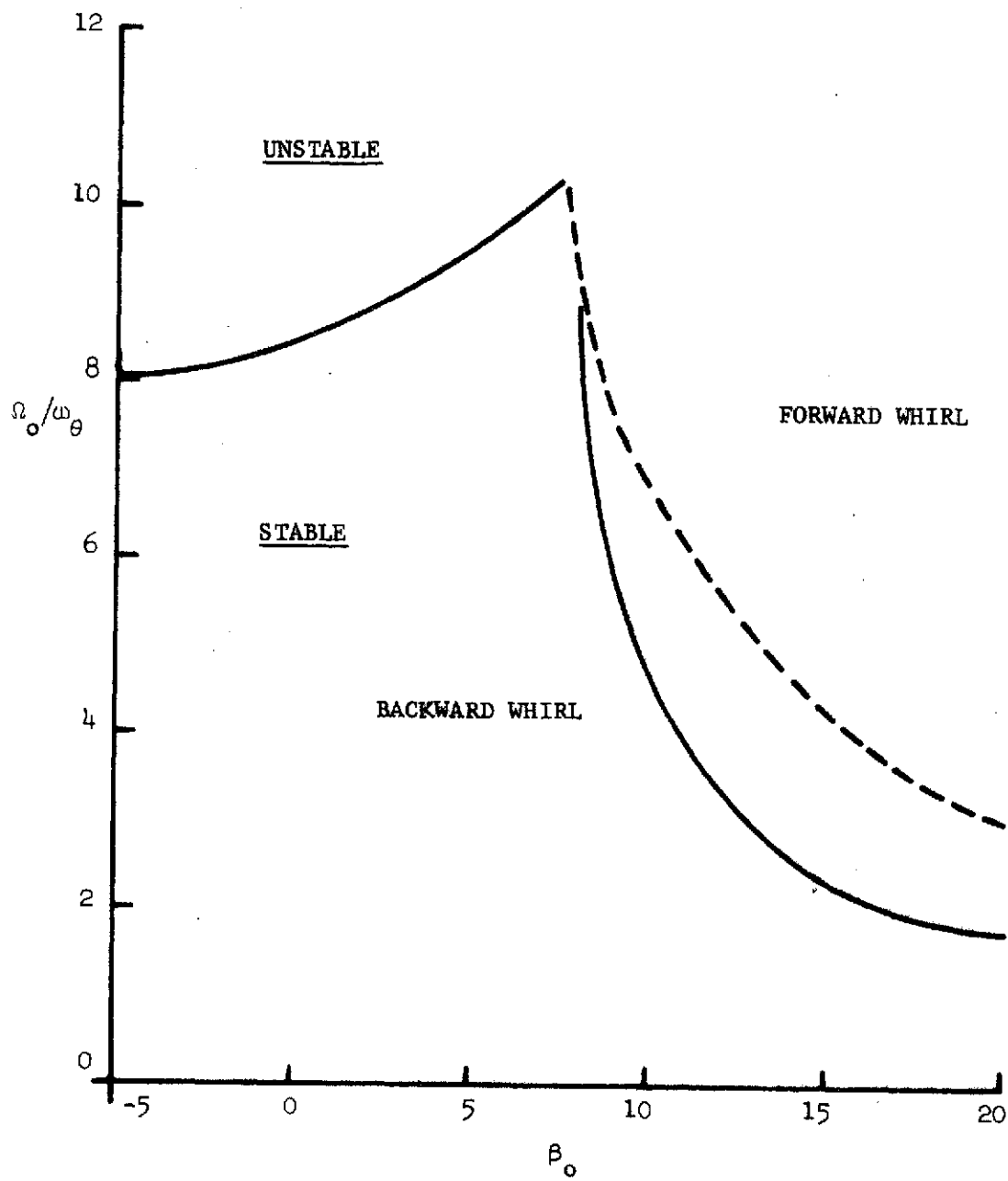
FIG. 6.5--Effect of coning angle on flutter speed — $\epsilon = 0.08$; $\omega_\theta/\omega_\psi = 1$; $\zeta_\theta = \zeta_\psi = 0.04$; $\zeta_\beta = 0$ (see Table 6.1).

from forward to backward. The magnitude of this backward speed is in agreement with that of the forward speed noticed in the tunnel. Thus the effect of the coning angle may not be the reason for the disagreement between theory and experiment on this model, but it certainly has a marked influence on the stability, both divergence and flutter.

The effect of ζ_β on the flutter speed for the case of fully flapped rotors with $\omega_\beta/\omega_\theta$ as a parameter is shown in Figs. 6.6(a) and 6.6(b) for two values of β_0. The damped flapping frequency of the rotor is given by $\omega_{\beta 1 d} = \omega_{\beta 1} \sqrt{1 - \zeta_\beta^2}$, with respect to the blade fixed axis system. It is observed that a small amount of damping ζ_β (4% of critical) at the flapping hinge not only changes the predominant flutter mode from backward to forward but also reduces the flutter speed. This effect is analogous to that of internal damping in the rotor as discussed in Ref. 3.9. The difference in flutter speed between the pylon backward and forward modes decreases with an increase in the elastic restraint parameter $\omega_\beta/\omega_\theta$ and finally changes the predominant mode to backward whirl as expected.

Extending this study on the effect of flap damping to hinge offset bladed rotors, the parameters of the 8% and the 13% hinge offset models are selected. Unfortunately, the data on damping at the flapping hinge are not available, and hence the flutter boundary ζ_β versus Ω_0/ω_θ, with β_0 as a parameter, is shown in Fig. 6.7. Pylon damping effects in the presence of flap damping are also included in Fig. 6.7(b). As in the case of fully flapped rotors, the damping at the flapping hinge continuously reduces the backward flutter speed. It might even
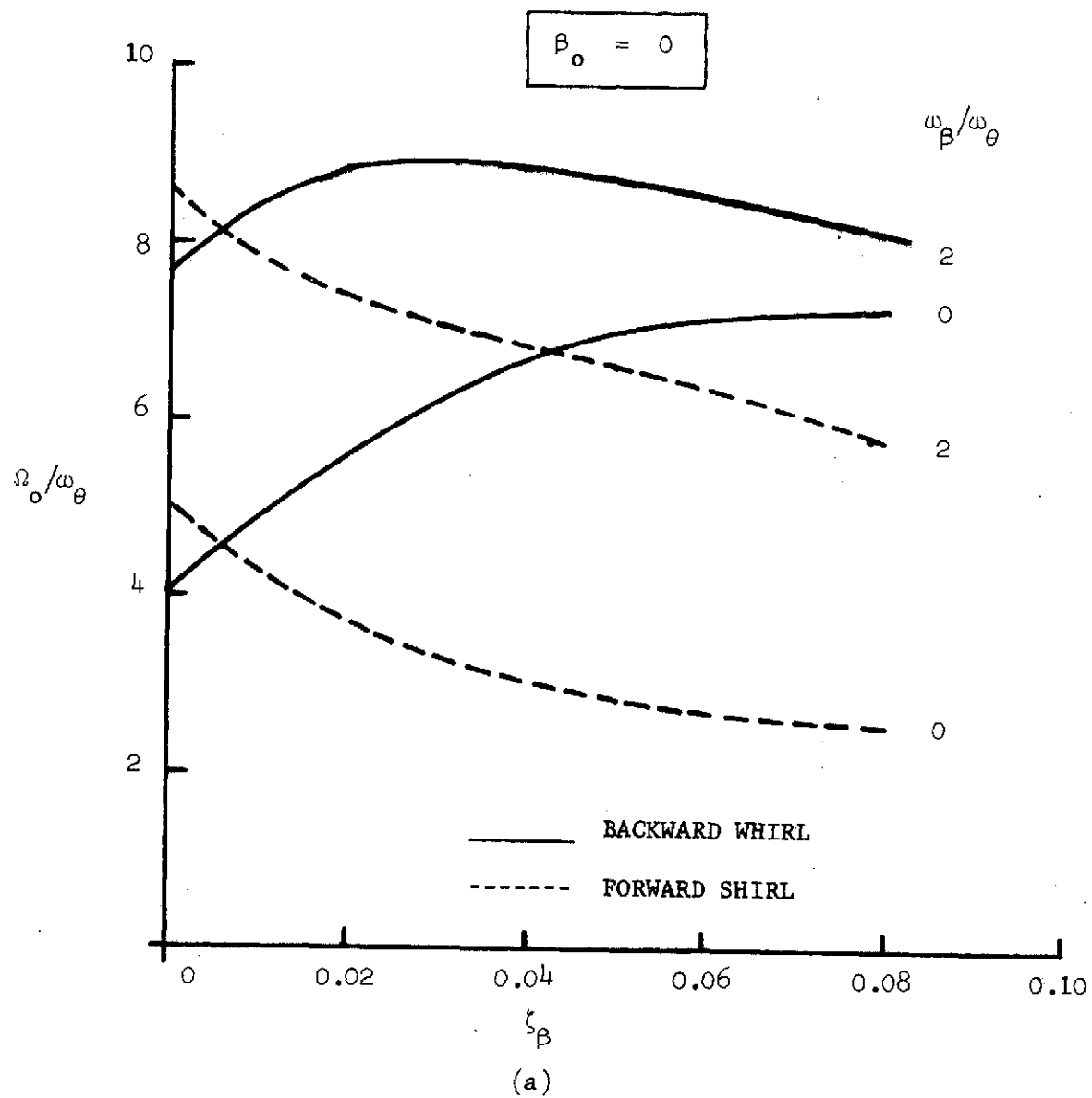
FIG. 6.6--Effect of flap damping on flutter speed — $\epsilon = 0$; $\omega_\theta/\omega_\psi = 1$; $\zeta_\theta = \zeta_\psi = 0.02$ (see Table 6.1).
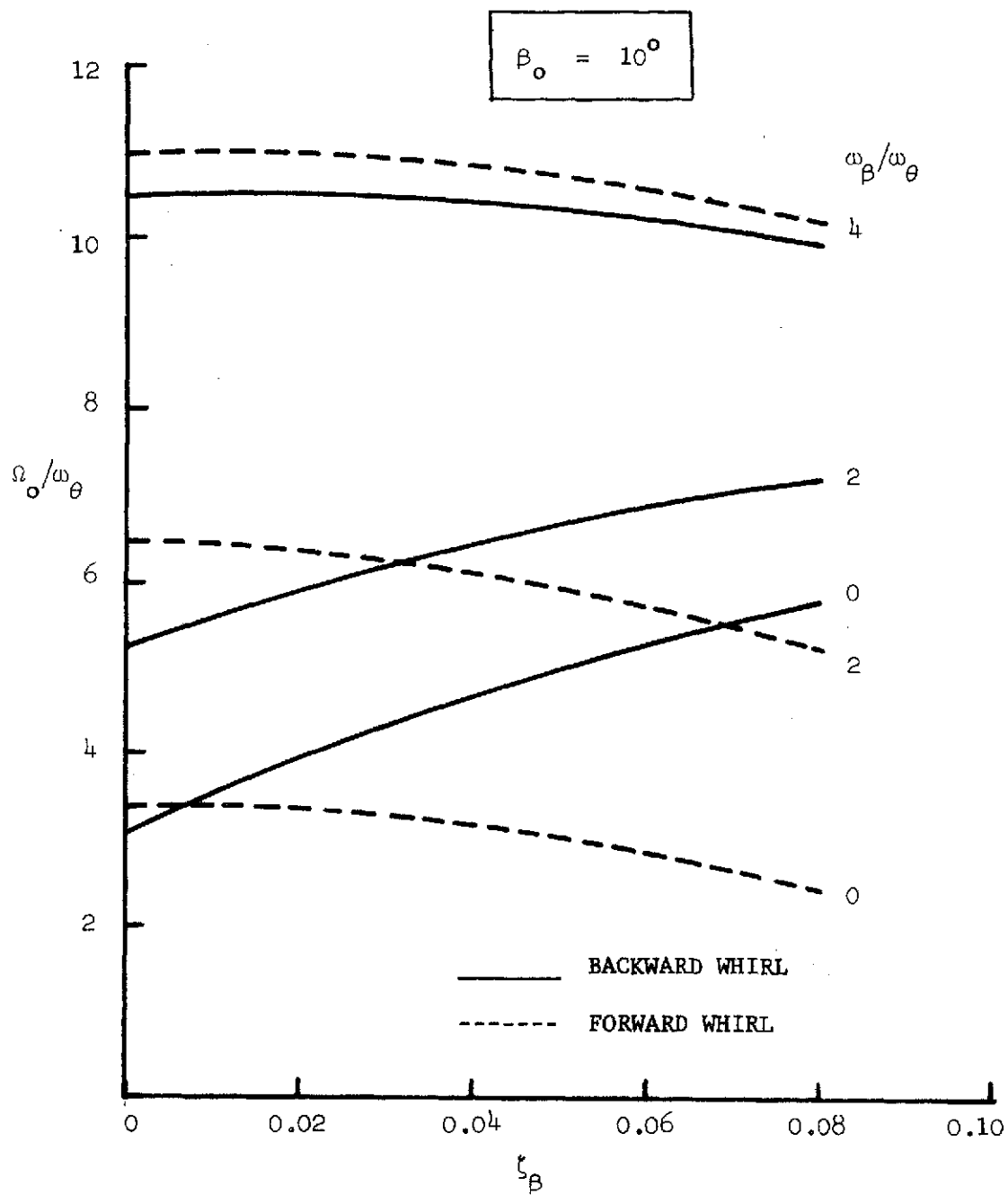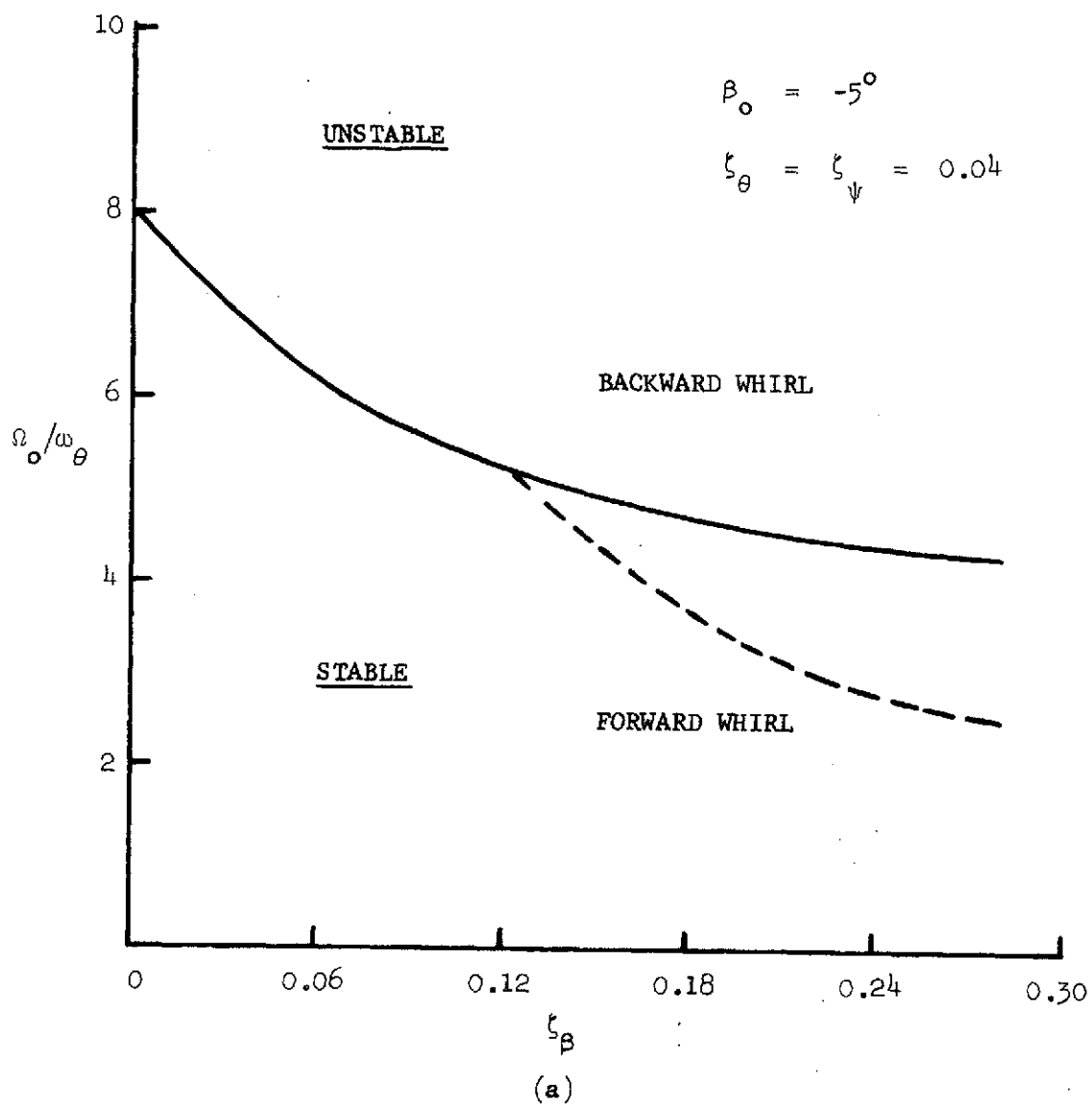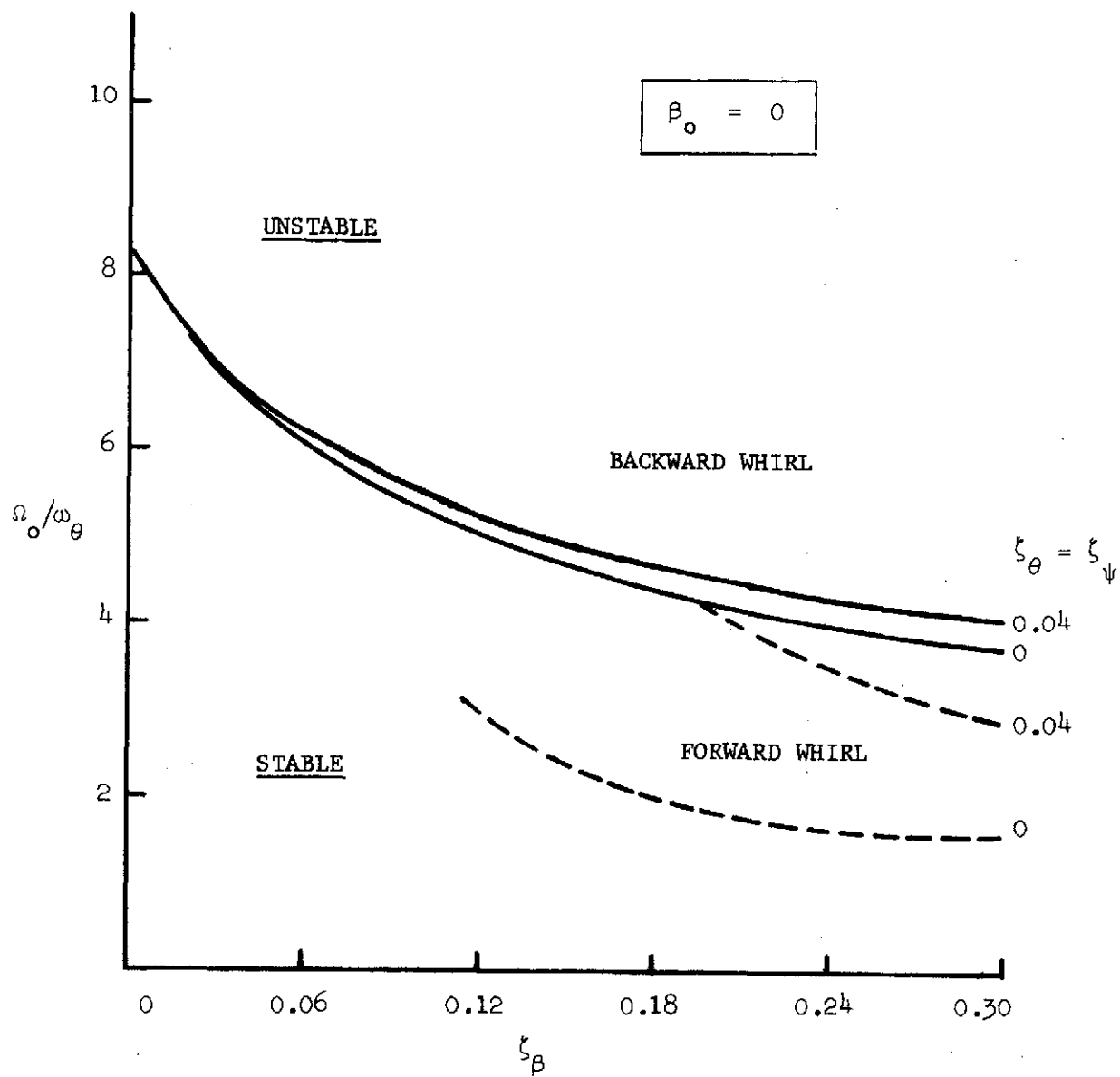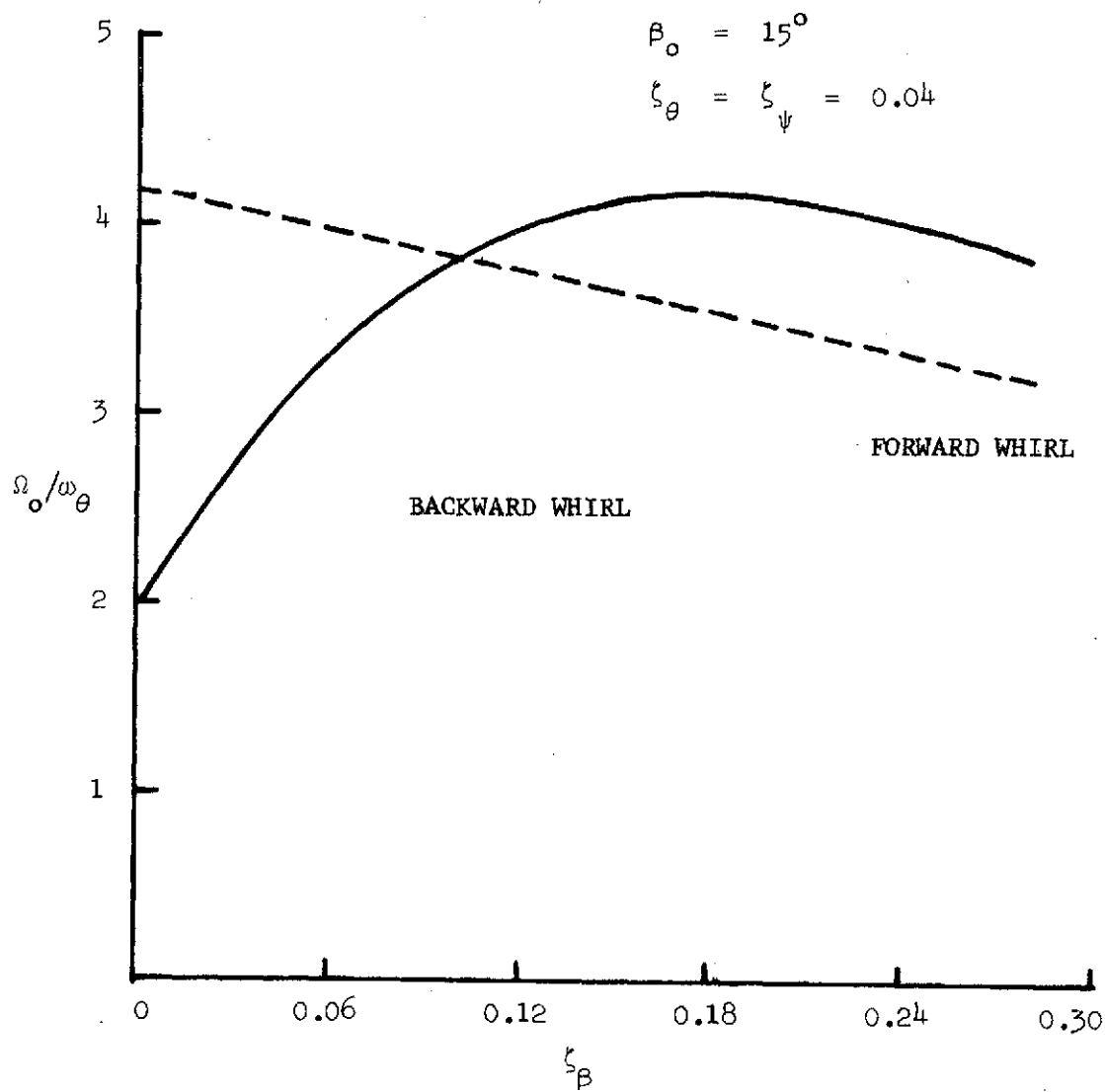
FIG. 6.6--Concluded.

FIG. 6.7—Influence of flap damping on flutter speed —
$\epsilon = 0.08$; $\omega_\beta/\omega_\theta = 0$; $\omega_\theta/\omega_\psi = 1$ (see Table 6.1).

FIG. 6.7--Continued.

$\beta_o = 15°$

$\zeta_\theta = \zeta_\psi = 0.04$

FORWARD WHIRL

BACKWARD WHIRL

(c)

FIG. 6.7--Concluded.

destabilize the forward whirl mode at a much lower speed than that of the backward whirl mode when ζ_β is more than 0.16. Also, when $\zeta_\beta = 0$, pylon damping has no appreciable effect on flutter speed. When ζ_β is more than 0.12, pylon damping has a very little effect on backward whirl mode instability and has a marked stabilizing effect on forward whirl instability. Comparing the present value of the flutter speed, Ω_o/ω_θ $= 8.4$ at $\zeta_\beta = 0$, $\beta_o = 0$, with the corresponding one $(\Omega_o/\omega_\theta = 8.4)$ evaluated from Fig. 9 of Ref. 6.1, shows that they are in good agreement. However, the present theory does not account for aerodynamic lag effects whereas Ref. 6.1 does. But when $\zeta_\beta \geq 0.1$, and ζ_θ and ζ_ψ lie in the range 0 to 0.04, the predominant flutter mode is forward and the speed Ω_o/ω_θ lies in the range 1.7 to 3.5. Hence, the forward flutter instability observed in the wind tunnel within the range Ω_o/ω_θ $= 1.32$ and 2.4 (from Fig. 9, Ref. 6.1) may be due to damping at the flapping hinge.

Figures 6.8 and 6.9 summarize the calculations for the 13% hinge offset model. The variations of both real and imaginary parts of the eigenvalues with Ω_o/ω_θ are shown in Fig. 6.8 along with the corresponding ones of Ref. 6.1. Comparing these results, the agreement is very good. The difference in the variation of damping for the rotor backward whirl mode may be due to the fact that we assumed an aerodynamic phase lag of zero whereas a lag of 15° was assumed in Ref. 6.1. The flutter mode is backward rotor whirl as observed in the wind tunnel.

The next question concerns the effect of ζ_β on the flutter speed for this case. The answer is in Fig. 6.9, which shows the variation of
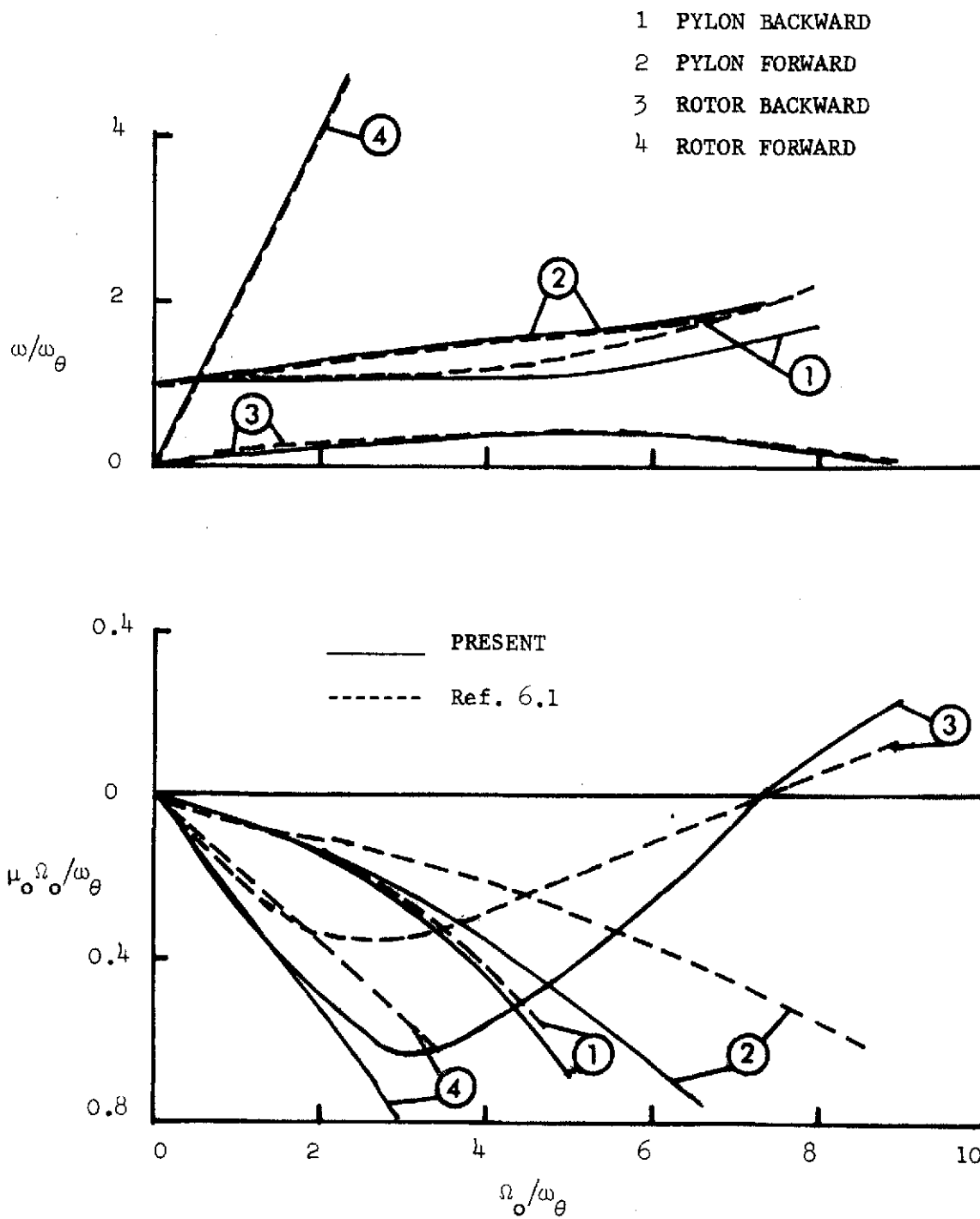
FIG. 6.8--Calculated flapping blade whirl modes — $\epsilon = 0.137$; $\omega_\theta/\omega_\psi = 1.0$; $\omega_\beta = 0$; $\beta_o = 0$; $\zeta_\beta = 0$ (see Table 6.1)
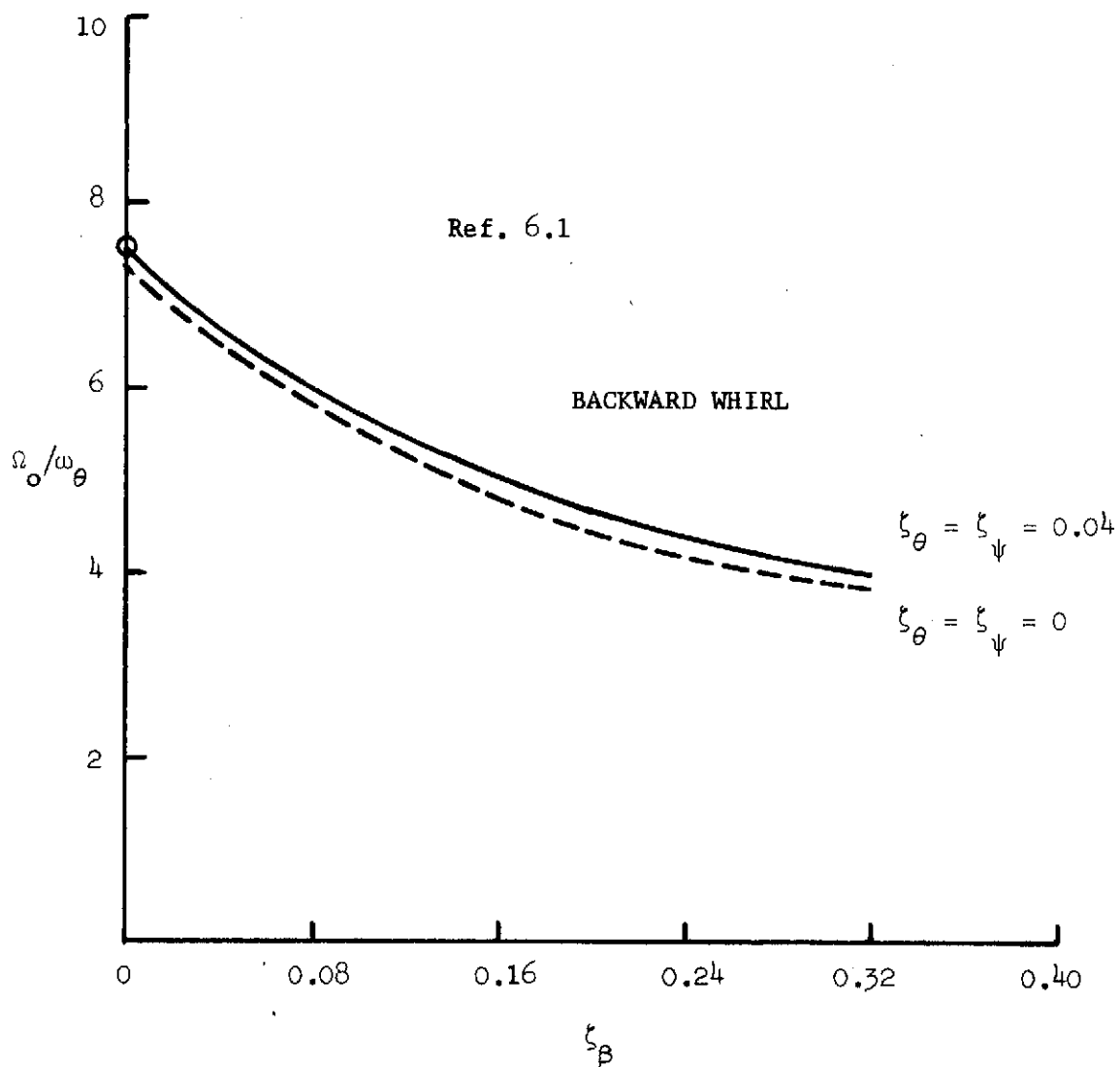
FIG. 6.9--Influence of flap damping on flutter speed — $\epsilon = 0.137$; $\omega_\theta/\omega_\psi = 1$; $\omega_\beta = 0$; $\beta_o = 0$ (see Table 6.1).

flutter speed with ζ_β , with ζ_θ/ζ_ψ as a parameter. It can be seen that there is no possibility for forward whirl flutter for ζ_β in the range 0 to 0.32, unlike the 8% hinge offset case. This reversal in the ζ_β effect is due to an increase in the flapping frequency parameter $\omega_{\beta 1}$, which increases with the hinge offset parameter ϵ . This is precisely what is expected from the calculations of a fully flapped rotor for large values of the flapping restraint parameter $\omega_\beta/\omega_\theta$; see Fig. 6.6(b). From Fig. 6.9, again it is clear that pylon damping has no appreciable effect on flutter speed.

In summary, it is seen that internal damping and coning angle have a marked influence on whirl flutter stability, depending on other parameters. In fact, the internal damping at the flapping hinge not only changes the flutter speed but also its predominant mode, depending on the other parameters. It is believed that a proper account of this internal damping might help to explain why some investigations show good correlation between theory and experiment and some do not.

VII. CONCLUSIONS

This dissertation covers four areas, vibration, stability, optimization, and aeroelasticity, considering elastic continuum models and concentrated mass and stiffness models. This study is undertaken with the following objectives: a) to group together at least some, if not all, of the problems involving effects of rotation; b) to identify the common features of this class of problems; c) to use this experience and observations profitably to study some problems which have not yet received a special treatment of their own, such as the stability of a coned beam and the least weight design of a rotating beam with a constraint on fundamental flapping frequency; and d) extrapolate this information for better understanding of the whirl flutter problem in flapped blade prop-rotors, particularly to resolve existing disagreement between theory and experiment in some earlier investigations under certain conditions.

At the outset, it is realized that the continuum mathematical model in the presence of rotation has a practical limit to the class of problems for which analytical solutions are possible. Adapting the common engineering philosophy that the understanding of any problem is helped if its relation to other problems is appreciated, the equations of motion of a general unrestrained, deformable, and rapidly rotating body are developed. The explicit need for the nonlinear theory of

elasticity under certain conditions is emphasized. Some common features such as the choice of axis system, self-adjointness, the phenomenon of frequency splitting, shortcomings of stability methods as applied to gyroscopic systems, and the consequent need for introduction of imperfections to extract all the instabilities by kinetic method of stability, are identified and discussed.

On the basis of a linear theory, vibration and stability of a rotating coned beam is examined. It is seen that the beam has several interesting bands of instability depending on the coning angle and the rotational speed. It must be pointed out that we assumed that the bearings are rigid and axially symmetric. If the beam is unsymmetric, and the bearings are considered to be flexible and also unsymmetric, the equations of motion will contain periodic coefficients. The solution of such partial differential equations is not at all possible at present. Numerically exact frequencies of the beam are obtained, and these results are used to validate approximate methods.

The field of parameter optimization and optimal control theory techniques are briefly reviewed, and a start is made in applying these techniques to simple rotating systems. Though these continuum models have practical limits as stated earlier, it is believed that these results can be extrapolated to understand the behavior of complicated systems. Optimum depth distributions of a solid rotating cantilever beam are obtained with rotational speed as a parameter and with a fixed first flapping frequency. It is shown that, even in the presence of

rotation, the optimal structure is characterized by the condition that Lagrangian density is constant.

Finally, guided by the experience of the above general study, the effect of two parameters — steady coning angle of the blades and internal damping at the flapping hinges — on whirl flutter in prop-rotors are studied. It is shown that these two parameters have a marked influence on stability. The effect of this internal damping for a certain range of model parameters is discovered to be analogous to that of internal damping in gyroscopic systems. It is also shown that this internal damping may help to resolve the disagreement between theory and experiment in the earlier investigations under certain conditions.

The study on the effect of rotation has not been completed in its entirety but several useful observations have been made and the experience gained has been applied to some practical cases. There is a vast amount of work to be done. Some examples are the dynamic response of a rotating coned blade with random inputs, the influence in depth of internal and external damping in gyroscopic systems, and continuation of optimization studies in rotating systems with aeroelastic constraints.

APPENDIX A

EQUATIONS OF MOTION USED IN WHIRL FLUTTER STUDY

The mathematical model of an idealized dynamical system considered here is shown in Fig. 6.1. The governing equations of motion are derived with respect to an inertial coordinate system using the classical Lagrangian approach and quasi-steady blade element aerodynamic theory. The coordinates of a point on the blade with respect to the inertial axis system X_s , Y_s , Z_s , 0_s can be written as

$$\{\bar{x}_s\} = \begin{Bmatrix} x_s \\ y_s \\ z_s \end{Bmatrix} = \begin{bmatrix} [T_\theta][T_\psi] & [T_\phi][T_{\beta_n}] \begin{Bmatrix} x_b \\ y_b \\ z_b \end{Bmatrix} \\ + [T_\phi] \begin{Bmatrix} x_e \\ y_e \\ z_e \end{Bmatrix} + \begin{Bmatrix} x_c \\ y_c \\ z_c \end{Bmatrix} \end{bmatrix} \qquad (A.1)$$

where

$$[T_\phi] = \begin{bmatrix} \cos\theta & 0 & \sin\theta \\ 0 & 1 & 0 \\ -\sin\theta & 0 & \cos\theta \end{bmatrix} \qquad (A.2)$$

and

$$[T_\psi] = \begin{bmatrix} \cos\psi & -\sin\psi & 0 \\ \sin\psi & \cos\psi & 0 \\ 0 & 0 & 1 \end{bmatrix} \qquad (A.3)$$

$$[T_\phi] = \begin{bmatrix} 1 & 0 & 0 \\ 0 & \cos\phi_n & -\sin\phi_n \\ 0 & \sin\phi_n & \cos\phi_n \end{bmatrix} \qquad (A.4)$$

$$[T_{\beta_n}] = \begin{bmatrix} \cos\beta_n & 0 & \sin\beta_n \\ 0 & 1 & 0 \\ -\sin\beta_n & 0 & \cos\beta_n \end{bmatrix} \qquad (A.5)$$

Aligning the Z_b axis along the axis of the Nth blade, the position vector of an arbitrary point on the axis with respect to a blade fixed axis system is

$$\begin{Bmatrix} x_b \\ y_b \\ z_b \end{Bmatrix} = \begin{Bmatrix} 0 \\ 0 \\ r' \end{Bmatrix} \qquad (A.6)$$

When the hinge offset of the blades is uniform, the position vector of the flapping hinge of the Nth blade is

$$\left\{ \begin{array}{c} x_e \\ y_e \\ z_e \end{array} \right\} = \left\{ \begin{array}{c} 0 \\ 0 \\ r_e \end{array} \right\} \tag{A.7}$$

Considering the case that the pylon is restrained elastically in pitch and yaw directions at an equal distance from the propeller center, we can write the position vector of the point O as

$$\left\{ \begin{array}{c} x_c \\ y_c \\ z_c \end{array} \right\} = \left\{ \begin{array}{c} h \\ 0 \\ 0 \end{array} \right\} \tag{A.8}$$

Analogous to $\overline{x}_s$, the position vector of an arbitrary point on the axis of the symmetric nacelle with respect to the inertial axis system becomes

$$\{\overline{x}_{gn}\} = \left\{ \begin{array}{c} x_{gn} \\ y_{gn} \\ z_{gn} \end{array} \right\} = [T_\theta][T_\psi] \left\{ \begin{array}{c} s \\ 0 \\ 0 \end{array} \right\} \tag{A.9}$$

The expression for the total kinetic energy of the system is

$$T = \frac{1}{2} \sum_{n=1}^{N} \int_{0}^{R} \{\dot{x}_s\}^T \{\dot{x}_s\} \, dm_b + \frac{1}{2} \int_{0}^{h} \{\dot{x}_{gn}\}^T \{\dot{x}_{gn}\} \, dm_n \qquad (A.10)$$

All the ingredients required in this equation are given by Eqs. A.1 to A.9. The flapping angle β_n of the Nth blade is expressed with respect to the rotating coordinate system X_r , Y_r , Z_r and 0 . However, this can also be expressed conveniently for the case of rigid blades with respect to the inertial coordinate system X_s , Y_s , Z_s and 0_s through quasi-coordinates β_θ and β_ψ and a steady-state coning angle β_0 as

$$\beta_n = \beta_0 + \bar{\beta}_n = \beta_0 + \beta_\theta \cos \phi_n + \beta_\psi \sin \phi_n \qquad (A.11)$$

This simplification is possible because the other possible patterns of the blade motion do not couple with the pylon freedoms. Considering $\bar{\beta}_n$ as small, we can further write

$$\cos \beta_n = \cos \beta_0 - \bar{\beta}_n \sin \beta_0 - \frac{\cos \beta_0}{2} \bar{\beta}_n^2$$

$$\sin \beta_n = \sin \beta_0 + \bar{\beta}_n \cos \beta_0 - \frac{\sin \beta_0}{2} \bar{\beta}_n^2 \qquad (A.12)$$

Since θ and ψ are small, the trigonometric functions of these co-ordinates can be expanded in power series, and the terms higher than

the second order can be neglected. The azimuth angle ϕ_n for N

equispaced blades can be written as

$$\phi_n \;=\; \phi + \frac{2}{N} \,(N-1) \tag{A.13}$$

where

$$\phi \;=\; \Omega t \tag{A.14}$$

Substituting Eqs. A.11, A.12, A.13 and A.14 into Eq. A.10 and

applying Lagrange's equation (Ref. 2.1), we obtain the following gen-

eralized inertial forces:

$$P_\theta \;=\; \Omega^2 \,\{\overline{I}_\theta \theta'' + I_2 \beta''_\theta + 2\overline{I}_1 \psi'$$

$$+\; [I_\beta (1 + \cos 2\beta_o) + 2I_o \cos \beta_o]\, \beta'_\psi\} \tag{A.15}$$

$$P_\psi \;=\; \Omega^2 \,\{\overline{I}_\psi \psi' + I_2 \beta'_\psi - 2\overline{I}_1 \theta'$$

$$-\; [I_\beta (1 + \cos 2\beta_o) + 2I_o \cos \beta_o]\, \beta'_\theta\} \tag{A.16}$$

$$P_{\beta_\theta} \;=\; \Omega^2 \,\{I_\beta \beta''_\theta + 2I_\beta \beta'_\psi + I_2 \theta''$$

$$+\; [I_\beta (\cos 2\beta_o - 1) + I_o \cos \beta_o]\, \beta_\theta\}$$

$$+\; [I_\beta (1 + \cos 2\beta_o) + 2I_o \cos \beta_o]\, \beta' \tag{A.17}$$

and

$$P_{\beta_\psi} = \Omega^2 \{ I_\beta \beta_\psi'' + I_2 \psi'' - 2 I_\beta \beta_\theta'$$

$$+ \beta_\psi [(I_\beta \cos 2\beta_o - 1) + I_o \cos \beta_o]$$

$$- [I_\beta (1 + \cos 2\beta_o) + 2 I_o \cos \beta_o] \theta' \} \qquad (A.18)$$

where

$$I_1 = \frac{N}{2} \int_O^R m_b r^2 dr$$

$$\overline{I}_1 = I_1 + I_\beta (\cos^2 \beta_o - 1) + 2 I_o (\cos \beta_o - 1)$$

$$I_\beta = \frac{N}{2} \int_{r_e}^R m_b r'^2 dr$$

$$I_o = \frac{N}{2} \int_{r_e}^R m_b r_e r' dr$$

$$I_N = \frac{1}{2} \int_O^h m_n s^2 ds$$

$$I_2 = I_\beta + I_o \cos \beta_o + \frac{I_{ho}}{2} \sin \beta_o$$

$$I_{ho} = Nh \int_{r_e}^R r' m_b dr \qquad \text{(Cont'd)}$$

- 143 -

and

$$M = N \int_{0}^{R} m_b \, dr$$

$$\overline{Mh}^2 = Mh^2 + 2I_{ho} \sin \beta_o + 2I_{\beta} \sin^2 \beta_o$$

$$I_{\theta} = I_1 + Mh^2 + I_N$$

$$\overline{I}_{\theta} = (I_{\theta} - 2I_o) + 2I_o \cos \beta_o$$
$$+ \ I_{\beta} \sin^2 \beta_o + 2I_{ho} \sin \beta_o$$

$$I_{\psi} = I_1 + Mh^2 + I_N$$

$$\overline{I}_{\psi} = (I_{\psi} - 2I_o) + 2I_o \cos \beta_o$$
$$+ \ I_{\beta} \sin^2 \beta_o + 2I_{ho} \sin \beta_o$$

$$\tau = \Omega_o t$$

$$(\ )' = \frac{1}{\Omega_o} (\dot{ })$$

(Cont'd)

and

$$(\ )'' = \frac{1}{\Omega_o^2} (\ddot{\ })$$

$$\left. \begin{array}{rcl} \displaystyle\sum_{n=1}^{N} \sin^2 \phi_n & = & \dfrac{N}{2} \\[4mm] \displaystyle\sum_{n=1}^{N} \cos^2 \phi_n & = & \dfrac{N}{2} \\[4mm] \displaystyle\sum_{n=1}^{N} \sin \phi_n \cos \phi_n & = & 0 \end{array} \right\} \quad \text{for} \quad N \geq 3 \qquad \text{(A.19)}$$

The potential energy due to linear elastic springs in the pitch, yaw, and flapping modes can be written as

$$U_{PE} = \frac{1}{2} K_\theta \theta^2 + \frac{1}{2} K_\psi \psi^2 + \frac{1}{2} K_\beta' \sum_{n=1}^{N} \bar{\beta}_n^2 \qquad \text{(A.20)}$$

Substituting Eqs. A.11, A.12, A.13 and A.14 into the above equation, we get

$$U_{PE} = \frac{1}{2} (K_\theta \theta^2 + K_\psi \psi^2) + \frac{N}{2} K_\beta' \beta_\theta^2 + \frac{N}{2} K_\beta' \beta_\psi^2 \qquad \text{(A.21)}$$

Then the generalized elastic forces S_i follow from Eq. A.21

$$S_\theta = \bar{I}_\theta \gamma_\theta^2 \Omega^2 \theta \qquad \text{(Cont'd)}$$

- 145 -

and

$$S_\psi = \bar{I}_\psi \gamma_\psi^2 \Omega^2 \psi$$

$$S_{\beta_\theta} = I_\beta \gamma_\beta^2 \Omega^2 \beta_\theta$$

$$S_{\beta_\psi} = I_\beta \gamma_\beta^2 \Omega^2 \beta_\psi \tag{A.22}$$

where

$$\gamma_\theta = \frac{\omega_\theta}{\Omega_o} = \left(\frac{K_\theta}{\bar{I}_\theta}\right)^{\frac{1}{2}} \frac{1}{\Omega_o}$$

$$\gamma_\psi = \frac{\omega_\psi}{\Omega} = \left(\frac{K_\psi}{\bar{I}_\psi}\right)^{\frac{1}{2}} \frac{1}{\Omega_o}$$

$$\gamma_\beta = \frac{\omega_\beta}{\Omega_o} = \left(\frac{K_\beta}{I_\beta}\right)^{\frac{1}{2}} \frac{1}{\Omega_o}$$

$$K_\beta = K_\beta' \frac{N}{2} \tag{A.23}$$

A viscous type of damping is assumed in the θ, ψ, and β_n motions. Then the dissipation potential is given by

$$D_C = \frac{1}{2} C_\theta \dot{\theta}^2 + \frac{1}{2} C_\psi \dot{\psi}^2 + \frac{1}{2} C_\beta' \sum_{n=1}^{N} \dot{\beta}_n^2 \tag{A.24}$$

Again the Lagrangian equations lead to the following generalized damping forces

$$d_\theta \;=\; 2\Omega_o^2 \bar{I}_\theta \gamma_\theta \zeta_\theta \theta'$$

$$d_\psi \;=\; 2\Omega_o^2 \bar{I}_\psi \gamma_\psi \zeta_\psi \psi'$$

$$d_{\beta_\theta} \;=\; 2\Omega_o^2 I_\beta \gamma_{\beta 1} \zeta_\beta (\beta_\theta' + \beta_\psi)$$

$$d_{\beta_\psi} \;=\; 2\Omega_o^2 I_\beta \gamma_{\beta 1} \zeta_\beta (\beta_\psi' - \beta_\theta) \qquad\qquad \text{(A.25)}$$

where

$$\zeta_\theta \;=\; \frac{C_\theta}{2\bar{I}_\theta \omega_\theta}$$

$$\zeta_\psi \;=\; \frac{C_\psi}{2\bar{I}_\psi \omega_\psi}$$

$$\zeta_\beta \;=\; \frac{C_\beta}{2I_\beta \omega_{\beta 1}}$$

$$C_\beta \;=\; \frac{N}{2}\, C_\beta'$$

$$\gamma_{\beta 1} \;=\; \left(\cos 2\beta_o + \frac{I_o}{I_\beta} \cos \beta_o + \gamma_\beta^2 \right)^{\frac{1}{2}} \qquad\qquad \text{(A.26)}$$

The quasi-steady aerodynamic forces are derived from the well known blade element theory of the propeller. A typical blade element is illustrated in Fig. 6.2. The elemental lift and drag expressions are given by

$$dL_n = \frac{1}{2} \rho c U^2 C_\ell dr$$

$$dD_n = \frac{1}{2} \rho c U^2 C_d dr \qquad (A.27)$$

where

$$C_\ell = a\alpha$$

$$C_d = K_{d0} + K_{d1}\alpha + K_{d2}\alpha^2 \qquad (A.28)$$

By resolving dL_n and dD_n, the elemental thrust dT_n and the elemental inplane force dH_n can be obtained as

$$dT_n = \frac{1}{2} \rho c dr \left\{ aUU_T \left(\nu - \tan^{-1} \frac{U_p}{U_T} \right) - UU_p \left[K_{d0} + K_{d1} \left(\nu - \tan^{-1} \frac{U_p}{U_T} \right) \right. \right.$$

$$\left. \left. + K_{d2} \left(\nu - \tan^{-1} \frac{U_p}{U_T} \right)^2 \right] \right\} \qquad \text{(Cont'd)}$$

and

$$dH_n = \frac{1}{2} \rho c d r \left\{ a U U_p \left(v - \tan^{-1} \frac{U_p}{U_T} \right) + U U_T \left[K_{d0} + K_{d1} \left(v - \tan^{-1} \frac{U_p}{U_T} \right) \right. \right.$$

$$\left. \left. + K_{d2} \left(v - \tan^{-1} \frac{U_p}{U_T} \right)^2 \right] \right\} \qquad (A.29)$$

where U_p and U_T are the perpendicular and inplane components of velocity in blade fixed coordinates.

Referring to Fig. 6.1, the velocity vector with respect to the inertial axis system is given by

$$\overline{V}_s = \left\{ \begin{array}{c} -V - \dot{x}_s \\ - \dot{y}_s \\ - \dot{z}_s \end{array} \right\} \qquad (A.30)$$

From Eqs. A.1 and A.30 the velocity components experienced by a blade element can be written as

$$\left\{ \begin{array}{c} \dot{x}_b \\ \dot{y}_b \\ \dot{z}_b \end{array} \right\} = \left\{ \begin{array}{c} -U_p \\ U_T \\ U_r \end{array} \right\} = \left\{ [T_{\beta_n}]^t [T_\varphi]^t [T_\psi]^t [T_\theta]^t \right\} \{ \overline{V}_s \} \qquad (A.31)$$

Expansion of Eq. A.31 yields

$$U_p = V(\cos\theta\cos\psi\cos\beta_n - \cos\theta\sin\psi\sin\varphi_n\sin\beta_n$$

$$- \sin\theta\cos\varphi_n\sin\beta_n) + \dot\theta\cos\psi\cos\varphi_n(r + h\sin\beta_n)$$

$$+ \dot\psi\sin\varphi_n(r + h\sin\beta_n) + r'\dot\beta_n$$

$$U_T = V(\cos\theta\sin\psi\cos\varphi_n - \sin\theta\sin\varphi_n)$$

$$+ r\dot\theta(\sin\psi\cos\beta_n + \cos\psi\sin\varphi_n\sin\beta_n)$$

$$+ h\dot\theta\sin\varphi_n\cos\psi - r\dot\psi\cos\varphi_n\sin\beta_n$$

$$- h\dot\psi\cos\varphi_n + r'\Omega\cos\beta_n + r_e\Omega + r_e\dot\theta\sin\psi \qquad (A.32)$$

The elemental force vector $\{dF_n\}$ in the inertial system follows from Eqs. A.1 and A.29

$$\{dF_n\} = [T_\theta][T_\psi][T_\varphi][T_\beta] \begin{Bmatrix} dT_n \\ dH_n \\ 0 \end{Bmatrix} \qquad (A.33)$$

From the principle of virtual work, the generalized aerodynamic forces are

$$Q_i = \sum_{n=1}^{N} \int_0^R \{dF_n\}^T \frac{d\bar{x}_s}{\partial q_i} \qquad (A.34)$$

These forces are nonlinear. Hence, they are expanded in Taylor series about the steady initial values of θ, ψ, and β_n, and the series are truncated at the first derivatives. For a particular case in which the blades are twisted such that α_o is constant, the linearized aerodynamic forces, after neglecting the effects of the hub and the airloads on the nonflapping portion of the blades, are given by

$$Q_{\beta_\theta} = k\Omega_o^2 \left[M_1\beta_\theta - M_2\beta_\psi + M_3\theta - M_4\psi + M_5\beta_\theta' + M_6\theta' - M_7\psi' \right]$$

$$Q_{\beta_\psi} = k\Omega_o^2 \left[M_2\beta_\theta + M_1\beta_\psi + M_4\theta + M_3\psi + M_5\beta_\psi' + M_7\theta' + M_6\psi' \right]$$

$$
\begin{aligned}
Q_\theta = k\Omega_o^2 \, [& (M_1 + M_1' - N_2 - N_2')\,\beta_\theta - (M_2 + M_2' + N_1 + N_1')\,\beta_\psi \\
& + (M_3 + M_3' - N_4 - N_4')\,\theta - (M_4 + M_4' + N_3 + N_3')\,\psi \\
& + (M_5 + M_5')\,\beta_\theta' - (N_5 + N_5')\,\beta_\psi' + (M_6 + M_6' - N_7 - N_7')\,\theta' \\
& - (M_7 + M_7' + N_6 + N_6')\,\psi']
\end{aligned}
$$

$$
\begin{aligned}
Q_\psi = k\Omega_o^2 \, [& (M_2 + M_2' + N_1 + N_1')\,\beta_\theta + (M_1 + M_1' - N_2 - N_2')\,\beta_\psi \\
& + (M_4 + M_4' + N_3 + N_3')\,\theta + (M_3 + M_3' - N_4 - N_4')\,\psi \\
& + (N_5 + N_5')\,\beta_\theta' + (M_5 + M_5')\,\beta_\psi' + (M_7 + M_7' + N_6 + N_6')\,\theta' \\
& + (M_6 + M_6' - N_7 - N_7')\,\psi']
\end{aligned}
$$

(A.35)

where

$$M_1 = \frac{\sin\beta_o}{\cos\beta_o^3} \left\{ \left[-2\epsilon\lambda_c^3 \frac{C_{do}}{a} - \epsilon^2\lambda_c^2(\alpha_o - \mu_o) \right] \bar{\tau} \right.$$

(Cont'd)

$$+ \left[2 \frac{C_{do}}{a} \lambda_c^3 + 3\epsilon\lambda_c^2\alpha_o - \epsilon\lambda_c^2\mu_o - \lambda_c\epsilon^2\left(1 - \frac{C_{do}}{a}\right) \right] \bar{\tau}_1$$

$$+ \left[- 2\alpha_o(\lambda_c^2 + \epsilon^2) - 3\epsilon\lambda_c \frac{C_{do}}{a} + \epsilon\lambda_c \right] \bar{\tau}_2$$

$$+ \left[2\lambda_c \frac{C_{do}}{a} + 4\epsilon\alpha_o \right] \bar{\tau}_3 - 2\alpha_o\bar{\tau}_4 \bigg\}$$

$$M_2 = \frac{-1}{\cos^3\beta_o} \left\{ - 2\epsilon^2\lambda_c^2 \frac{C_{do}}{a} \bar{\tau}_0 + \left[4\epsilon\lambda_c^2 \frac{C_{do}}{a} + \epsilon^2\lambda_c(\alpha_o + \mu_o) \right] \bar{\tau}_1 \right.$$

$$+ \left[- 2\lambda_c^2 \frac{C_{do}}{a} - 2\epsilon\lambda_c(\alpha_o + \mu_o) - \epsilon^2\left(1 + \frac{C_{do}}{a}\right) \right] \bar{\tau}_2$$

$$+ \left[\lambda_c(\alpha_o + \mu_o) + 2\epsilon\left(1 + \frac{C_{do}}{a}\right) \right] \bar{\tau}_3 - \left(1 + \frac{C_{do}}{a}\right)\bar{\tau}_4 \bigg\}$$

$$M_3 = \frac{-\lambda_c \sin\beta_o}{\cos^3\beta_o} \left\{ 2 \frac{C_{do}}{a}\lambda_c^2\epsilon\bar{\tau}_0 - \left[2\lambda_c^2 \frac{C_{do}}{a} - 2\epsilon\lambda_c(\alpha_o + \mu_o) \right] \bar{\tau}_1 \right.$$

$$+ \left[\lambda_c(\alpha_o + \mu_o) + \epsilon\left(1 + \frac{C_{do}}{a}\right) \right] \bar{\tau}_2 - \left(1 + \frac{C_{do}}{a}\right)\bar{\tau}_3 \bigg\}$$

$$M_4 = \frac{\lambda_c}{\cos^3\beta_o} \left\{ \epsilon\lambda_c^2(\alpha_o - \mu_o)\bar{\tau}_0 + \left[- \lambda_c^2(\alpha_o - \mu_o) + \lambda_c\epsilon\left(1 - \frac{C_{do}}{a}\right) \right] \bar{\tau}_1 \right.$$

$$+ \left[2\epsilon\alpha_o - \lambda_c\left(1 - \frac{C_{do}}{a}\right) \right] \bar{\tau}_2 - 2\alpha_o\bar{\tau}_3 \bigg\}$$

$$M_5 = - M_2 \hspace{4cm} \text{(Cont'd)}$$

and

$$M_6' = -M_2 + \frac{(\epsilon + \ell_h \sin \beta_o)}{\cos^2 \beta_o} \left\{ 2\epsilon\lambda_c^2 \frac{C_{do}}{a} \bar{\tau}_0 \right.$$

$$+ \left[-2\lambda_c^2 \frac{C_{do}}{a} - \epsilon\lambda_c(\alpha_o + \mu_o) \right] \bar{\tau}_1$$

$$\left. + \left[\lambda_c(\alpha_o + \mu_o) + \epsilon\left(1 + \frac{C_{do}}{a}\right) \right] \bar{\tau}_2 - \left(1 + \frac{C_{do}}{a}\right) \bar{\tau}_3 \right\}$$

$$M_7 = \frac{\sin \beta_o}{\cos \beta_o^3} \left\{ \lambda_c^2 \epsilon^2 (\alpha_o - \mu_o) \bar{\tau}_0 + \left[\epsilon\lambda_c \left(1 - \frac{C_{do}}{a}\right) - 2\epsilon\lambda_c^2(\alpha_o - \mu_o) \right] \bar{\tau}_1 \right.$$

$$+ \left[2\epsilon^2\alpha_o - 2\epsilon\lambda_c\left(1 - \frac{C_{do}}{a}\right) + \lambda_c^2(\alpha_o - \mu_o) \right] \bar{\tau}_2$$

$$\left. + \left[-4\epsilon\alpha_o + \lambda_c\left(1 - \frac{C_{do}}{a}\right) \right] \bar{\tau}_3 + 2\alpha_o\bar{\tau}_4 \right\}$$

$$\times \frac{-\ell_h}{\cos^2 \beta_o} \left\{ \epsilon\lambda_c^2(\alpha_o - \mu_o) \bar{\tau}_0 + \left[-\lambda_c^2(\alpha_o - \mu_o) + \lambda_c\epsilon\left(1 - \frac{C_{do}}{a}\right) \right] \bar{\tau}_1 \right.$$

$$\left. + \left[2\epsilon\alpha_o - \lambda_c\left(1 - \frac{C_{do}}{a}\right) \right] \bar{\tau}_2 - 2\alpha_o\bar{\tau}_3 \right\}$$

$$M_1' = (\epsilon + \ell_n \tan \beta_o) \tan \beta_o \left\{ \left[2\lambda_c^3 \frac{C_{do}}{a} + \epsilon\lambda_c^2(\alpha_o - \mu_o) \right] \bar{\tau}_0 \right.$$

$$+ \left[-2\lambda_c^2\alpha_o + \epsilon\lambda_c\left(1 - \frac{C_{do}}{a}\right) \right] \bar{\tau}_1 \qquad \text{(Cont'd)}$$

- 153 -

$$+ \left[2\lambda_c \frac{C_{do}}{a} + 2\epsilon\alpha_o \right] \bar{\tau}_2 - 2\alpha_o \bar{\tau}_3$$

$$M_2' = - \left(\frac{\epsilon + \ell_n \tan \beta_o}{\cos \beta_o} \right) \left\{ + 2\lambda_c^2 \epsilon \frac{C_{do}}{a} \bar{\tau}_0 \right.$$

$$+ \left[- 2\lambda_c^2 \frac{C_{do}}{a} - \lambda_c \epsilon (\alpha_o + \mu_o) \right] \bar{\tau}_1$$

$$\left. + \left[\lambda_c (\alpha_o + \mu_o) + \epsilon \left(1 + \frac{C_{do}}{a} \right) \right] \bar{\tau}_2 - \left(1 + \frac{C_{do}}{a} \right) \bar{\tau}_3 \right\}$$

$$M_3' = - (\epsilon \tan \beta_o + \ell_h \tan^2 \beta_o) \left[- 2\lambda_c^3 \frac{C_{do}}{a} \bar{\tau}_0 \right.$$

$$\left. + \lambda_c^2 (\alpha_o + \mu_o) \bar{\tau}_1 - \lambda_c \left(1 + \frac{C_{do}}{a} \right) \bar{\tau}_2 \right]$$

$$M_4' = - \left(\frac{\epsilon \cos \beta_o + \ell_h \sin \beta_o}{\cos^2 \beta_o} \right) \left[\lambda_c^3 (\alpha_o - \mu_o) \bar{\tau}_0 \right.$$

$$\left. + \lambda_c^2 \left(1 - \frac{C_{do}}{a} \right) \bar{\tau}_1 + \alpha_o \bar{\tau}_2 \right]$$

$$M_5' = \frac{\epsilon \cos \beta_o + \ell_h \sin \beta_o}{\cos^2 \beta_o} \left\{ 2\epsilon \frac{C_{do}}{a} \lambda_c^2 \bar{\tau}_0 - \left[2 \frac{C_{do}}{a} \lambda_c^2 \right. \right.$$

$$\left. + \epsilon\lambda_c (\alpha_o + \mu_o) \right] \bar{\tau}_1 \qquad\qquad \text{(Cont'd)}$$

$$+ \left[\lambda_c (\alpha_o + \mu_o) + \epsilon \left(1 + \frac{C_{do}}{a} \right) \right] \bar{\tau}_2 - \left(1 + \frac{C_{do}}{a} \right) \bar{\tau}_3 \Bigg\}$$

$$M_6' = \frac{\epsilon \cos \beta_o + \ell_h \sin \beta_o}{\cos^2 \beta_o} \left\{ \left[2\epsilon \frac{C_{do}}{a} \lambda_c^2 (1 - \cos \beta_o) \right. \right.$$

$$\left. - 2\ell_h \sin \beta_o \cos \beta_o \lambda_c^2 \frac{C_{do}}{a} \right] \bar{\tau}_0$$

$$+ \left[- 2 \frac{C_{do}}{a} \lambda_c^2 - \epsilon \lambda_c (\alpha_o + \mu_o)(1 - \cos \beta_o) \right.$$

$$\left. + \lambda_c \ell_h \sin \beta_o \cos \beta_o (\alpha_o + \mu_o) \right] \bar{\tau}_1$$

$$+ \left[\lambda_c (\alpha_o + \mu_o) + \epsilon \left(1 + \frac{C_{do}}{a} \right) (1 - \cos \beta_o) \right.$$

$$\left. - \ell_h \sin \beta_o \cos \beta_o \left(1 + \frac{C_{do}}{a} \right) \right] \bar{\tau}_2 - \left(1 + \frac{C_{do}}{a} \right) \bar{\tau}_3 \Bigg\}$$

$$M_7' = \left(\frac{\epsilon \cos \beta_o + \ell_h \sin \beta_o}{\cos^2 \beta_o} \right) \left\{ (\ell_h \cos \beta_o - \epsilon \sin \beta_o) \lambda_c^2 (\alpha_o - \mu_o) \bar{\tau}_0 \right.$$

$$+ \left[\lambda_c^2 (\alpha_o - \mu_o) \sin \beta_o + (\ell_h \cos \beta_o - \epsilon \sin \beta_o) \lambda_c \left(1 - \frac{C_{do}}{a} \right) \right] \bar{\tau}_1$$

$$+ \left[\lambda_c \left(1 - \frac{C_{do}}{a} \right) \sin \beta_o + (\ell_h \cos \beta_o - \epsilon \sin \beta_o) 2\alpha_o \right] \bar{\tau}_2$$

$$+ 2\alpha_o \sin \beta_o \bar{\tau}_3 \Bigg\} \qquad \text{(Cont'd)}$$

and

$$N_1 = -\frac{\sin^2 \beta_o}{\cos^3 \beta_o} \left\{ \left[-2\epsilon\lambda_c^3\alpha_o + \epsilon^2\lambda_c^2\left(1 + \frac{C_{do}}{a}\right)\right]\bar{\tau}_0 \right.$$

$$+ \left[2\lambda_c^3\alpha_o - 3\lambda_c^2\epsilon\frac{C_{do}}{a} - \epsilon\lambda_c^2 + \lambda_c\epsilon^2(\alpha_o + \mu_o)\right]\bar{\tau}_1$$

$$+ \left[2\lambda_c^2\frac{C_{do}}{a} - 3\lambda_c\epsilon\alpha_o - \lambda_c\epsilon\mu_o + 2\epsilon^2\frac{C_{do}}{a}\right]\bar{\tau}_2$$

$$\left. + \left[2\lambda_c\alpha_o - 4\epsilon\frac{C_{do}}{a}\right]\bar{\tau}_3 + 2\frac{C_{do}}{a}\bar{\tau}_4\right\}$$

$$N_1' = -\frac{\ell_h \sin \beta_o}{\cos^2 \beta_o} \left\{ \left[2\lambda_c^3\alpha_o - \epsilon\lambda_c^2\left(1 + \frac{C_{do}}{a}\right)\right]\bar{\tau}_0 \right.$$

$$+ \left[2\lambda_c^2\frac{C_{do}}{a} - \epsilon\lambda_c(\alpha_o + \mu_o)\right]\bar{\tau}_1$$

$$\left. + \left[2\lambda_c\alpha_o - 2\epsilon\frac{C_{do}}{a}\right]\bar{\tau}_2 + 2\frac{C_{do}}{a}\bar{\tau}_3\right\}$$

$$N_2 = \frac{\sin \beta_o}{\cos^3 \beta_o} \left\{ 2\lambda_c^2\epsilon^2\alpha_o\bar{\tau}_0 + \left[-4\epsilon\lambda_c^2\alpha_o - \epsilon^2\lambda_c\left(1 - \frac{C_{do}}{a}\right)\right]\bar{\tau}_1 \right.$$

$$+ \left[2\lambda_c^2\alpha_o + 2\epsilon\lambda_c\left(1 - \frac{C_{do}}{a}\right) + \epsilon^2(\alpha_o - \mu_o)\right]\bar{\tau}_2$$

$$\left. + \left[-\lambda_c\left(1 - \frac{C_{do}}{a}\right) - 2\epsilon(\alpha_o - \mu_o)\right]\bar{\tau}_3 + (\alpha_o - \mu_o)\bar{\tau}_4\right\}$$

(Cont'd)

and

$$N_2' = - \frac{\ell_h}{\cos^2 \beta_o} \left\{ - 2\epsilon\lambda_c^2\alpha_o\bar{\tau}_0 + \left[\epsilon\lambda_c \left(1 - \frac{C_{do}}{a} \right) + 2\lambda_c^2\alpha_o \right]\bar{\tau}_1 \right.$$

$$\left. + \left[- \epsilon (\alpha_o - \mu_o) - \lambda_c \left(1 - \frac{C_{do}}{a} \right) \right]\bar{\tau}_2 + (\alpha_o - \mu_o)\,\bar{\tau}_3 \right\}$$

$$N_3 = - \frac{\sin^2 \beta_o}{\cos^3 \beta_o} \left\{ - 2\epsilon\lambda_c^3\alpha_o\bar{\tau}_0 + \left[2\lambda_c^3\alpha_o + \lambda_c^2\epsilon \left(1 - \frac{C_{do}}{a} \right) \right]\bar{\tau}_1 \right.$$

$$\left. + \left[- \lambda_c^2 \left(1 - \frac{C_{do}}{a} \right) - \epsilon\lambda_c(\alpha_o - \mu_o) \right]\bar{\tau}_2 + (\alpha_o - \mu_o)\,\lambda_c\bar{\tau}_3 \right\}$$

$$N_3' = - \frac{\ell_h \sin \beta_o}{\cos^2 \beta_o} \left[2\lambda_c^3\alpha_o\bar{\tau}_0 - \lambda_c^2 \left(1 - \frac{C_{do}}{a} \right)\bar{\tau}_1 + \lambda_c(\alpha_o - \mu_o)\,\bar{\tau}_2 \right]$$

$$N_4 = - \frac{\sin \beta_o}{\cos^3 \beta_o} \left\{ - \epsilon\lambda_c^3 \left(1 + \frac{C_{do}}{a} \right)\bar{\tau}_0 \right.$$

$$+ \left[- \epsilon\lambda_c^2(\alpha_o + \mu_o) + \lambda_c^3 \left(1 + \frac{C_{do}}{a} \right) \right]\bar{\tau}_1$$

$$\left. + \left[\lambda_c^2(\alpha_o - \mu_o) - 2\epsilon\frac{C_{do}}{a} \right]\bar{\tau}_2 + 2\lambda_c\frac{C_{do}}{a}\,\bar{\tau}_3 \right\}$$

$$N_4' = - \frac{\ell_h}{\cos^2 \beta_o} \left[\lambda_c^3 \left(1 + \frac{C_{do}}{a} \right)\bar{\tau}_0 + \lambda_c^2(\alpha_o + \mu_o)\,\bar{\tau}_1 + 2\lambda_c\frac{C_{do}}{a}\bar{\tau}_2 \right]$$

$$N_5 + N_5' = - [N_2 + N_2']$$

and

$$N_6 = \frac{\sin \beta_o}{\cos^3 \beta_o} \left\{ \left\{ 2\epsilon^2 \lambda_c^2 \alpha_o \bar{\tau}_0 + \left[-4\epsilon\lambda_c^2\alpha_o - \epsilon^2 \left(1 - \frac{C_{do}}{a}\right)\lambda_c \right] \bar{\tau}_1 \right. \right.$$

$$+ \left[\epsilon^2(\alpha_o - \mu_o) + 2\epsilon\lambda_c \left(1 - \frac{C_{do}}{a}\right) + 2\lambda_c^2\alpha_o \right] \bar{\tau}_2$$

$$+ \left[-2\epsilon(\alpha_o - \mu_o) - \lambda_c \left(1 - \frac{C_{do}}{a}\right) \right] \bar{\tau}_3 + (\alpha_o - \mu_o) \bar{\tau}_4 \right\}$$

$$+ \left[(\epsilon + \ell_h \sin \beta_o) \cos \beta_o \right] \left\{ -2\epsilon\lambda_c^2\alpha_o \bar{\tau}_0 \right.$$

$$+ \left[2\lambda_c^2\alpha_o + \lambda_c\epsilon \left(1 - \frac{C_{do}}{a}\right) \right] \bar{\tau}_1$$

$$+ \left. \left. \left[-\lambda_c \left(1 - \frac{C_{do}}{a}\right) - \epsilon(\alpha_o - \mu_o) \right] \bar{\tau}_2 + \bar{\tau}_3(\alpha_o - \mu_o) \right\} \right\}$$

$$N_6' = \frac{\ell_h}{\cos^2 \beta_o} \left\{ 2\lambda_c^2\alpha_o \bar{\tau}_0 \left[(\cos \beta_o - 1)\epsilon + \ell_h \sin \beta_o \cos \beta_o \right] \right.$$

$$+ \left\{ 2\lambda_c^2\alpha_o - \lambda_c \left(1 - \frac{C_{do}}{a}\right) \left[(\cos \beta_o - 1)\epsilon + \ell_h \sin \beta_o \cos \beta_o \right] \right\} \bar{\tau}_1$$

$$+ \left\{ -\lambda_c \left(1 - \frac{C_{do}}{a}\right) + (\alpha_o - \mu_o) \left[(\cos \beta_o - 1)\epsilon \right. \right.$$

$$+ \left. \left. \left. \ell_h \sin \beta_o \cos \beta_o \right] \right\} \bar{\tau}_2 + (\alpha_o - \mu_o) \bar{\tau}_3 \right\} \qquad \text{(Cont'd)}$$

- 158 -

and

$$N_7 = \frac{\sin^2 \beta_o}{\cos^3 \beta_o} \left\{ \epsilon^2 \lambda_c (\alpha_o + \mu_o) \, \bar{\tau}_0 + \left[\epsilon^2 \lambda_c^2 \left(1 + \frac{C_{do}}{a} \right) - 2\epsilon \lambda_c (\alpha_o + \mu_o) \right] \bar{\tau}_1 \right.$$

$$+ \left[2\epsilon^2 \frac{C_{do}}{a} - 2\epsilon \lambda_c^2 \left(1 + \frac{C_{do}}{a} \right) + \lambda_c^2 \left(1 + \frac{C_{do}}{a} \right) \right] \bar{\tau}_2$$

$$\left. + \left[-4\epsilon \frac{C_{do}}{a} + \lambda_c (\alpha_o + \mu_o) \right] \bar{\tau}_3 + 2 \frac{C_{do}}{a} \bar{\tau}_4 \right\}$$

$$+ \frac{2\ell_h \sin \beta_o}{\cos^2 \beta_o} \left\{ - \epsilon \lambda_c^2 \left(1 + \frac{C_{do}}{a} \right) \bar{\tau}_0 \right.$$

$$+ \left[- \epsilon \lambda_c (\alpha_o + \mu_o) + \lambda_c^2 \left(1 + \frac{C_{do}}{a} \right) \right] \bar{\tau}_1$$

$$\left. + \left[- 2\epsilon \frac{C_{do}}{a} + \lambda_c (\alpha_o + \mu_o) \right] \bar{\tau}_2 + 2 \frac{C_{do}}{a} \bar{\tau}_3 \right\}$$

$$N_7' = \frac{\ell_h^2}{\cos \beta_o} \left[\lambda_c^2 \left(1 + \frac{C_{do}}{a} \right) \bar{\tau}_0 + \lambda_c^2 (\alpha_o + \mu_o) \, \bar{\tau}_1 + 2 \frac{C_{do}}{a} \bar{\tau}_2 \right]$$

$$\lambda_c = \lambda \cos \beta_o$$

$$\mu_o = \frac{K_{d1} + 2K_{d2}\alpha_o}{a}$$

$$\bar{\tau}_m = \int_\epsilon^{(1-\epsilon) \cos \beta_o + \epsilon} \frac{\bar{X}^m}{\sqrt{\lambda_c^2 + \bar{X}^2}} \, d\bar{X} \qquad \left. \begin{array}{c} \\ \\ \\ \\ \\ \end{array} \right\} \qquad \text{(Cont'd)}$$

and

$$m = 0, 1, 2, 3, 4$$

$$\overline{X} = (X - \epsilon) \cos \beta_o + \epsilon$$

$$\lambda = V/\Omega_o R$$

$$\alpha_o = \nu - \tan^{-1} (\lambda_c/\overline{X})$$

$$k = \frac{N}{4} \rho c a R^4$$

$$\ell_h = h/R$$

$$C_{do} = K_{d0} + K_{d1}\alpha_o + K_{d2}\alpha_o^2$$

$$\epsilon = r_e/R$$

$$X = r/R \tag{A.36}$$

The final equations of motion are obtained by simply adding together all the forces acting on the system, and finally they are

written below in matrix notation as

$$[AN]\{q''\} + \Big[[SD] - [AD]\Big]\{q'\} + \Big[[SS] - [AS]\Big]\{q\} = 0 \qquad (A.37)$$

where

$$\{q\} = \begin{Bmatrix} \beta_\theta \\ \theta \\ \beta_\psi \\ \psi \end{Bmatrix}$$

$$[AN] = \Omega_o^2 \begin{bmatrix} I_\beta & I_2 & 0 & 0 \\ I_2 & \overline{I}_\theta & 0 & 0 \\ 0 & 0 & I_\beta & I_2 \\ 0 & 0 & I_2 & \overline{I}_\psi \end{bmatrix}$$

$$[SD] = \Omega_o^2 \begin{bmatrix} 2I_\beta \zeta_\beta \gamma_{\beta 1} & 0 & 2I_\beta & I_\beta(1+\cos 2\beta_o)+2I_o\cos\beta_o \\[2ex] 0 & 2\bar{I}_\theta \zeta_\theta \gamma_\theta & I_\beta(1+\cos 2\beta_o)+2I_o\cos\beta_o & 2\bar{I}_1 \\[2ex] -2I_\beta & -[I_\beta(1+\cos 2\beta_o)+2I_o\cos\beta_o] & 2I_\beta \zeta_\beta \gamma_{\beta 1} & 0 \\[2ex] -[I_\beta(1+\cos 2\beta_o)+2I_o\cos\beta_o] & -2\bar{I}_1 & 0 & 2\zeta_\psi \bar{I}_\psi \gamma_\psi \end{bmatrix}$$

$$[SS] = \Omega_o^2 \begin{bmatrix} I_\beta(\cos 2\beta_o - 1)+I_o\cos\beta_o+\gamma_\beta^2 I_\beta & 0 & 2I_\beta \zeta_\beta \gamma_{\beta 1} & 0 \\[2ex] 0 & \bar{I}_\theta \gamma_\theta^2 & 0 & 0 \\[2ex] -2I_\beta \zeta_\beta \gamma_{\beta 1} & 0 & I_\beta(\cos 2\beta_o - 1)+I_o\cos\beta_o+\gamma_\beta^2 I_\beta & 0 \\[2ex] 0 & 0 & 0 & \bar{I}_\psi \gamma_\psi^2 \end{bmatrix}$$

(Cont'd)

$$[AS] = k\Omega_o^2 \begin{bmatrix} M_1 & M_3 & -M_2 & -M_4 \\ M_1 + M_1' - (N_2 + N_2') & M_3 + M_3' - N_4 - N_4' & -(M_2 + M_2' + N_1 + N_1') & -(M_4 + M_4' + N_3 + N_3') \\ M_2 & M_4 & M_1 & M_3 \\ M_2 + M_2' + N_1 + N_1' & M_4 + M_4' + N_3 + N_3' & M_1 + M_1' - N_2 - N_2' & M_3 + M_3' - N_4 - N_4' \end{bmatrix}$$

$$[AD] = k\Omega_o^2 \begin{bmatrix} M_5 & M_6 & 0 & -M_7 \\ M_5 + M_5' & M_6 + M_6' - N_7 - N_7' & -N_5 - N_5' & -(M_7 + M_7' + N_6 + N_6') \\ 0 & M_7 & M_5 & M_6 \\ N_5 + N_5' & M_7 + M_7' + N_6 + N_6' & M_5 + M_5' & M_6 + M_6' - N_7 - N_7' \end{bmatrix}$$

$$(A.38)$$

REFERENCES

CHAPTER II

2.1   Novozhilov, V. V., <u>Foundations of the Nonlinear Theory of Elas-</u>
        <u>ticity</u> (English Translation by F. Bagemihl, H. Komm, and W.
        Seidel), Graylock Press, Rochester, New York, 1953.

2.2   Bisplinghoff, R. L. and Ashley, H., <u>Principles of Aeroelasticity,</u>
        John Wiley & Sons, Inc., New York, 1962.

2.3   Milne, R. D., "Some Remarks on the Dynamics of Deformable Bodies,"
        <u>AIAA Journal,</u> Vol. 6, No. 3, March 1968, pp. 556-558.

2.4   Milne, R. D., "Dynamics of the Deformable Airplane," ARC R & M
        3345, 1964.

CHAPTER III

3.1   Milne, R. D., "Some Remarks on the Dynamics of Deformable Bodies,"
        <u>AIAA Journal,</u> Vol. 6, No. 3, March 1968, pp. 556-558.

3.2   Courant, R. and Hilbert, D., <u>Methods of Mathematical Physics,</u>
        Interscience Publishers, Inc., New York, 1955.

3.3   Bisplinghoff, R. L. and Ashley, H., <u>Principles of Aeroelasticity,</u>
        John Wiley & Sons, Inc., New York, 1962.

3.4   Bolotin, V. V., <u>Nonconservative Problems of Theory of Elastic</u>
        <u>Stability,</u> edited by G. Herrmann, Translated from the Russian
        by T. K. Lusher, The Macmillan Company, New York, 1963.

3.5 Backus, G. and Gilbert, F., "The Rotational Splitting of the Free Oscillations of the Earth," <u>Proceedings of the National Academy of Sciences</u>, Vol. 47, 1961, pp. 362-371.

3.6 Gilbert, F. and Backus, G., "The Rotational Splitting the Free Oscillations of the Earth," <u>Reviews of Geophysics</u>, Vol. 3, No. 1, February 1965, pp. 1-9.

3.7 Ashley, H., "Observations on the Dynamic Behaviour of Large Flexible Bodies in Orbit," <u>AIAA Journal</u>, Vol. 5, No. 1, March 1967, pp. 460-469.

3.8 Bishop, R. E. D., "The Vibration of Rotating Shafts," <u>Journal of Mechanical Engineering Science</u>, Vol. 1, No. 1, June 1959, pp. 50-65.

3.9 Ziegler, H., <u>Principles of Structural Stability</u>, Blaisdell Publishing Company, Waltham, Mass., 1968.

3.10 Leipholz, H., <u>Stability Theory</u>, Academic Press, New York, pp. 1-21, 1970.

3.11 Stoker, J. J., "Stability of Continuous Systems," "Dynamic Stability of Structures," Proceedings of International Conference held at Northwestern University, Evanston, Illinois, 1965, pp. 45-48.

3.12 Herrmann, G., "Stability of Equilibrium of Elastic Systems Subjected to Non-conservative Forces," <u>Applied Mechanics Reviews</u>, Vol. 20, No. 2, February 1967, pp. 103-108.

3.13 Bryan, G. H., "On the Stability of Elastic Systems," <u>Proceedings of the Cambridge Philosophical Society</u>, Vol. 6, 1886-1889, pp. 199-287.

3.14 Meirovitch, L., _Methods of Analytical Dynamics_, McGraw-Hill, New York, 1970, pp. 209-322.

3.15 Wang, P. K. C., "Stability Analysis of Elastic and Aeroelastic Systems via Liapunov's Direct Method," _Journal of the Franklin Institute_, Vol. 281, No. 1, 1966, pp. 51-72.

3.16 Parks, P. C., "A Stability Criterion for Panel Flutter via the Second Method of Liapunov," _AIAA Journal_, Vol. 4, No. 9, September 1966, pp. 175-177.

3.17 Meirovitch, L., "A Method for Liapunov Stability Analysis of Force-Free Dynamical Systems," _AIAA Journal_, Vol. 9, No. 9, September 1971, pp. 1695-1701.

3.18 Meirovitch, L. and Calico, R. A., "Stability of Motion of Force-Free Spinning Satellites with Flexible Appendages," _Journal of Spacecraft and Rockets_, Vol. 9, No. 4, April 1972, pp. 237-245.

3.19 Fung, Y. C., _An Introduction to the Theory of Aeroelasticity_, Dover Publications, Inc., New York, 1969.

3.20 Garrick, I. E., ed., _Aerodynamic Flutter_, AIAA Selected Reprints, March 1969.

3.21 Herrmann, G. and Bungay, R. W., "On the Stability of Elastic Systems Subjected to Nonconservative Forces," _Journal of Applied Mechanics_, Vol. 31, No. 3, September 1964, pp. 435-440.

3.22 Routh, E. J., _Advanced Rigid Dynamics_, Dover Publications, New York, 1955.

3.23 Thomson, Sir W. (Lord Kelvin) and Tait, P. G., _Principles of Mechanics and Dynamics_, Vol. 1, Dover Publications, New York, 1962.

3.24 Meirovitch, L., <u>Analytical Methods in Vibrations</u>, The Macmillan Company, New York, 1967.

3.25 Theodorsen, T. and Garrick, I. E., "Mechanism of Flutter — A Theoretical and Experimental Investigation of the Flutter Problem," NACA Rept. 685, 1940.

3.26 Bisplinghoff, R. L., Ashley, H. and Halfman, R. L., <u>Aeroelasticity</u>, Addison Wesley Publishing Company, Reading, Mass., 1955.

3.27 Scanlan, R. H. and Rosenbaum, R., <u>Aircraft Vibration and Flutter</u>, Dover Publications, Inc., New York, 1968.

3.28 Houbolt, J. C. and Reed, W. H., III, "Propeller-Nacelle Whirl Flutter," <u>Journal of the Aerospace Sciences</u>, Vol. 29, No. 3, 1962, pp. 333-346.

3.29 Reed, W. H., III and Bland, S. R., "An Analytical Treatment of Aircraft Propeller Precession Instability," NASA TN D-659, 1961.

3.30 Richardson, J. R., McKillop, J. A., Naylor, H. F. W. and Bandler, P. A., "Whirl Flutter of Propellers with Flexible Twisted Blades," Rept. No. 43, Directorate Eng. Res., Defence Board, (Canada), 1963.

3.31 Young, M. I. and Lytwyn, R. T., "The Influence of Blade Flapping Restraint on the Dynamic Stability of Low Disk Loading Propeller-Rotors," <u>Journal of the American Helicopter Society</u>, Vol. 12, No. 4, October 1967, pp. 38-60.

3.32 Milne, R. D., "Dynamics of the Deformable Airplane," ARC R & M 3345, 1964.

3.33   Ariaratnam, S. T., "The Vibration of Unsymmetrical Rotating

Shafts," <u>Journal of Applied Mechanics</u>, Vol. 32, No. 1, March

1965, pp. 157-162.

3.34   Yntema, R. T., "Simplified Procedures and Charts for the Rapid

Estimation of Bending Frequencies of Rotating Beams," NACA TN

3459, 1955.

3.35   Houbolt, J. C. and Brooks, G. W., "Differential Equations of

Motion for Combined Flapwise Bending, Chordwise Bending and

Torsion of Twisted Rotating Beams," NACA TN 3905, 1957.

3.36   Brooks, G. W., "On the Determination of the Chordwise Bending

Frequencies of Rotor Blades," <u>Journal of American Helicopter</u>

<u>Society</u>, Vol. 3, No. 3, July 1958, pp. 40-43.

3.37   Pederson, P. T., "On Forward and Backward Precession of Rotors,"

Report No. 17, The Technical University of Denmark, Lyngby,

Denmark, September 1971.

3.38   Lamb, H. and Southwell, R. V., "The Vibration of Spinning Disc,"

<u>Proceedings of the Royal Society (London)</u>, Vol. 99, July 1921,

pp. 272-280.

3.39   Eversman, W. and Dodson, R. O. Jr., "Free Vibration of a Cen-

trally Clamped Spinning Circular Disc," <u>AIAA Journal</u>, Vol. 7,

No. 10, September 1969, pp. 2010-2012.

3.40   Carrier, G. F., "On the Vibration of the Rotating Ring," <u>Quarterly</u>

<u>Journal of Mathematics</u>, Vol. III, No. 3, October 1945, pp. 235-

245.

3.41 Johnson, D. C., "Free Vibration of a Rotating Elastic Body," *Aircraft Engineering*, Vol. XXIV, No. 282, August 1952, pp. 234-236.

3.42 Meirovitch, L., "Stability of a Spinning Body Containing Elastic Parts Via Liapunov's Direct Method," *AIAA Journal*, Vol. 8, No. 7, July 1970, pp. 1193-1200.

3.43 Meirovitch, L. and Calico, R. A., "A Comparative Study of Stability Methods for Flexible Satellites," *AIAA Journal*, Vol. 11, No. 1, January 1973, pp. 91-98.

CHAPTER IV

4.1 Yntema, R. T., "Simplified Procedures and Charts for the Rapid Estimation of Bending Frequencies of Rotating Beams," NACA TN 3459, 1955.

4.2 Brooks, G. W., "On the Determination of the Chordwise Bending Frequencies of Rotor Blades," *Journal of the American Helicopter Society*, Vol. 3, No. 3, July 1958, pp. 40-43.

4.3 Hildebrand, F. B., *Introduction to Numerical Analysis*, McGraw-Hill Book Company, New York, 1956.

CHAPTER V

5.1 Turner, M. J., "Design of Minimum-Mass Structures with Specified Natural Frequencies," *AIAA Journal*, Vol. 5, No. 3, March 1967, pp. 406-412.

5.2 Keller, J. B. and Niordson, F. I., "The Tallest Column," *Journal of Mathematics and Mechanics*, Vol. 16, No. 5, November 1966, pp. 443-446.

5.3 Niordson, F. I., "On the Optimal Design of a Vibrating Beam," _Quarterly of Applied Mathematics_, Vol. XXIII, No. 1, April 1965, pp. 47-53.

5.4 Olhoff, N., "Optimal Design of Vibrating Circular Plates," Department of Applied Mechanics, The Technical University of Denmark, Copenhagen, 1969.

5.5 Sheu, C. Y. and Prager, W., "Recent Developments in Optimal Structural Design," _Applied Mechanics Reviews_, Vol. 21, No. 10, October 1968, pp. 985-992.

5.6 Prager, W. and Taylor, J. E., "Problems of Optimal Structural Design," _Journal of Applied Mechanics_, Vol. 35, No. 1, March 1968, pp. 102-106.

5.7 Ashley, H. and McIntosh, S. C., Jr., "Application of Aeroelastic Constraints in Structural Optimization," Proceedings of the Twelfth International Congress of Applied Mechanics, Stanford University, Stanford, California, August 1968, Springer-Verlag, Berlin, 1969, pp. 100-113.

5.8 Armand, J.-L. and Vitte, W. J., "Foundations of Aeroelastic Optimization and Some Applications to Continuous Systems," SUDAAR 390, January 1970, Department of Aeronautics and Astronautics, Stanford University, Stanford, California.

5.9 Weisshaar, T. A., "An Application of Control Theory Methods to the Optimization of Structures Having Dynamic or Aeroelastic Constraints," SUDAAR 412, October 1970, Department of Aeronautics and Astronautics, Stanford University, Stanford, California.

5.10 Armand, J.-L., "Application of the Theory of Optimal Control of Distributed Parameter Systems to Structural Optimization," Ph.D. Dissertation, August 1971, Department of Aeronautics and Astronautics, Stanford University, Stanford, California.

5.11 Vepa, K., "Optimally Stable Structural Forms," Ph.D. Dissertation, February 1972, Department of Civil Engineering, University of Waterloo.

5.12 Haug, E. J., Jr., Streeter, T. D. and Newell, R. S., "Optimal Design of Elastic Structural Elements," SY-RI-69, April 1969, System Analysis Directorate, U. S. Army Weapons Command, Rock Island, Illinois.

5.13 MacCart, B. R., Haug, E. J., Jr. and Streeter, T. D., "Optimal Design of Structures with Constraints on Natural Frequency," AIAA Journal, Vol. 8, No. 6, June 1970, pp. 1012-1019.

5.14 Fox, R. L. and Kapoor, M. P., "Structural Optimization in the Dynamic Response Regime: A Computational Approach," AIAA Journal, Vol. 8, No. 10, October 1970, pp. 1798-1804.

5.15 Rubin, C. P., "Minimum-Weight Design of Complex Structures Subjected to a Frequency Constraint," AIAA Journal, Vol. 8, No. 5, May 1970, pp. 923-927.

5.16 Turner, M. J., "Optimization of Structures to Satisfy Flutter Requirements," AIAA Structural Dynamics and Aeroelasticity Specialist Conference, New Orleans, La., April 1969, Volume of Technical Papers, pp. 1-8.

5.17 Bryson, A. E., Jr. and Ho, Y.-C., <u>Applied Optimal Control</u>, The
Blaisdell Publishing Company, Waltham, Massachusetts, 1969.

5.18 Halfman, R. L., <u>Dynamics Volume II</u>, Addison-Wesley, Reading,
Mass., 1962, Chapter 10.

5.19 Caratheodory, C., <u>Calculus of Variations and Partial Differential
Equations of the First Order</u>, Holden Day Inc., San Francisco,
1968.

5.20 Pontryagin, L. S., Boltyanskii, V. G., Gumkrelidge, R. V. and
Mishchenko, E. F., <u>The Mathematical Theory of Optimal Processes</u>,
John Wiley & Sons, New York, 1962.

CHAPTER VI

6.1 Reed, W. H., III, "Review of Propeller-Rotor Whirl Flutter,"
NASA TR R-264, July 1967.

6.2 Richardson, J. R. and Naylor, H. F. W., "Whirl Flutter of
Propellers with Hinged Blades," Report No. 24, Engineering
Research Associates, Toronto, Canada, March 1962.

6.3 Young, M. I. and Lytwyn, R. T., "The Influence of Blade Flapping
Restraint on the Dynamic Instability of Low Disc Loading Pro-
peller-Rotors," <u>Journal of the American Helicopter Society</u>,
Vol. 12, No. 4, October 1967, pp. 38-60.

6.4 Kaza, K. R. V. (Krishna Rao, K. V.), "A Preliminary Investigation
of Whirl Flutter Studies in High-Bypass Ratio Fan Jet Engines,"
NASA Langley, Working Paper, LWP-523, 1967.

6.5   Kaza, K. R. V. (Krishna Rao, K. V.), "Whirl Flutter Studies in High-Bypass Ratio Fan Jet Engines," Paper Presented at the 20th Annual General Meeting of the Aeronautical Society of India, Indian Institute of Science, Bangalore, 1968.

6.6   Kaza, K. R. V. (Krishna Rao, K. V.) and Sundararajan, D., "Whirl Flutter of Flapped Blade Rotor Systems," TN-18, October 1969, National Aeronautical Laboratory, Bangalore, India.

6.7   Gaffey, T. M., "Whirl Flutter Calculations for Reed's Flapping Blade Propeller Model" (Unpublished Results Obtained from Reed, November 1969), Bell Helicopter Company, Fort Worth, Texas.

6.8   Baird, E. F., Bauer, E. M. and Kohn, J. S., "Model Tests and Analysis of Prop-Rotor Dynamics for Tilt-Rotor Aircraft," Paper Presented at the Mideast Region Symposium of American Helicopter Society, Philadelphia, Pennsylvania, October 1972.

6.9   Kvaternik, R. G., "Studies in Tilt-Rotor VTOL Aircraft Aeroelasticity," Ph.D. Dissertation, Department of Solid Mechanics, Structures and Mechanical Design, Case Western Reserve University, June 1973.

6.10   Loewy, R. G., "Review of Rotary-Wing V/STOl Dynamic and Aeroelastic Problems," AIAA Paper No. 69-202, 1969.

6.11   Kaza, K. R. V., "The Effect of Steady State Coning Angle and Damping on Whirl Flutter Stability," Journal of Aircraft, Vol. 10, November 1973, pp. 664-669.

6.12   Fair, G., "ALLMAT: A TSS/360 Fortran IV Subroutine for Eigenvalues and Eigenvectors of a General Complex Matrix," NASA TN D-7032, January 1971.